Phase Behavior of Polymers in Supercritical Fluid Solvents

Christopher F. Kirby and Mark A. McHugh*

Department of Chemical Engineering, 3400 N. Charles Street, Johns Hopkins University, Baltimore, Maryland 21218

Received July 6, 1998 (Revised Manuscript Received October 13, 1998)

Contents

I. Introduction

Scientists and engineers have been aware of the unique solvent characteristics of supercritical fluids (SCF) for more than 100 years, but it is only in the past three decades that SCF solvents have been the focus of active research and development programs especially in the area of polymer processing. SCF solvents have been touted as candidate media for polymerization processes, polymer purification and fractionation, and as environmentally preferable solvents for solution coatings and powder formation. Understanding the underlying physics and chemistry of SCF−polymer solution behavior provides the opportunity to fully exploit the potential of SCF-based polymer processing. Although a detailed understanding of the physics and chemistry of polymer−liquid mixtures has emerged in the past four decades, significant challenges remain for developing the same level of understanding of polymer−SCF solution behavior. At present, efficient development of SCF-based polymer processing technology suffers from the limitation that equations of state utilized for process simulation and modeling are still not facile enough to describe the unique characteristics of a long-chain polymer in solution. The underlying issue is how to account for the intra- and intersegmental interactions of the many segments of the polymer connected to a single backbone relative to the small number of segments in a solvent molecule. In addition, the challenge of calculating the density dependence of intermolecular potential functions is exacerbated when dealing with SCF−polymer solutions that by their very nature, are highly compressible mixtures which precludes the application of a rigid lattice description of solution properties. As a consequence, the approach taken in this review is to describe a molecular thermodynamic basis for interpreting polymer−SCF phase behavior that relies on a physicochemical interpretation of experimental data. With this approach the types and the strengths of energetic interactions are related to the chemical nature of the SCF solvent and to the chemical architecture of the polymer. Phase diagrams for polymer−solvent mixtures are developed and used to interpret as well as catalog polymer−SCF solution behavior so as to provide a template for designing experimental studies that cover a broad pressure−temperature−composition (P−T−x) space with a minimum of experimental data.

In principle, it is possible to extend the results of a phase behavior study using an equation of state to model and calculate solubility behavior at other temperatures, pressures, and in the presence of alternate cosolvents. Although, as alluded to earlier, equations of state for polymer solutions have certain limitations, they are in a state of continual development, they can be used to correlate data, and, with caution, they can be used to simulate other experimental conditions not explicitly measured. The strengths and limitations of equation of state modeling are presented in this review. It should also be mentioned that an alternative approach to extending phase behavior results is to perform computer simulations based on first principles. However, computer simulation techniques suffer from convergence difficulties as the number of repeat units in the polymer

10.1021/cr970046j CCC: $35.00
Published on Web 01/13/1999

Christopher Kirby received his B.S. degree in Chemical Engineering from Johns Hopkins University in 1993. As an undergraduate, he conducted research with Dr. Mark A. McHugh on the phase behavior of hydrocarbon polymers in liquid and supercritical fluid (SCF) solvents. He is currently a senior graduate student at Johns Hopkins University working with Dr. McHugh to develop high-pressure optical techniques to characterize polymer configurational properties in SCF solvents across wide ranges of pressure–temperature space. His is major focus is on the application of time-resolved light-scattering methods to investigate the kinetics of phase separation and the microstructures produced via pressure quenches in polymer-supercritical fluid (SCF) solvent solutions. The objective of his research is to correlate the microscopic properties of a polymer–solvent mixture with the observable macroscopic phase behavior.

Mark A. McHugh received his Ph.D. from the University of Delaware in 1981. He was on the faculty of Chemical Engineering at the University of Notre Dame for four and a half years before joining the Department of Chemical Engineering at the Johns Hopkins University where he is Professor of Chemical Engineering. He has conducted research in the area of high-pressure phase equilibria, including extensive studies on polymer–supercritical fluid (SCF) mixtures and solid–SCF mixtures. His main research interest is in the physical chemistry of hydrocarbon and fluorocarbon (co)polymers in SCF solvents at high-pressures. His research group has incorporated video techniques with high-pressure techniques to visualize and record phase behavior and they are currently integrating light, X-ray, and neutron scattering techniques with high-pressure phase behavior techniques to elucidate and characterize polymer dimensions and intermolecular interactions at the macromolecular length scale.

chain exceeds a few hundred, as compared to many thousands found with real polymers, and as realistic intermolecular potential functions are used either with the polymer or with the solvent. Computer simulation studies of polymer solution behavior are not reviewed here.

Historically the high-pressure, free-radical polyethylene polymerization process developed in the late 1930s represents the earliest applications of SCF solvents for processing polymers. Although these processes were commercialized in the late 1930s and early 1940s, a thorough understanding of the phase and kinetic behavior of these systems was still developing at this time. Ehrlich and co-workers were the first to develop fundamental phase behavior information that resolved much of the contradictory kinetic data that were actually obtained while operating in a two-phase region rather than the presumed one-phase region.[1] The resiliency of free radical polyolefin polymerization is exemplified by the 1997 statistic that more than six billion pounds of polyethylene alone were produced at kilobar pressures and elevated temperatures that are certainly supercritical conditions. The phase behavior of a polymer in a given solvent depends on polymer molecular weight, molecular weight dispersity, and degree and type of chain branching as well as solvent quality. Examples of these types of dependencies are provided in this review.

The need to understand high-pressure polymer solution behavior was not alleviated once the specifics of the polyethylene-ethylene system were resolved. The polyethylene manufacturing industry recognized the potential of producing higher value added, ethylene-based copolymers using existing high-pressure process facilities. Three examples of these type copolymers are poly(ethylene-*co*-vinyl acetate), poly(ethylene-*co*-methyl acrylate), and poly(ethylene-*co*-acrylic acid). Poly(ethylene-*co*-vinyl acetate) copolymers have higher gloss and are more flexible than low-density PE (LDPE),[2] making them preferable to LDPE for film applications. Poly(ethylene-*co*-vinyl acetate) is a biocompatible copolymer that has been used as the matrix for controlled drug release devices.[3,4] Poly(ethylene-*co*-methyl acrylate) copolymers have elastomeric properties and they possess excellent temperature and chemical resistance.[2] Poly(ethylene-*co*-acrylic acid) copolymers have very good adhesion to metalized film, paper, and foil, which makes them excellent as packaging materials and films.[2] Maintaining a single phase in the reactor is significantly more challenging with ethylene-based copolymers since nonpolar ethylene repeat units can be copolymerized with acids, acrylates, and acetates which means that functionalized branch points are incorporated in the backbone and chemical composition distribution can have a significant effect on phase behavior. Consider that it takes on the order of seconds to form a high molecular weight ethylene-based copolymer yet the copolymer needs to remain in solution during and after the polymerization process for perhaps minutes before purposefully being precipitated from solution. It is apparent that for some fraction of reactor residence time ethylene, comonomer, and copolymer species are all present in the solution. With certain copolymers it may be necessary to add a cosolvent to maintain a single phase during the isobaric polymerization process. Hence, the range of variables has now expanded with the addition of a comonomer or a cosolvent to the solution. Included in this review are phase behavior studies on ternary mixtures consisting of a polymer, an SCF solvent, and a cosolvent.

By themselves, experimental polymer−SCF data are used as a basis for designing polymerization, separation, and recycle processes for polymers and copolymers. For example, high-pressure phase behavior data are useful for identifying an SCF solvent for fractionation of polymers and copolymers by both molecular weight and backbone composition. Information on the molecular weight and chemical composition polydispersity provides a means to determine the validity of the assumptions used in reactor simulation studies (e.g., is the reactor well stirred, is it isothermal, is there hold-up in the reactor, etc.). These data can also be used to assess the reliability of the various kinetic rate constants used to model the reaction. Likewise, phase behavior data provides guidance in choosing a particular solvent for a polymer purification process. For example, to design a process for removing residual solvent, monomer, spent catalyst, and other low molecular weight components, it is necessary to know the operating temperatures and pressures where these components preferentially dissolve relative to the polymer. Purity issues may be especially important when dealing with fluorocopolymers since the removal of "impurities" is essential if these polymers are to be used in the high-tech, medical, and electronic industries.

II. Molecular Thermodynamics of Polymer–SCF Mixtures

The principles of molecular thermodynamics provide the vehicle for connecting classical thermodynamics with the physicochemical properties of the components in solution.[5] A molecular thermodynamics approach coupled with an experimental protocol in which solvent and solvent properties are varied systematically elucidates the underlying chemical features of the components that fix the conditions needed to dissolve a polymer in an SCF solvent. This type of molecularly directed experimental approach provides the insight needed by polymer chemists to design polymers and copolymers that are miscible in SCF solvents at low pressures. In addition, it provides a rational methodology for choosing cosolvents to reduce operating pressures and temperatures needed to obtain a single phase.

To form a stable polymer−SCF solvent solution at a given temperature and pressure, the Gibbs free energy must be negative and at a minimum.[5] The Gibbs free energy of mixing is

$$\Delta G_{\mathrm{mix}} = \Delta H_{\mathrm{mix}} - T\Delta S_{\mathrm{mix}} \qquad (1)$$

where ΔH_{mix} and ΔS_{mix} are the change of enthalpy and entropy, respectively, on mixing. Enthalpic interactions depend predominately on solution density and on polymer segment−segment, solvent−solvent, and polymer segment−solvent interaction energies. ΔS_{mix} depends on both the combinatorial entropy of mixing and the noncombinatorial contribution associated with the volume change on mixing, a so-called equation of state effect.[6] It is reasonable to assume that the combinatorial entropy of mixing a polymer with an SCF solvent should not vary significantly with temperature and pressure near the conditions where the polymer dissolves in solution as long as the solvent density does not change dramatically. The combinatorial entropy always promotes the mixing of a polymer with a solvent. Although it is not possible to rigorously decouple the impact of energetic and entropic contributions to the Gibbs free energy of mixing, it is possible to design phase behavior experiments that magnify or attenuate the impact of energetic relative to entropic contributions. For those situations, the principles of molecular thermodynamics provide a means for quantifying the interactions that govern the phase behavior of polymer−SCF mixtures.

For a dense SCF solution, ΔH_{mix} is expected to be approximately equal to the change in internal energy on mixing, ΔU_{mix}. The scaling of the solution energetics with density, assuming pairwise additivity, is shown in the following expression for the internal energy of an isotropic, homogeneous mixture relative to an ideal gas mixture:[7]

$$\Delta U_{\mathrm{mix}} \approx \frac{2\pi\rho(P,T)}{kT} \sum_{i,j} x_i x_j \int \Gamma_{ij}(r,T)\, g_{ij}(r,\rho,T)\, r^2\, \mathrm{d}r \qquad (2)$$

where x_i and x_j are mole fractions of components i and j, respectively, $\Gamma_{ij}(r,T)$ is the intermolecular pair-potential energy of the solvent and the polymer segments, $g(r,\rho,T)$ is the radial distribution function, r is the distance between molecules, $\rho(P,T)$ is the solution density, and k is the Boltzmann constant. Imbedded in eq 2 is the radial distribution function that describes the spatial positioning of molecules or segments of molecules with respect to one another. It is in this spatial description of the solution that the connectivity of the segments in the backbone of the polymer chain precludes the possibility of rigorously decoupling energetics from chain conformation in solution, i.e., the solution of segments is not random. Nevertheless, important generalities can still be gleaned from this approach. For example, given that the internal energy of the mixture is roughly proportional to density, the solubility of a polymer is expected to improve by increasing the system pressure or using a denser SCF solvent. However, the polymer will dissolve only if the energetics of polymer segment−solvent interactions outweigh polymer segment−segment and solvent−solvent interactions. In other words, the integral in eq 2 cannot be ignored completely. Stated differently, for certain polymer−SCF solvent mixtures, hydrostatic pressure alone will not overcome a mismatch in energetics between the components in solution. The balance of such interactions in solution is described by the interchange energy, ω, defined as

$$\omega = z[\Gamma_{ij}(r,T) - {}^1/_2(\Gamma_{ii}(r,T) + \Gamma_{jj}(r,T))] \qquad (3)$$

where z is the coordination number, or number of different pairs in solution.[5] An approximate form of

the attractive part of the intermolecular potential energy, $\Gamma_{ij}(r,T)$, for small molecule mixtures is

$$\Gamma_{ij}(r,T) \approx -\left[C_1\frac{\alpha_i\alpha_j}{r^6} + C_2\frac{\mu_i^2\mu_j^2}{r^6\,kT} + C_3\frac{\mu_i^2Q_j^2}{r^8\,kT} + C_4\frac{\mu_j^2Q_i^2}{r^8\,kT} + C_5\frac{Q_i^2Q_j^2}{r^{10}\,kT} + \text{complex formation}\right] \quad (4)$$

where α is the polarizability, μ is the dipole moment, Q is the quadrupole moment, and C_{1-5} are constants.[5]

Equation 4 serves only as a guide for qualitatively evaluating the effects of intermolecular interactions on polymer−solvent phase behavior. Induction interactions are not shown in eq 4 since their contribution to the potential energy tends to be much smaller than dispersion and polar interactions.[5] Equation 4 is not expected to describe rigorously the interaction of a polymer segment with another segment or with the solvent since segmental motion is constrained by chain connectivity. Note that nonpolar dispersion interactions, the first term in eq 4, depend only on the polarizability of the components in solution and not on temperature. Therefore, the pressures needed to dissolve a nonpolar polymer in a nonpolar SCF solvent should decrease as the polarizability of the solvent increases—a trend expected for SCF solvents from the same chemical family. SCF solvents consisting of heteroatoms have bond dipoles due to the difference in electron affinity of the various atoms that results in a dipole moment or, higher order polar moments, such as a quadrupole moment. The leading terms in the expansions for the potential energy of dipolar and quadrupolar interactions in eq 4 are inversely proportional to temperature. At elevated temperatures thermal energy disrupts the configurational alignment of the polar moments of the molecules so that they behave as if they were nonpolar. Hence, it may be possible to dissolve a nonpolar polymer in a polar SCF solvent, such as dimethyl ether ($D = 1.3$), if the temperature is high enough to diminish ether−ether polar interactions that are quite significant at lower temperatures. Hydrostatic pressure can now be applied to the solution to obtain a single phase at a suitable SCF density. Specific interactions such as complex formation or hydrogen bonding can also contribute to the attractive pair potential energy. Once again the strength of these "directional" interactions are also very temperature sensitive. Equations 2−4 describe how the solvent quality of a supercritical fluid can be tuned with changes in pressure as well as temperature, a degree of flexibility not available with liquid solvents.[8]

Table 1 lists the properties for a variety of different SCF solvents. Notice that the polarizability within a given chemical family increases with increasing molecular size of the solvent. Although the critical properties of the alkenes do not differ significantly from those of the alkanes, the double bond in the alkenes provides a quadrupole moment and a potential site for π complexing. Examples are provided in this review where the presence of the double bond can shift the binodal curve by 10 to 100 degrees. The properties of the fluorocarbon solvents are utilized in the section describing fluoropolymer−SCF solvent phase behavior. Finally, note that the polarizability of CO_2 is similar to that of perfluoromethane, fluoroform, and dihydrodifluoromethane. In fact, it is also very close to that of methane, a very weak SCF solvent. Insight into the effect of SCF solvent properties on the phase behavior will be described by comparing the solubility characteristics of a single polymer or copolymer in a series of SCF solvents.

Table 1. Physical Properties of Supercritical Fluid Solvents[208,209a]

solvent	T_c (°C)	P_c (bar)	$\alpha \times 10^{25}$ (cm^3)	μ (D)
ethane	32.3	48.8	45.0	0.0
propane	96.7	42.5	62.9	0.1
butane	152.1	38.0	81.4	0.0
hexane	234.1	29.7	118.3	0.0
ethylene	9.2	50.4	42.3	0.0
propylene	91.9	46.2	62.6	0.4
1-butene	146.5	39.7	82.4	0.3
2-*trans*-butene	155.5	39.9	84.9	0.0
dimethyl ether	126.9	52.4	51.6	1.3
tetrafluoromethane	−45.6	37.4	28.6	0.0
hexafluoroethane	19.7	29.8	47.6	0.0
octafluoropropane	71.9	26.8	66.7	0.0
hexafluoropropylene	94.0	29.0	60.4	0.4
difluoromethane	78.5	53.4	24.8	2.0
trifluoromethane	26.2	48.6	26.5	1.6
chlorotrifluoromethane	28.8	38.7	45.8	0.5
chlorodifluoromethane	96.2	49.7	44.4	1.4
difluoroethane	113.1	45.2	41.5	2.3
tetrafluoroethane	101.1	40.6	43.8	2.1
pentafluoroethane	66.3	36.3	45.6	?
sulfur hexafluoride	45.4	37.6	54.6	0.0
carbon dioxide	31.0	73.8	27.6	0.0

[a] The polarizability, α, is calculated with the method of Miller and Savchik.[210] The dipole moments, μ, of C_3F_8 and C_3F_6 are assumed to be equal to those of propane and propylene, respectively. C_2F_6 has a quadrupole moment of (-0.65×10^{-26}) erg$^{1/2}$ cm$^{5/2}$ and carbon dioxide has a quadrupole moment of (-4.3×10^{-26}) erg$^{1/2}$ cm$^{5/2}$.

It is important to note that configurational interactions such as dipolar and quadrupolar moments scale differently with respect to volume. The strength of dipole interactions scale inversely with the square root of the molar volume, v, where $\mu_i^* = \mu_i/v_i^{1/2}$ whereas the strength of quadrupole interactions scale inversely with the molar volume to the $^5/_6$ power, $Q_i^* = Q_i/v_i^{5/6}$.[5] Recognition of this scaling becomes important when interpreting solubility data of polymers from the same chemical family dissolved in a given SCF solvent.

III. Phase Diagrams of Polymer–SCF Mixtures

Although there are countless polymer−SCF solvent binary mixtures possible, fortunately there are essentially only two types of phase diagrams that describe the characteristic phase behavior observed for these mixtures. These polymer−SCF solvent phase diagrams are best described by comparison to the diagrams for binary mixtures of low molecular weight components.[8] Throughout this review the cataloging scheme adapted by McHugh and Krukonis[8] is utilized to classify different types of phase diagrams. The reader is directed to the work

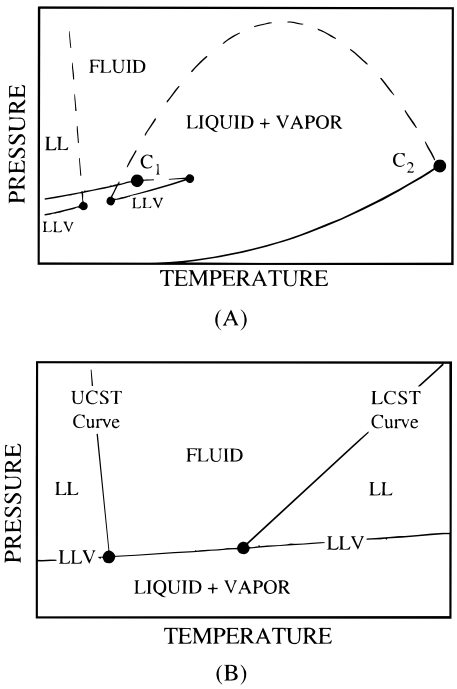

Figure 1. Schematic pressure−temperature phase diagrams for binary mixtures of low molecular weight solvent with a low molecular weight solute (A) and with a high molecular weight polymer (B). Points C_1 and C_2 represent the critical points of components 1 and 2. LL represents a liquid−liquid region, LV represents a liquid−vapor region, and LLV represents a liquid−liquid−vapor line.[8]

of Scott and van Konynenburg[9,10] for an alternative approach to cataloging phase diagrams. Figure 1A shows a generalized $P-T$ diagram of type III phase behavior for binary mixtures of small molecules. In Figure 1A the two pure-component critical points are labeled C_1 and C_2, where component 1 represents the more volatile component and component 2 represents the less volatile component. In Figure 1A the dashed line with a steep, negative slope at low temperatures is an upper-critical-solution-temperature (UCST) curve which describes the pressure dependency of a liquid+liquid (LL) → liquid transition as the temperature is isobarically increased. Enthalpic interactions between the two components in solution typically govern the location of the UCST curve.[11] Since the temperatures are fairly low and the phases in question are dense liquids, it is not too surprising that this UCST curve is relatively insensitive to pressure. Not shown in this diagram are the compositions of the mixtures at each point along the UCST curve. It should also be noted that for certain mixtures the UCST curve does not occur. This type of phase behavior is termed type V in both the Scott and van Konynenburg[9,10] and the McHugh and Krukonis[8] cataloging schemes.

The dashed curve starting at C_2 in Figure 1A is a slightly different type of critical solution temperature curve; it is a critical-mixture curve that represents the locus of liquid−vapor critical points for mixtures of differing composition. As the temperature is lowered the critical-mixture curve exhibits a maximum in pressure and eventually intersects a three phase, liquid + liquid + vapor (LLV) line near C_1. As this critical-mixture curve approaches C_1 it takes on the characteristics of a lower-critical-solution-temperature (LCST) curve which describes the pressure dependency of a liquid+vapor (LV) → liquid transition as the temperature is isobarically decreased. The location of the LCST curve is generally, but not always, controlled by the free volume difference between each component in solution. As the temperature increases one of the components exhibits a much greater volume expansion relative to the other component (i.e., the so-called free volume difference[6]) leading to a large negative entropy of mixing that eventually induces the solution to phase separate. The difference in free volume decreases with increasing pressure, which then requires higher temperatures for the entropy of mixing to dominate the enthalpy of mixing and induce the solution to phase separate. The phase behavior shown in Figure 1A is typical for small molecule mixtures in which there is significant size difference between the two species, such as methane and hexane, or the intermolecular potential functions of the two species differs considerably, such as ethane and ethanol.[12]

Type III phase behavior for small molecules is extrapolated to that expected for a polymer−solvent mixture in Figure 1B. It is possible to induce the single fluid phase to split into two phases by isobarically lowering the temperature and crossing the UCST curve or increasing the temperature and crossing the LCST curve. At high temperatures, the LCST curve does not reach a distinct end point since polymers do not have critical points. Also, the LLV lines for a polymer−solvent mixture essentially superpose onto the vapor pressure curve of the solvent. Note that the LCST curve is more sensitive to pressure since it is typically at temperatures in the vicinity of the solvent critical temperature where the solvent is highly compressible. Hence, increased hydrostatic pressure decreases the molar volume of the solvent and reduces the free volume difference between the solvent and polymer. Numerous polymer−solvent phase behavior studies are available in the literature demonstrating the effect of solvent quality on the location of the LCST for type III mixtures.[11−19]

It is important to be aware that the binary polymer−solvent diagram in Figure 1B actually represents multicomponent phase behavior since all polymers have a molecular weight polydispersity fixed by the synthesis technique used to make the polymer. For polymer−solvent mixtures the transition from a transparent single phase to an opaque two-phase system at either the UCST or LCST is termed a cloud-point which is the multicomponent analogue of a binodal point.[20−26] The maximum of the isothermal P−x loop measured as a cloud-point does not coincide with the mixture-critical point[12] as it would for a binary mixture of monodisperse components. The critical point is shifted to higher overall polymer concentration and lower pressure than the maximum in the P−x loop. For polydisperse systems the composition of the two coexisting phases at each pressure of a P−x loop is not defined by a horizontal line as it would be for a true binary mixture since each of the coexisting phases contain oligomers with

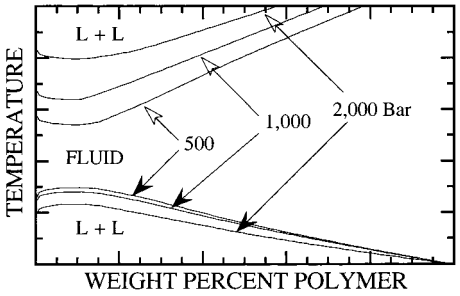

Figure 2. Schematic representation of the impact of pressure on the UCST (maximum) and LCST (minimum) temperature for a polymer−solvent mixture. The curves are relatively flat at the maximum (minimum) in the range of 3−15 wt % polymer. L + L represents a two-phase region.

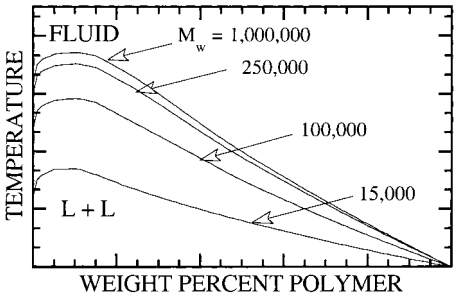

Figure 3. Schematic representation of the influence of polymer molecular weight on the phase behavior of a polymer−SCF solvent mixture at an arbitrary pressure. The same type of behavior is expected if pressure is substituted for the temperature axis.

different molecular weights, which leads to a partial fractionation of the parent polymer. A so-called "shadow curve" is determined by measuring the composition of the phase that precipitates at the cloud-point. The true critical point of the polydisperse polymer−solvent mixture is the intersection of the shadow and cloud-point curves which also occurs at the intersection of the spinodal and binodal curves. Although spinodal curves exist for both polydisperse and monodisperse polymer−solvent mixtures, these curves are not reported in this review since few of them have been measured at high pressures. Polymer molecular weight polydispersity will be ignored in this review although it is noted that the cloud-point transition does occur over a pressure interval that is greater than that observed for a mixture of monodisperse components. In practice the cloud-point pressure transition is usually on the order of 5−7 bar as long as the polymer has a molecular weight polydispersity of less than ∼3.0. If the molecular-weight polydispersity of the polymer is large the LLV line shown schematically in Figure 1A actually represents the highest pressure at which three phases exist.

Another distinction between small molecule and polymer−SCF solvent behavior shown in Figure 1 is that the curves in the small molecule diagram are the locus of points for mixtures with differing compositions and the curves in polymer−SCF solvent diagram are at essentially one fixed composition. Figure 2 shows that the maximum/minimum temperature of the temperature−composition loop for a polymer−SCF solution is relatively insensitive to composition in the range of 3−15 wt % polymer. The pressure maximum/minimum of a pressure−composition (P−x) loop is also insensitive to composition. This means that a single cloud-point curve in the composition range of 3−15 wt % polymer defines the maximum pressure of the P−T trace of the P−x loops—that is, cloud-point curves with compositions between 3 and 15 wt % essentially superpose.[14,27−29] The reader is cautioned, however, that the pressure maximum of the P−x loop does shift to lower and lower polymer concentrations as the molecular weight becomes very high and as the molecular weight polydispersity becomes greater than ∼3.0. In these instances, a cloud-point curve at a fixed polymer concentration between 3 and 15 wt % may not represent the maximum pressure needed to maintain a single phase at all concentrations.[22]

Fortunately, the effect of polymer molecular weight on the phase behavior in an SCF solvent is analogous to that observed in a liquid solvent. Figure 3 shows a schematic representation of the diminishing effect of polymer molecular weight on the UCST in a liquid solvent for a molecular weight greater than ∼100 000. The same diminishing effect is observed with polymer−SCF mixtures for both the UCST and LCST curves which suggests that experiments should be conducted with molecular weights near 100 000. If molecular weight effects are a concern, it is possible to obtain a straight-line extrapolation of the effect of molecular weight by plotting the inverse UCST temperature versus the inverse square root of molecular weight from several cloud-point curves.

When the two components in solution differ considerably with respect to their molecular size and/or intermolecular potentials, such as CO_2 and hexadecane, the UCST curve shifts to higher temperatures and merges with the LCST curve to give type IV behavior[8] shown in Figure 4A. The dashed curve starting at C_2 in Figure 4A no longer intersects an LLV line but rather it exhibits a minimum in pressure and then exhibits a steep negative slope reminiscent of the UCST curve. Type IV phase behavior is extended to a polymer−solvent mixture in Figure 4B. For the polymer−solvent system, the pressures of the cloud-point curve are relatively constant at high temperatures, and rise sharply with decreasing temperature. Many polymer−SCF solvent mixtures exhibit this type of phase behavior especially if one of the two components is nonpolar and the other component is polar.

Figure 5 shows that some of the fluid-phase behavior can be obscured if the polymer is semicrystalline. Polymer solubility is extremely low at temperatures less than the solidification temperature of the polymer, which depends on solvent quality and hydrostatic pressure. For all practical purposes the solubility is so low at temperatures below the solidification boundary that polymer fractionation or extraction processes would not be operated in this regime. It should be recognized that most of the experimental data presented in this review are obtained at a fixed temperature with changes in pressure. As a general observation, the solution remains very dark at temperatures below the

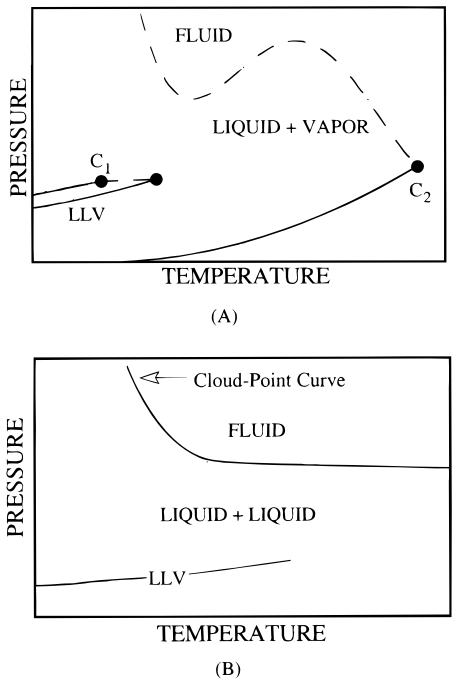

Figure 4. Schematic pressure−temperature phase diagrams for binary mixtures of a low molecular weight solvent with a low molecular weight solute (A) and with a high molecular weight polymer (B).[8] The notation is the same as that in Figure 1.

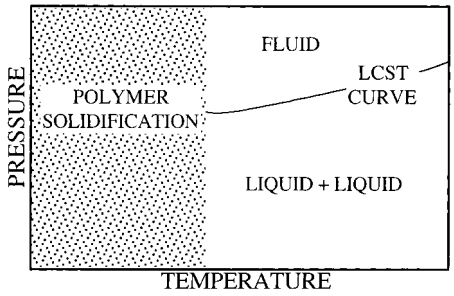

Figure 5. Effect of polymer solidification on the phase behavior of polymer−SCF mixtures.

"crystallization" or "solidification" boundary regardless of the system pressure. To ascertain whether this region represents solid + fluid or liquid + fluid equilibria the temperature is increased rapidly while maintaining the pressure constant. If the solution becomes clear once the temperature increases one-to-two degrees, a liquid + fluid region exists at the lower temperature. However, if it takes 10−20 °C to make the solution clear a solid + fluid region exists at the lower temperature.

It should now be apparent that a very good representation of polymer−SCF phase behavior can be obtained with a single cloud-point curve at a fixed composition and molecular weight. The experimental technique used to obtain a cloud-point curve is mentioned briefly before proceeding to examples of polymer−SCF phase behavior.[8,30,31] Figure 6 shows a diagram of a high-pressure cell used to obtain cloud-point data. A known amount of polymer is loaded into the cell along with a known amount of SCF. It is much more efficient to hold the system temperature constant and vary the pressure than to vary the temperature since the thermal mass of the

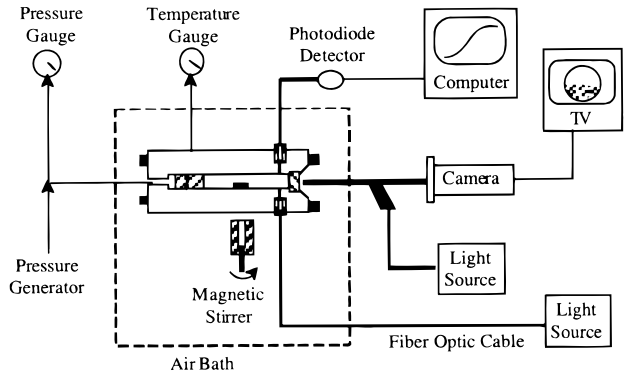

Figure 6. Schematic diagram of the experimental equipment used to obtain polymer−SCF cloud-points.[8]

cell is very large. The cell is fitted with a sapphire window and a fiber optic light source and detector so that the turbidity of the solution can be observed both visually and photoelectrically as the pressure is changed. To obtain a single phase the solution is heated, pressurized, and well stirred. Once in solution, the pressure is slowly decreased until the solution becomes hazy. The cloud-point is determined when the stir bar is no longer visible, similar to the technique used by Cowie and McEwan,[19] or when the light transmitted through the solution decreases to 10% of its original value.[32] Usually both methods are in good agreement as long as the polymer has a molecular weight polydispersity of less than ~3.0. However, visual turbidity measurements are not reliable when working with copolymers that have broad chemical composition distributions. For example, McHugh and DiNoia report that the cloud-point for a solution with 5 wt % poly(vinylidene fluoride-*co*-4.5 mol % hexafluoropropylene) in difluoromethane at 213 °C is 1170 bar as measured visually and is 910 bar as measured by fiber optics.[33] This result, and similar results reported in the literature,[34] reinforce the need to fractionate copolymers with respect to backbone composition before measuring the phase behavior. With the apparatus shown in Figure 6 it is not possible to obtain cloud-point data for solutions with greater than ~25 wt % polymer since the stir bar cannot be dislodged from the polymer-rich phase.

A wide range of polymer−SCF phase behavior studies is described in the following sections. Table 3 provides a compilation of polymer−SCF phase behavior studies found in the literature. Likewise, Table 4 provides a compilation of polymer−CO_2 studies found in the literature.

IV. Homopolymer–SCF Phase Behavior

1. SCF Solvent Quality

The phase behavior of the polyethylene−ethylene system appears as perhaps one of the earliest polymer−SCF phase behavior studies reported in the technical literature likely due to its commercial interest.[35,36] Since those early studies, other polyethylene−SCF phase behavior studies appeared[37] perhaps because now it is possible to synthesize polyethylene with a variety of different chain archi-

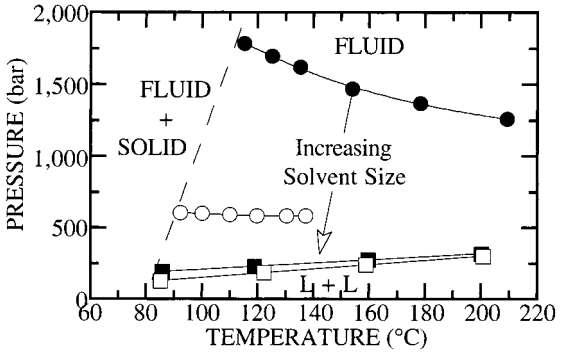

Figure 7. Impact of solvent quality on polyethylene (M_w = 108 000, M_w/M_n = 3.0, T_m = 113 °C) solubility at 5 wt % in normal alkenes (closed circles, ethylene; open circles, propylene; closed squares, 1-butene; open squares, 2-butene).[39,41]

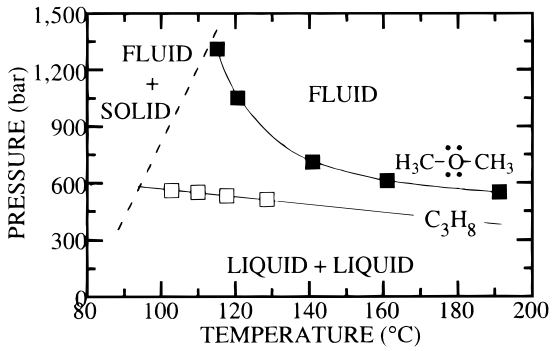

Figure 8. Phase behavior of 5 wt % polyethylene (M_w = 108 000, M_w/M_n = 3.0, T_m = 113 °C) in propane[44] and in dimethyl ether.[28]

tectures that lend themselves to fundamental studies.[38] The phase behavior of nonpolar polyethylene in a variety of different solvents is considered in this section. Figure 7 shows the phase behavior of 5 wt % polyethylene (LDPE, M_w = 108 900; M_w/M_n = 3.0; T_{melt} = 113 °C) in ethylene,[39] propylene,[39] 1-butene,[40] and 2-*trans*-butene.[41] Several trends are evident in this figure. Note that the pressures needed to obtain a single phase decrease significantly with increasing size of the solvent. For example, at 120 °C it takes 1600 bar to obtain a single phase in ethylene. With propylene the cloud-point pressure decreases 1000 bar to ~600 bar and with the two slightly different butenes the pressure drops another 400 bar to ~200 bar. The increase in SCF solvent quality follows directly from the increase in polarizability with molecular size (see Table 1). However the reduction in cloud-point pressure is less dramatic as the size of the solvent increases, or, stated differently, as the solvent quality increases. This diminishing returns of solvent quality with increasing solvent size is a recurring theme that suggests that the largest changes in phase behavior will be observed with much smaller hydrocarbon solvents.

In 1963, Ehrlich and Kurpen[1,42] showed that polyethylene−alkane mixtures exhibit very similar trends to those found with the alkene solvents shown in Figure 7. The polyethylene−propane and polyethylene−butane curves essentially superpose onto the propylene and butene curves but the ethane curve is more than 400 bar lower pressures than the ethylene curve.[1,39−41] The reason for the large disparity for the C2 hydrocarbon case is that the double bond of ethylene makes it a strong quadrupolar solvent that favors ethylene−ethylene interactions relative to nonpolar PE−ethylene interactions. As the system temperature increases the PE−ethylene cloud-point curve drops in pressure as quadrupolar ethylene−ethylene interactions decrease as described in eq 4. The location of the ethane and ethylene curves is intimately related to the balance of polymer segment−solvent energetic interactions since these two solvents have similar densities at their respective cloud-point conditions.

The double bond, quadrupolar effect is attenuated in propylene and butene because the quadrupole moment is distributed over a larger molar volume reducing its effectiveness by a factor of molar volume to the $-5/6$ power. Whaley and co-workers[43] show that there is a small but discernible difference in the LCST curve of atactic polypropylene in propane and propylene. The propylene curve is ~30 bar higher in pressure than the propane curve. The phase behavior of PE in 1-butene and 2-*trans*-butene also exhibit some subtle effects as a consequence of polar butene−butene interactions. At temperatures near 80 °C the PE−1-butene curve is approximately 50 bar greater in pressures than the 2-*trans*-butene curve since 2-*trans*-butene is slightly less polar than 1-butene due to symmetry. The difference between the two PE−butene curves is noticeable at low temperatures because PE is very nonpolar which makes the interchange energy very sensitive to any intermolecular potential mismatch between the components in solution. The difference in cloud-point pressures of these two butene curves decreases with increasing temperature. Solvent density is not a major factor in this instance since 1-butene and 2-*trans*-butene have similar densities and critical properties. The impact of an interchange energy that favors solvent−solvent interactions is apparent in the comparison of the cloud-point curves in Figure 8 for PE in propane[44] and PE in dimethyl ether (DME)[28] which has a dipole moment of 1.3 D. The DME curve changes slope and increases in pressure as the temperature is lowered to the region where DME−DME polar interactions are favored. As a general rule, the cloud-point curve will eventually exhibit a negative slope with decreasing temperature for mixtures containing one component that is polar and the other component that is nonpolar.

2. Polymer Molecular Weight

The effect of polymer molecular weight on the phase behavior is shown in Figure 9 for the polyisobutylene−butane system.[17] It is readily apparent in this case that the location of the LCST curve becomes less sensitive to polymer molecular weight when the molecular weight exceeds a few hundred thousand. The effect of molecular weight on the phase behavior of the PE−ethylene system also becomes far less pronounced as the molecular weight increases above ~100 000.[22,45−47] For example, at 150 °C the cloud-point pressure increases by 300 bar for a linear PE as the M_w increases from 3700 to 9200; it

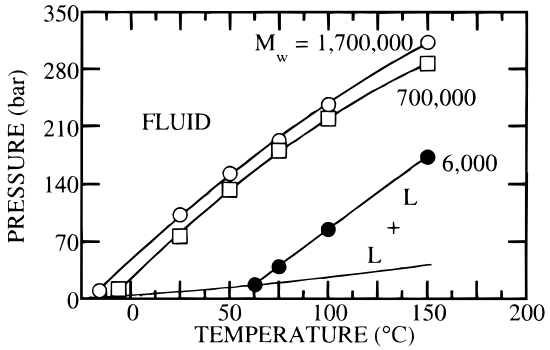

Figure 9. Effect of polyisobutylene molecular weight on the location of the cloud-point curve in butane.[17] The polymer concentration is ~5 wt % in each case.

increases again by 300 bar as the M_w increases from 9200 to 55 000; and it only increases by 100 bar as the M_w increases from 55 000 to 118 000.[22]

Hamada et al. also show that the LCST for the PE−pentane system only decreases from 160 to 149 °C as the M_w is increased from 34 900 to 97 200, it decreases another 4 °C as the molecular weight is increased further to 204 900, and it only decreases four more degrees as the molecular weight is increased once again to 442 100.[48] Kiran and co-workers also show quite convincingly that the cloud-point pressures of PE−pentane and poly(ethylene−butane) mixtures are insensitive to molecular weight once the M_w is increased above 108 000.[49−52]

3. Melting Point Depression

It is interesting to note the impact of solvent quality on the solidification temperature of the semicrystalline PE (~36% crystallinity as measured by DSC and referenced to a pure PE crystal) used in the previous discussion. Figure 7 shows that the melting point of PE increases from 113 °C at one bar to 115 °C at 1600 bar in ethylene, it decreases to 90 °C at 600 bar in propylene, and it decreases further still to ~80 °C at 400 bar in butene. The solidification temperature is the result of two competing effects, hydrostatic pressure which raises the melting point of PE at rate of 0.01 °C/bar and the solubility of the SCF solvent in the polymer-rich liquid phase which depresses the melting point at a rate proportional to the SCF solvent concentration. For example, PE should melt at 129 °C at 1600 bar, but the melting point actually occurs at 115 °C due to the solubility of ethylene in the PE-rich phase.

The melting point depression of a crystalline polymer can have significant ramifications for processing these materials in SCF solvents. For example, Conway et al.,[53] show that the melting point of a low molecular weight, semicrystalline polyester can be reduced from 105 °C to 75 °C in pure CO_2, to 65 °C in CO_2 with 11 wt % acetone, and to 35 °C in CO_2 with 11 wt % ethanol. Even though it is not possible to dissolve this polyester in neat CO_2, it is possible to suppress the crystallization of the polyester and to obtain the wetting characteristics needed to coat particles at low operating temperatures and pressures. When the pressure is released, the polyester coating crystallizes and ensures that the particles do not agglomerate as long as they remain at temperatures below 105 °C, the normal melting point of the polyester.

4. Polymer Backbone Branching

Chain branching is an important variable that can affect polymer solubility in subtle ways. Branching increases the free volume of the polymer, which makes it easier to dissolve in an SCF solvent. Also, branching reduces the intermolecular interactions between polymer segments that would arise due to short-range molecular orientation offered by a high content of linear segments without pendant groups.[54] The impact of chain branching is most noticeable if the molecular weight polydispersity is minimized. Klientjens and co-workers[55] show that for PE−diphenyl ether mixtures, the two-phase region with a linear PE is shifted slightly more than 10 °C higher temperature compared with that of a branched PE with virtually the same M_w and M_n. The same effect of branching occurs with an SCF solvent although the effect is exacerbated since most SCF solvents are much weaker compared to liquid diphenyl ether.

Krukonis and co-workers investigated the impact of chain branching on the phase behavior of linear low-density PE (LLDPE) in supercritical ethane and propane.[56] The LLDPE was fractionated twice—first by molecular weight and then the fractions were again fractionated but now with respect to chain branching.[57] The LLDPE is actually a copolymer of ethylene with low amounts of octene incorporated into the backbone during the polymerization using a Ziegler−Natta catalyst that results in branches that are C6 hydrocarbon chains. For this study, fraction PE_{40B} (M_w = 50 100; M_w/M_n = 1.27; ΔH^{fus} = 108 J/g) is fractionated again, but now by backbone structure. Fractions PE_{36} (ΔH^{fus} = 97 J/g), PE_{49} (ΔH^{fus} = 133 J/g), and PE_{57} (ΔH^{fus} = 154 J/g) each have the same molecular weight characteristics as PE_{40B}, but different amounts of chain branching as implied by the heats of fusion. (Here the x subscript on PE_x represents the percent crystallinity relative to a perfect PE crystal.) These fractions were used in a phase behavior study with ethane and propane. The solvents in this case were chosen to match as closely as possible the intermolecular potential of the solvent with that of a repeat unit of LLDPE. Figure 10 shows that the cloud-point curves for PE_{36}, PE_{49}, and PE_{57} in ethane increase in pressure with increasing crystallinity or, conversely, with decreasing chain branching.[56] The cloud-point pressures for the PE_{40B}−ethane system are slightly greater than those for the PE_{49}−ethane system since PE_{40B} contains a finite amount of polymer with a low branch density. The difference in cloud-point pressures for the PE_{57}−ethane and the PE_{36}−ethane systems is ~140 bar. In propane the difference in cloud-point pressures for the PE_{57}−propane and the PE_{36}−propane systems is approximately half that found with SCF ethane. Again we see the principle that the weaker of the two solvents magnifies the effect of the polymer properties on the phase behavior. The authors also note that the effect of branching is obscured if there is a large

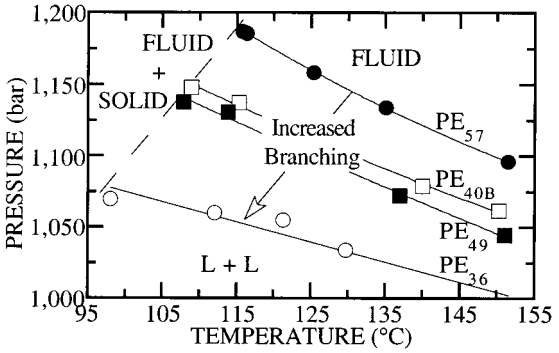

Figure 10. Effect of backbone structure on the cloud-point behavior of 5 wt % PE in ethane.[56] The subscript *x* on PE_x represents the percent crystallinity of the polymer. PE_{40B} is only fractionated once with respect to molecular weight while the other three PE_x polymers are fractionated first with respect to molecular weight and then with respect to ethyl side-chain branches.

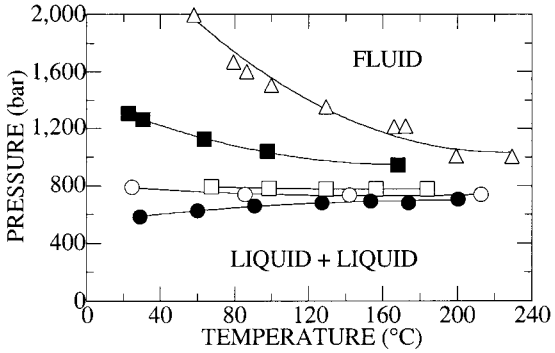

Figure 11. Effect of alkyl tail length on the phase behavior of 5 wt % poly(acrylates) in ethylene.[61] The open triangles are data for poly(ethyl acrylate), the closed squares are data for poly(propyl acrylate), the open squares are data for poly(butyl acrylate), the open circles are data for poly(octadecyl acrylate), and the closed circles are data for poly(ethyl hexyl acrylate).

molecular weight polydispersity or if there is a large branching polydispersity.[56]

Chen and Radosz show that side-chain branching has a significant effect on the pressures needed to solubilize linear poly(ethylene-*co*-1-butene) (PEB) in supercritical propane.[58,59] The copolymers used in this study were synthesized in a controlled manner to produce PEB copolymers with molecular weights close to 100 000, molecular weight polydispersities near 1.1, and fixed amounts of ethyl branches. At a fixed temperature of 160 °C the cloud-point decreases from slightly greater than 600 bar for PE to 300 bar for PEB with 39.5 ethyl branches per 100 carbons. The difference between linear and branched PEB cloud-point pressures increases with decreasing temperature which reflects the change in the phase behavior from type IV for highly linear PEBs to type III as the branch content approaches that in pure poly(butene). Ehrlich and co-workers have also verified these results.[60] de Loos and co-workers have also demonstrated that branched PE dissolves at a lower pressure in ethylene compared to more linear PE[29] consistent with earlier work published in the literature.[45]

5. Polymer Chemical Architecture

The phase behavior of vinyl polymers in hydrocarbon SCF solvents is very sensitive to the backbone chemical architecture. For example, Lora et al.[61] show that the conditions needed to obtain a single phase for poly(acrylates) in ethylene varies in an nonlinear manner with the length of the alkyl tail on the acrylate. Figure 11 shows the phase behavior of poly(ethyl acrylate) (PEA), poly(propyl acrylate) (PPA), poly(butyl acrylate) (PBA), poly(ethyl-hexyl acrylate) (PEHA), and poly(octadecyl acrylate) (PODA) in ethylene. The molecular weight characteristics of the poly(acrylates) are given in Table 2. Lora et al.[61] report that it is not possible to dissolve PMA in ethylene to pressures of 2500 bar and temperatures to 250 °C even though PMA has a very low weight average molecular weight. More than likely, PMA remains insoluble in ethylene due to methyl acrylate segment−segment polar interactions that are much stronger than acrylate segment−ethylene interactions. PEA dissolves in ethylene at pressures near 1200 bar and temperatures in excess of 150 °C. However, as the temperature decreases, the PEA−ethylene curve exhibits a gradual increase in pressure to 2200 bar at 50 °C which suggests that polar ethyl acrylate−ethyl acrylate interactions also gradually increase over this temperature range. As the length of the alkyl tail on the acrylate increases from methyl to ethyl the impact of the polar acrylate interactions decreases since dipolar interactions scale inversely with the square root of the molar volume and quadrupolar interactions scale inversely with the volume to the 5/6 power.[5] Figure 11 shows that it takes progressively less pressure to dissolve PPA, PBA, and PEHA compared to PEA. At high temperatures where configurational polar interactions are reduced, similar cloud-point pressures are observed for each of the poly(acrylates). At temperatures near 60 °C there is much greater difference in the location of each of the cloud-point curves. As the acrylate tail is increased from ethyl-hexyl to octadecyl, the cloud-point curve increases in pressure and falls virtually on top of the PBA−ethylene curve even though PODA has a smaller molecular weight than PBA. There is an optimum alkyl tail length that balances the acrylate−acrylate, ethylene−ethylene, and acrylate−ethylene energies of this system. In addition the free volume of the poly(acrylate) is expected to increase as the tail length of the acrylate group increases which makes it easier to dissolve the poly(acrylate) in highly expanded, supercritical ethylene. PODA should have a higher free volume than PEHA, but, the balance of PODA−ethylene interactions are probably less favorable than those of PEHA−ethylene since the polar character of the octadecyl acrylate is spread over such a large volume. This study rein-

Table 2. Molecular Weight Data for the Poly(alkyl acrylates) Shown in Figure 11

	M_w	M_w/M_n
poly(methyl acrylate) (PMA)	30 700	2.90
poly(ethyl acrylate) (PEA)	119 300	4.83
poly(propyl acrylate) (PPA)	140 000	3.78
poly(butyl acrylate) (PBA)	61 800	2.99
poly(ethylhexyl acrylate) (PEHA)	112 800	2.97
poly(octadecyl acrylate) (PODA)	23 300	1.79

forces the need to consider both energetic and entropic effects when interpreting the effect of chemical architecture on polymer−SCF phase behavior.

6. Effect of End Groups

Typically the effect of end groups on phase behavior is ignored for polymers with molecular weights in excess of ∼100 000. However, as with branching impact on phase behavior, end groups can have a significant effect on the phase behavior in certain situations. Krukonis and co-workers demonstrated the impact of hydroxyl end groups on the solubility of hydroxy-terminated poly(butadiene) (HTPB) with an M_n of 2960, an M_w of 6250, and a hydroxyl equivalent weight of 1256 (0.796 meq/g).[8] Carbon dioxide only dissolves ∼12% of the HTPB at pressures to 600 bar. Propane at 130 °C dissolves virtually all of the parent material at pressures less than 600 bar. Krukonis used propane to fractionate the HTPB and obtained fractions with M_ns ranging from 780 to 11 750 and M_w from 970 to 21 525. Most of the fractions had polydispersities of ∼1.2. However, the hydroxy equivalent weight was nonlinear with molecular weight especially in the fractions with-higher molecular weight.

7. Cosolvent/Antisolvent Effects

A cosolvent can greatly enhance polymer solubility in a given solvent due to several factors. If the solvent is highly expanded, the addition of a dense, liquid cosolvent reduces the free volume difference between the polymer and the solvent that results in a reduction in the pressure needed to obtain a single phase.[62] If the cosolvent provides favorable physical interactions, such as polar interactions, the region of miscibility should expand more than expected from just a density effect.[63] In the case where a polar cosolvent is used with a polar polymer, cloud-points monotonically decrease in pressure and temperature as long as the cosolvent does not form a complex with the polar repeat units in the polymer.[44,63,64] The cloud-point will decrease much more dramatically if the polar cosolvent can form a complex with the polymer since the interaction energy of complex formation, such as hydrogen bonding, is typically an order of magnitude greater than that expected from dispersion or polar interactions. Decoupling the effect of a cosolvent from that of hydrostatic pressure is sometimes complicated since increasing the system pressure also reduces the free volume difference between the solvent and the polymer and increases the probability of interaction between polymer, solvent, and cosolvent segments in solution.[64]

It is worthwhile to mention briefly some of the results from studies done with polar homopolymers in liquid cosolvent mixtures,[19,62,65−71] since there are direct corollaries to high-pressure polymer−SCF solvent phase behavior. For example, Wolf and Blaum[63] show that small amounts of 2-butanol reduce the UCST of the poly(methyl methacrylate) (PMMA)−chlorobutane system by as much as 70 °C as the 2-butanol hydrogen bonds to the basic acrylate

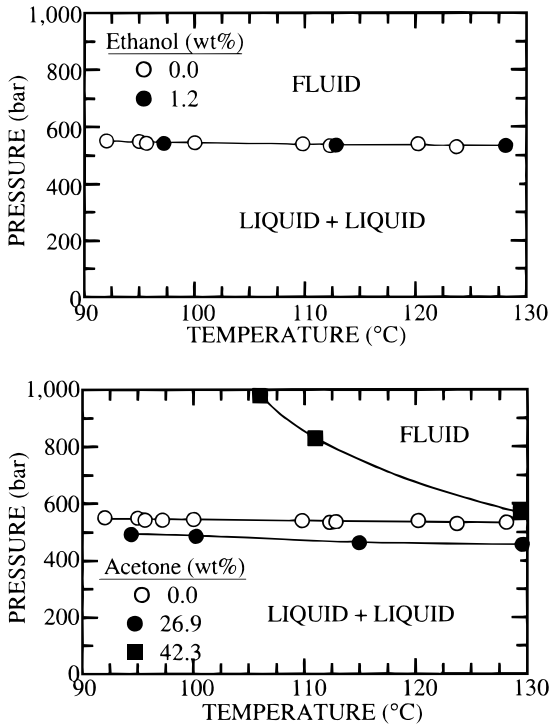

Figure 12. Effect of ethanol and acetone on the phase behavior of polyethylene in propane.[44] The polymer concentration is 5 wt %, and the polymer molecular weight characteristics are the same as those in Figure 7.

group in the backbone of the polymer. However, subsequent addition of butanol to the mixture causes an increase in the UCST. At low concentration, butanol hydrogen bonds with the acrylate groups, which promotes miscibility. However, once the acrylate groups are titrated with butanol, further increase in butanol concentration favors cosolvent−cosolvent hydrogen bonding that decreases the region of miscibility. Many authors report findings for other polymer−solvent−cosolvent systems that are consistent with this behavior.[19,62,65−70,72] More modest changes in solubility behavior are observed if a polar cosolvent is used that does not hydrogen bond. For example, when 4-heptanone is added to PMMA−chlorobutane mixtures, the UCST decreases monotonically with heptanone concentration over only a 10 °C range.[63]

Figure 12 shows the experimental results for two different PE−propane−cosolvent mixtures.[44] The cloud-point curves in Figure 12 terminate at the solidification boundary so that only liquid + liquid → fluid transitions are shown. At ∼1.0 wt %, ethanol has no effect on the cloud-point pressure. This low concentration of ethanol apparently does not increase the solvent density of propane sufficiently enough to improve the quality of the mixed solvent. Also, the small increase in favorable dispersion and induced dipolar interactions between ethanol and PE apparently does not outweigh strong ethanol−ethanol interactions that include dispersion, dipolar, and hydrogen bonding forces. In fact, if the ethanol concentration is increased to ∼5.0 wt %, PE falls out of solution. Since there are no polar groups in the backbone of PE, ethanol hydrogen bonds to itself forming polar ethanol multimers that have an effec-

Table 3. Experimental (Co)Polymer−SCF Data[a]

SCF solvent	temperature (°C)	pressure (bar)	$M_w \times 10^{-3}$	comments	ref(s)
			Polyethylene		
butane	75−225	200−400	106	P−T (LDPE)	28
	110−200	0−300	2.1−420	P−T, P−x	52
	80−160	0−1300	17−246	P−x, P−T	42
butane/CO_2	110−200	200−800	2.2−420	P−T, P−x	52
butene	75−225	200−400	106	P−T (LDPE)	28
	220	0−200	5.4	P−x	168
DME	100−200	500−1500	106	P−T (LDPE)	28
	110−170	600−1500	65−113	P−T (LDPE)	200
ethane	115−150	1000−1300	46−108	P−T, linear PE	56
	100−130	1200	108,246	P−T,P−x	39,42
ethylene	110−140	1600−1800	108	P−T (LDPE)	39
	110−140	1600−1800	246	P−T	42
	105−140	1400−2000	315	P−T	36
	120−200	1300−2000	28−100 (M_V)	P−T, P−x	35
	110−170	900−2000	4−118	P−T, P−x	22
	130−250	1000−1700	6−374	P−T, P−x	105
	115−180	1000−2000	30−2000	P−T, P−x, branched PE	29
	170	0−1000	5.4	P−x	168
4-methyl-1-pentene (4MP)	220	0−60	5.4	P−x	168
4MP/ethylene	220	250	5.4	P−x	168
heptane	180−190	n/a	77−202 (M_V)	LCST	48
hexane	140−165	n/a	35−440 (M_V)	LCST	48
	120−180	0−70	177 (HDPE)	P−T	83
hexane/nitrogen	120−180	0−70	177 (HDPE)	P−T	83
n-pentane	125−210	20−200	2.1−420	P−x, P−T	50
	110−145	n/a	5−23 (M_V)	LCST	48
	80−160	0−1300	17−246	P−x, P−T	42
octane	220−230	n/a	77−202 (M_V)	LCST	48
propane	100−140	400−700	13−120	P−T, (linear PE)	38
	100−130	400−600	106	P−T (LDPE)	28
	60−165	0−2000	30−340	P−T (LDPE)	31
	90−135	600	108	P−T (LDPE)	39
	105−150	450−600	46−108	P−T (linear PE)	56
	90−140	600	108	P−T	42
	110−130	650	120	P−T	60
	95−130	0−600	36	P−T (LDPE)	44
propane/acetone	95−130	500−1000	36	P−T (LDPE)	44
propylene	90−140	600	108	P−T (LDPE)	39
propylene	80−140	400−600	106	P−T (LDPE)	28
			Polystyrene		
acetone	20−200	0−300	20−97	T−x, P−T	17
butane	125−200	350−500	4−9	P−T, P−x	169
	100−180	400−600	9	P−T	81
	155−200	90−130	22	P−x	211
butane/pentane	125−200	250−450	4−9	P−T, P−x	169
cyclopentane	150−220	n/a	6−600 (M_V)	T−x	14
diethyl ether (DEE)	−75 to 175	0−300	20.4−110	P−T	72
DEE/acetone	−75 to 175	0−300	20.4−110	P−T	72
hexane	50−170	0−600	4−50	P−T	81
methyl acetate	0−200	0−300	51−1800	P−T	17
n-pentane	125−200	250	4−9	P−T, P−x	169
toluene/CO_2	20−80	0−140	235	P−T	82
	25−120	0−200	239	P−T	76
toluene/ethane	25−120	0−200	239	P−T	76
	0−160	0−200	150	P−T	78
tetrahydrofuran/CO_2	20−80	0−140	235	P−T	82
cyclohexane/CO_2	140−240	0−160	40−160	P−T	212
dichlorotrifluoroethane	75−145	30−350	114 900	P−T	213
			Poly(ethylene-*co*-methyl acrylate) (EMA_x, where *x* represents the mol % MA)		
butane	60−250	400−2500	109−140	P−T (EMA_{10}, EMA_{18}, EMA_{31}, EMA_{41})	90
butene	40−150	500−2200	109−140	P−T (EMA_{10}, EMA_{18}, EMA_{31}, EMA_{41})	90
$CHClF_2$	60−150	0−400	30−350	P−T (EMA_{10}, EMA_{36})	31
	60−150	40−400	34−59	P−T (EMA_{10}, EMA_{31})	44
	70−160	100−300	92−108	P−T (EMA_{36})	108
	75−140	0−400	109−140	P−T (EMA_{18}, EMA_{31}, EMA_{41})	90
$CHClF_2$/acetone	60−150	40−400	34−59	P−T (EMA_{10}, EMA_{31})	44
	70−140	0−250	92−108	P−T (EMA_{36})	108
$CHClF_2$/ethanol	60−150	40−400	34−59	P−T (EMA_{10}, EMA_{31})	44
	70−130	0−150	92−108	P−T (EMA_{36})	108
ethane	60−180	1200−3000	∼100	P−T (EMA_{10}, EMA_{31})	39
ethylene	20−180	1400−3000	∼100	P−T (EMA_{10}, EMA_{31}, EMA_{41})	39
	25−250	1250−2800	75−185	P−T (EMA_x; $x = 0-41$)	95

Table 3. (Continued)

SCF solvent	temperature (°C)	pressure (bar)	$M_w \times 10^{-3}$	comments	ref(s)
Poly(ethylene-*co*-methyl acrylate) (EMA_x, where x represents the mol % MA)					
ethylene/methyl acrylate	100−210	1200−1700	210−295	P−T (EMA_x; x = 34, 38, 45)	107
hexane	145−180	400−2800	105	P−T (EMA_{31})	64
propane	60−165	0−2000	30−340	P−T (EMA_{10}, EMA_{36})	31
	20−140	600−1400	∼100	P−T (EMA_{10}, EMA_{31})	39
	135−160	1600−2200	105	P−T (EMA_{31})	64
	65−160	600−2000	34−59	P−T (EMA_{10}, EMA_{31})	44
	150−160	1600−2000	92	P−T (EMA_{36})	108
	100−175	800−2500	109−140	P−T (EMA_{10}, EMA_{18}, EMA_{31})	90
propane/acetone	65−160	200−2000	34−59	P−T (EMA_{10}, EMA_{31})	44
	40−140	300−2000	92	P−T (EMA_{36})	108
propane/ethanol	60−160	600−2800	105	P−T (EMA_{31})	64
	65−160	400−2000	34−59	P−T (EMA_{10}, EMA_{31})	44
	115−150	1000−2000	92	P−T (EMA_{36})	108
propane/hexane	135−160	1200−2500	105	P−T (EMA_{31})	64
propane/hexene	130−160	1200−2800	105	P−T (EMA_{31})	64
propane/methanol	70−160	600−2800	105	P−T (EMA_{31})	64
propane/1-propanol	50−160	600−2800	105	P−T (EMA_{31})	64
propane/1-butanol	60−160	600−2800	105	P−T (EMA_{31})	64
propylene	20−140	400−2500	∼100	P−T (EMA_{10}, EMA_{31}, EMA_{41})	39
	50−150	600−2200	109−140	P−T (EMA_{10}, EMA_{18}, EMA_{31}, EMA_{41})	90
Poly(ethylene-*co*-propylene)					
butene	0−250	600	0.8	LCST	86
	60−220	0−250	0.8−96	P−T	84
butene/ethylene	80−200	0−400	26	P−T, P−x	85
ethylene	0−200	500−2000	0.8−96	P−T	87
hexene	0−250	600	0.8−96	LCST	85
	60−220	0−500	0.8−96	P−T	84
hexene/ethylene	−50 to 200	0−400	26	P−T, P−x	85
mixed solvent/ethylene	20−80	40−220	145	P−T	75
mixed solvent/propylene	120−165	20−70	145	P−T	75
mixed solvent/methane	20−100	70−300	145	P−T	75
mixed solvent/CO_2	95−130	50−120	145	P−T	75
propane	0−220	0−700	60−210	P−T	58
	0−150	20−300	100−570	P−T	60
propane/1-butanol	0−175	0−400	100−570	P−T	60
propane/1-propanol	0−175	0−400	100−570	P−T	60
propylene	0−250	0−450	0.8	P−T	86
	100−150	150−450	6−96	P−x	87
	0−210	20−500	0.8−96	P−T	84
pentane	125−170	10−80	140	P−T	27
n-hexane	165−225	10−100	140−400	P−T	27
methylcyclopentane	220−275	20−80	140	P−T	27
3-methylpentane	175−210	15−70	140	P−T	27
Poly(ethylene-*co*-butyl acrylate)					
ethylene	50−250	700−2000	35−404	P−T (EBA_x; x = 0−41)	95
Poly(propylene oxide)					
propane	−20 to 150	0−300	0.8−3.9	T−x, P−T	17
Poly(tetrafluoroethylene)					
Freon 113	280−340	0−200	n/a	P−T	126
Fluorinert FC-75	280−340	0−200	n/a	P−T	126
n-perfluorohexane	280−340	0−200	n/a	P−T	126
perfluorodecalin	280−340	0−200	n/a	P−T	126
Poly(butyl acrylate)					
butyl acrylate/CO_2	20−175	50−1500	62	P−T	73
ethylene	25−200	800	62	P−T	61
Poly(ethylhexyl acrylate)					
ethylhexyl acrylate/CO_2	30−220	50−1500	113	P−T	73
ethylene	25−200	600	113	P−T	61
Poly(ethylene-*co*-acrylic acid) (EAA_x, where x represents the mol % AA)					
butane	120−250	200−2800	34−100	P−T ($EAA_{2.4}$, $EAA_{3.9}$)	28
butane/dimethyl ether	75−250	400−2000	123	P−T ($EAA_{3.9}$)	198
butane/ethanol	75−250	0−2000	123	P−T ($EAA_{3.9}$)	198
butene	100−250	200−2800	34−100	P−T ($EAA_{2.4}$, $EAA_{3.9}$, $EAA_{6.9}$)	28
	120−220	400−2700	24.3−247	P−T ($EAA_{4.1}$)	200
	90−220	400−2500	240−403	P−T ($EAA_{2.4}$.$EAA_{4.1}$)	100
DME	75−200	200−1300	34−100	P−T ($EAA_{2.4}$, $EAA_{3.9}$, $EAA_{6.9}$, $EAA_{9.2}$)	28
ethylene	160−220	600−2000	126−183	P−x ($EAA_{1.0}$, $EAA_{1.5}$, $EAA_{3.5}$)	103
	100−250	1500−2500	240−403	P−T ($EAA_{2.4}$, $EAA_{4.1}$)	100
propane	100−225	600−2500	34−100	P−T ($EAA_{2.4}$, $EAA_{3.9}$)	28
propylene	80−270	600−2800	104−403	P−T ($EAA_{2.4}$, $EAA_{4.1}$, $EAA_{8.1}$)	100
propylene	80−225	600−2500	34−100	P−T ($EAA_{2.4}$, $EAA_{3.9}$)	100

Table 3. (Continued)

SCF solvent	temperature (°C)	pressure (bar)	$M_w \times 10^{-3}$	comments	ref(s)
Poly(ethylene-*co*-methacrylic acid) (EMAA$_x$, where x represents the mol % MAA)					
butane	110−240	500−2500	70−123	P−T (EMAA$_x$; x = 0−5.4)	40
butane/DME	75−200	200−1250	70−123	P−T (EMAA$_x$; x = 0−5.4)	40
butane/ethanol	70−215	100−2000	70−123	P−T (EMAA$_x$; x = 0−5.4)	40
butene	90−225	400−2000	70−123	P−T (EMAA$_x$; x = 0−5.4)	40
DME	75−210	300−1300	70−123	P−T (EMAA$_x$; x = 0−5.4)	40
ethylene	175−240	1500−2500	70−123	P−T (EMAA$_x$; x = 0−5.4)	40
propane	175−240	800−2500	70−123	P−T (EMAA$_x$; x = 0−5.4)	40
Poly(dimethylsiloxane)					
butane	0−200	0−400	14.2−626 (M_v)	P−T	16
ethane	0−200	0−400	14.2−626 (M_v)	P−T	16
propane	0−200	0−400	14.2−626 (M_v)	P−T	16
Polyisobutylene					
butane	0−200	0−300	6.0−1660 (M_v)	P−T	16
	150−210	70−100	50	P−T	211
$CHClF_2$	100−200	500−1300	4	P−T (3-arm star)	196
	50−200	0−500	1	P−T (telechelic and nonfunctional)	161
	50−200	0−500	11	P−T (telechelic and nonfunctional)	162
DME	0−150	0−700	4	P−T (3-arm star PIB)	196
	0−200	0−200	1	P−T (telechelic and nonfunctional)	161
	0−150	200−600	11	P−T (telechelic and nonfunctional)	162
ethane	−50 to 150	600	4	P−T (3-arm star PIB)	196
	0−150	200−600	1	P−T (telechelic and nonfunctional)	161
	0−150	200−1200	11	P−T (telechelic and nonfunctional)	162
2-methylbutane	0−200	0−300	6.0−1660 (M_v)	P−T	16
hexane	0−200	0−300	6.0−1660 (M_v)	P−T	16
n-alkanes	45−310	n/a	630−3600 (M_v)	LCST	11
pentane	0−200	0−300	6.0−1660 (M_v)	P−T	16
propane	0−150	0−300	4	P−T (telechelic PIB)	196
	0−150	0−250	1	P−T (telechelic and nonfunctional)	161
	0−150	0−500	11	P−T (telechelic and nonfunctional)	162
Polypropylene					
propane	0−220	0−700	60−210	P−T	58
Isotactic Polypropylene					
propane	100−170	150−550	29−290	P−x, P−T	43
	65−200	400−600	91	P−T	59
pentane	140−210	0−100	216	P−T	80
Atactic Polypropylene					
propane	0−160	0−400	400	P−x, P−T	43
Poly(methyl acrylate)					
$CHClF_2$	90−150	200−400	360	P−T	31
	60−130	0−250	31	P−T	44
$CHClF_2$/acetone	80−160	0−200	31	P−T	44
$CHClF_2$/ethanol	80−160	0−200	31	P−T	44
toluene/CO_2	20−80	0−200	120	P−T	82
tetrahydrofuran/CO_2	20−80	0−200	120	P−T	82
Poly(ethyl acrylate)					
ethylene	40−240	1000−2000	120	P−T	61
Poly(propyl acrylate)					
ethylene	20−240	400−2000	140	P−T	61
Poly(octadecyl acrylate)					
ethylene	25−225	800	23	P−T	61
Poly(vinylidene fluoride-*co*-hexafluoropropylene$_{22}$)					
C_3F_6	160−240	800−2800	85	P−T	131
$CClF_3$	200−250	1500−3000	85	P−T	131
CHF_3	230−250	1500−3000	85	P−T	131
Poly(butadiene)					
toluene/CO_2	20−80	0−200	420	P−T	82
tetrahydrofuran/CO_2	20−80	0−200	420	P−T	82
Poly(tetrafluoroethylene-*co*-hexafluoropropylene$_{19}$)					
CF_4	180−250	1750−2250	210	P−T	30
C_2F_6	160−240	1000	210	P−T	30
C_3F_6	150−210	400	210	P−T	30
C_3F_8	150−230	0−500	210	P−T	30
$CClF_3$	130−220	600−800	210	P−T	30
CHF_3	230−260	1500−2800	210	P−T	131
SF_6	120−240	500	210	P−T	30

Table 3. (Continued)

SCF solvent	temperature (°C)	pressure (bar)	$M_w \times 10^{-3}$	comments	ref(s)
		Poly(tetrafluoroethylene-*co*-hexafluoropropylene$_{48}$)			
CF_4	130−240	1500−2500	191	P−T	130
SF_6	50−160	400−500	191	P−T	130
		Poly(vinyl fluoride)			
CH_2F_2	170−230	1500−1900	125	P−T	216
		Poly(vinylidene fluoride)			
CH_2F_2	120−230	1700	125	P−T	216
		Poly(ethylene-*co*-vinyl acetate)[b]			
ethylene	140−240	900−1100	44	P−x ($EVA_{42.7}$)	105
	100−200	1000−1500	120	P−x (EVA_x; $x = 11-58$)	102
ethylene/VA	120−180	600−800	41	P−x (ethylene$_{64}$[b]/VA_{36}[b])	104
	140−240	600−1300	44−145	P−x ($EVA_{7.5}$, $EVA_{12.7}$, $EVA_{27.3}$ $EVA_{31.8}$,$EVA_{42.7}$)	105,101
	200	200−800	5.7	P−T (EVA_{29})	106
	100−200	300−1500	120	P−x ($EVA_{18.0}$, EVA_{33})	102
		Poly(vinyl ethyl ether)			
toluene/CO_2	20−80	0−200	3.8	P−T	82
tetrahydrofuran/CO_2	20−80	0−200	3.8	P−T	82
		Poly(ethylene-1-butene)			
propane	25−220	0−800	60−120	P−T	58
	25−200	200−800	80−120	P−T	59
propane	80−160	200−300	570	P−T	60
		Poly(ethylene-1-hexene)			
propane	50−200	450−700	70−100	P−T	59
		Poly(ethylene-*co*-octene)$_x$			
propane	80−160	300−700	95−203	P−T (P(E-*co*-O)$_x$, $x = 0-8.4$)	60
propane	75−200	500−600	94	P−T	59
		Poly(4-methyl 1-pentene)			
propane	130−180	150−200	n/a	P−T	60
		Polybutene-1			
propane	0−200	0−700	100−570	P−T	60
		Poly(*E*-caprolactone)			
$CHClF_2$	50−150	50−350	15−41	P−T	184
$CHClF_2$	50−150	50−350	15−41	P−T	214
		Poly(methyl methacrylate)			
$CHClF_2$	60−150	0−300	74	P−T	184
$CHClF_2$	60−150	0−300	50	P−T	214
		Poly(ethyl methacrylate)			
$CHClF_2$	60−150	0−300	280	P−T	214
		Poly(decyl methacrylate)			
pentane	190−250	0−100	470	P−T	215
cyclopentane	210−300	0−100	470	P−T	215
hexane	200−300	0−100	470	P−T	215
heptane	240−300	0−100	470	P−T	215
isooctane	240−300	0−100	470	P−T	215
toluene	275−300	0−100	470	P−T	215
		Poly(lactic acid)			
$CHClF_2$	60−150	0−300	50	P−T	214

[a] Table 4 provides entries for CO_2 as the SCF solvent. However, CO_2 entries can be found in Table 3 when it is used as a cosolvent. The reader is directed to the book of McHugh and Krukonis for other sundry polymer−SCF data.[8] [b] Volume percent.

tive dipole moment which is much greater than that of an isolated ethanol molecule. As the amount of ethanol multimers increases, the polarity of the solvent increases in a nonlinear manner and reduces the solvent quality of the mixed solvent sufficiently to force nonpolar PE to precipitate from solution. Whaley and co-workers present a more detailed study of the effect of an alcohol cosolvent on the phase behavior of nonpolar atactic polypropylene in nonpolar propane.[60]

Figure 12 also shows that adding 27 wt % acetone to the PE−propane solution reduces the cloud-point pressure by ∼50 bar. In this instance, acetone contributes to the solvent quality by contributing favorable dispersion and induced dipolar interactions between itself and PE and increasing the solvent density and, thus, reducing the polymer−solvent free volume difference. However, as the concentration of acetone is further increased to 42 wt %, polar acetone−acetone interactions far outweigh acetone−PE interactions which results in a dramatic increase in the cloud-point pressures. If the concentration of acetone is further increased to 62 wt %, PE falls out of solution. The negative slope exhibited by the cloud-point curve with 42 wt % acetone is a result of the dipole−dipole interactions between acetone molecules that diminish with increasing temperature.[5]

Table 4. Experimental (Co)Polymer−CO_2 Data[a]

polymer	temperature (°C)	pressure (bar)	$M_w \times 10^{-3}$	comments	ref(s)
poly(dimethylsiloxane)	25−185	250−600	39−370	P−T	156
	25−100	150−750	2−486	P−T	154
polyisobutylene	50−200	0−2000	0.2,1	P−T (telechelic and nonfunctional)	161
	50−200	0−2000	1	P−T (telechelic and nonfunctional)	162
poly (vinylidene fluoride) (PVDF)	120−220	1700	∼200	P−T	216
PVDF w/acetone	90−220	300−1700	∼200	P−T	216
PVDF w/DME	100−220	1700	∼200	P−T	216
PVDF w/ethanol	100−220	1700	∼200	P−T	216
poly(vinyl fluoride) (PVF) w/acetone	130−250	500−2250	125	P−T	216
PVF w/DME	140−240	1000−2250	125	P−T	216
PVF w/ethanol	140−240	500−2250	125	P−T	216
poly(1,1-dihydroperfluorooctyl acrylate)	30−80	100−300	1200	P−x, T−x, P−T	217,218
poly(vinyl acetate)	20−160	500−1000	125	P−T	159
poly(methyl acrylate)	20−200	1700−2200	31	P−T	159
poly(ethyl acrylate)	50−200	1200−3000	119	P−T	159
poly(propyl acrylate)	100−180	1200−1500	140	P−T	159
poly(butyl acrylate)	80−200	1000−3000	62	P−T	159
poly(ethylhexyl acrylate)	150−220	1100−3000	113	P−T	159
poly(octadecyl acrylate)	210−260	1000−2600	23	P−T	159
poly(butyl methacrylate)	120−230	1100−3000	320, 100	P−T	159
EMA_{18}	80−280	1500−2800	∼100	P−T	159
EMA_{31}	80−280	1500−2800	∼100	P−T	159
EMA_{41}	80−280	1500−2800	∼100	P−T	159
$TFE−HFP_{19}$	180−250	1000−3000	210	P−T	159
	185−245	1000−3000	210	P−T	30
$TFE−HFP_{48}$	170−230	1000−2800	191	P−T	130
$VDF−HFP_{22}$	100−230	700−900	85	P−T	159
	0−230	400−900	85	P−T	131
$VDF−HFP_{22}$ w/acetone	0−250	0−1000	85	P−T	219
$VDF−CTFE_{74}$	120−210	1000−2750	∼100	P−T	219
oxidized polyethylene	200−270	1000−2500	3.6	P−T	219
Teflon AF160	50−180	500−1000	∼400	P−T	159
Teflon AF240	60−180	500−1000	n/a	P−T	33
poly(tetrahydroperfluorodecyl acrylate)	10−80	50−275	n/a	P−T	220

[a] Entries that show a polymer with the notation "w/cosolvent" indicate that a cosolvent is added to the solution. CO_2 entries can be found in Table 3 when it is used as a cosolvent. The reader is directed to the book of McHugh and Krukonis for other sundry polymer−CO_2 data.[8]

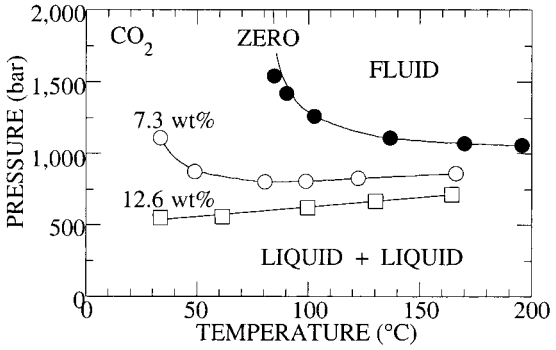

Figure 13. Impact of free butyl acrylate monomer (weight percents are given on a polymer-free basis) on the phase behavior of 5 wt % poly(butyl acrylate) in CO_2. (Reprinted with permission from ref 73. Copyright 1998 Elsevier.)

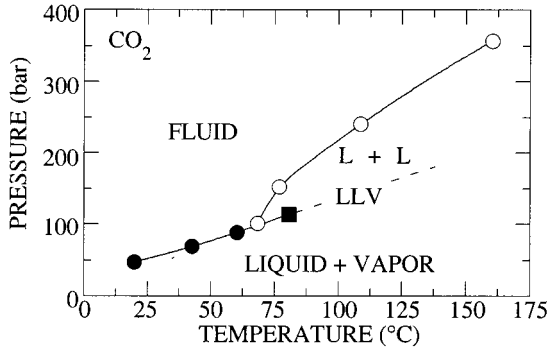

Figure 14. Impact of 32.0 wt % butyl acrylate monomer (on a polymer-free basis) on the phase behavior of the 5 wt % poly(butyl acrylate) in CO_2.[73] The open circles represent fluid → liquid + liquid transitions, the closed circles represent fluid → liquid + vapor transitions, and the closed square represents a liquid + liquid → $liquid_1$ + $liquid_2$ + vapor (LLV) transition. The dashed line is the suggested extension of the LLV line. (Reprinted with permission from ref 73. Copyright 1998 Elsevier.)

Although a later section of this review is devoted to polymer−supercritical CO_2 phase behavior, the effect of a comonomer as a cosolvent is best described with the poly(butyl acrylate) (PBA)−CO_2−butyl acrylate (BA) phase behavior study recently reported by McHugh et al.[73] It is not possible to dissolve PBA in CO_2 at temperatures less than ∼50 °C since the cloud-point curve exhibits a very steep slope at that point. Figure 13 shows that at 150 °C, the addition of ∼7 wt % BA to a PBA−CO_2 mixture lowers the cloud-point pressure from 1100 bar to 850 bar and that the sharp increase in the PBA−CO_2 cloud-point curve shifts from 85 to ∼30 °C. Note that the PBA−CO_2-12.6 wt % BA curve exhibits a positive slope over the range of 30−160 °C. Figure 14 shows that adding 32 wt % BA to the PBA−CO_2 solution significantly changes the phase behavior. Now the cloud-point curve takes on the appearance of a typical lower critical solution temperature (LCST) boundary.[8] At 150 °C the phase transition has shifted from 1100 bar in pure CO_2 to ∼350 bar in a CO_2 + 32 wt % BA mixture. The cloud-point curve intersects a liquid → liquid + vapor (LV) curve at ∼65 °C and 100 bar. A

liquid and vapor phase coexist at pressures below this curve. Note that the LV curve switches to a liquid$_1$ + liquid$_2$ + vapor (LLV) curve at temperatures greater than 65 °C. The slope of the PBA−CO_2−BA LCST curve, ~2.7 bar/°C, is approximately 40% greater than that observed for binary poly(isobutylene)−alkane mixtures reported by Zeman and Patterson.[17] At the same temperatures and pressures, the CO_2−BA mixture is more compressible than the alkanes used in the Zeman study. It should not be surprising that butyl acrylate is an excellent cosolvent for PBA since PBA dissolves in pure BA even at atmospheric pressure. Clearly it is possible to obtain a single phase that extends over a large temperature range at modest pressures if sufficient amounts of free acrylate monomer are added to the solution.

There are many cosolvent studies where an SCF solvent is added to solution with the express intent of decreasing the solvent quality of the liquid solvent to precipitate the polymer from solution. In this instance the supercritical fluid is an antisolvent. Irani et al.[27,74] were the first to demonstrate that the SCF dilates the solvent without raising its temperature, thus avoiding thermal degradation of the polymer. McHugh and co-workers,[75−79] extended the SCF-additive work of Irani and found that not only does the LCST curve shift to lower temperatures with the addition of a supercritical fluid to the mixture, but that the UCST also shifts to higher temperatures. Eventually the UCST and LCST curves merge if enough supercritical antisolvent is added to the solution. Many other studies have since been reported on the large effect supercritical CO_2 as an antisolvent.[51,52,80−82] The antisolvent effect is exacerbated when the operating temperatures are well above the critical point of the supercritical solvent.[83]

V. Copolymer–SCF Phase Behavior

1. Solvent Quality

With copolymers it is possible to develop systematic studies which vary the solvent properties, the copolymer backbone architecture, and the cosolvent quality. This approach facilitates the elucidation of the fundamental thermodynamic variables that fix the conditions needed to dissolve a polymer or copolymer in a pure SCF solvent or an SCF-cosolvent mixture. The examples presented in this section focus mainly on ethylene-based copolymers since they consist of a nonpolar ethylene group randomly distributed in the backbone with a nonpolar comonomer such as propylene or polar comonomers such an acrylate, acrylic and methacrylic acid, vinyl alcohol, vinyl acetate, and tetrafluoroethylene. Hence, large changes are anticipated in the observed phase behavior as a function of comonomer type and backbone content.

Radosz and co-workers have published extensively on the phase behavior of poly(ethylene-*co*-propylene) (PEP)−SCF solvent systems.[84−88] The phase behavior of the PEP−ethylene system follows type IV phase behavior, even if the "polymer" molecular weight is reduced to 790 g/mol.[87] This is not totally unexpected

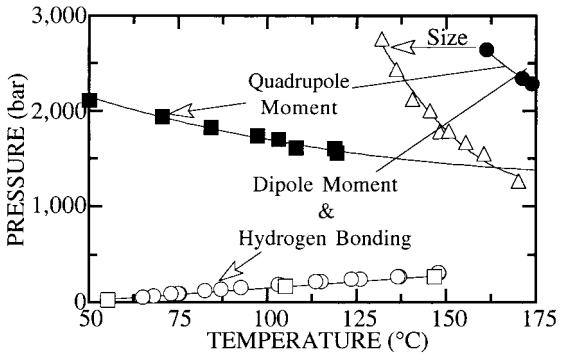

Figure 15. Phase behavior of 5 wt % poly(ethylene-*co*-31 mol % methyl acrylate) in ethane (closed circles),[39] propane (open triangles),[39] ethylene (closed squares),[39] dimethyl ether (DME) (open squares),[89] and chlorodifluoromethane (F22) (open circles).[90,91]

behavior since ethylene has both a significant quadrupole moment and a low polarizability and it is a poor solvent for PE. With SCF propylene, type III phase behavior is observed as long as the molecular weight of the copolymer remains below 6000. In this instance the location of the LCST curve decreases in temperature as the molecular weight of polymer increases. Eventually the PEP−propylene phase behavior changes from type III to type IV when the molecular weight is increased above 6000.

In contrast to PEP−SCF solvent phase behavior, the phase behavior of ethylene-based copolymers with a polar comonomer is very sensitive to the solvent quality and the type and amount of polar comonomer in the chain backbone. Figure 15 shows the phase behavior of poly(ethylene-*co*-31 mol % methyl acrylate) (EMA_{31}) in ethane,[39] ethylene,[39] propane,[39] dimethyl ether,[89] and chlorodifluoromethane.[90,91] High temperatures are needed before EMA_{31} dissolves in ethane since acrylate−acrylate dipolar interactions overwhelm dispersion and induction interactions between methyl acrylate and ethane. However, the temperature is so much higher than the critical temperature of ethane that very high pressures are needed to decrease the molar volume of ethane, which increase dispersion interactions. If the solvent is changed to propane, the cloud-point pressure at 175 °C decreases by ~1000 bar and the entire curve shifts ~30 °C to lower temperatures. The difference in the location of the ethane and propane curves reflects the impact of solvent polarizability since both of these solvents are nonpolar. Also, both curves are very steep which reflects the diminishing strength of the acrylate−acrylate dipolar interactions with increasing temperature.

A more significant shift in the cloud-point curve occurs in going from nonpolar ethane to ethylene, which has a quadrupole moment. In this case the cloud-point curve extends to temperatures as low as 50 °C due to favorable polar cross interactions between ethylene and methyl acrylate. However, note also that the ethylene curve is still at elevated pressures since ethylene is a highly expanded SCF solvent at the temperatures shown in Figure 15. The fate of the cloud-point curve was not determined at temperatures below 50 °C.

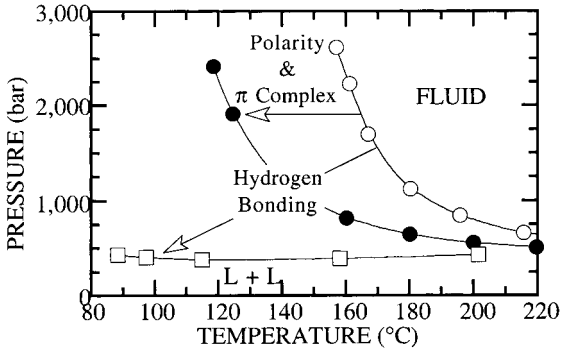

Figure 16. Phase behavior of 5 wt % poly(ethylene-*co*-3.9 mol % acrylic acid) in butane (open circles), butene (closed circles), and dimethyl ether (DME) (open squares).[28]

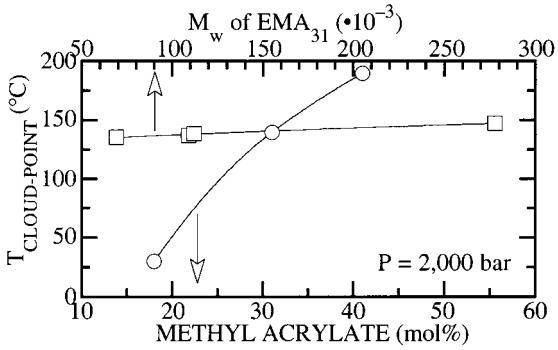

Figure 17. Impact of acrylate concentration[90] in the copolymer backbone (open circles) relative to copolymer molecular weight[200] (open squares) for mixtures of 5 wt % poly(ethylene-*co*-methyl acrylate) in butane.

The largest shift of the cloud-point curve is observed with dimethyl ether (DME) and chlorodifluoromethane (F22) relative to ethane. DME has a large dipole moment (1.3 D) that interacts favorably with the dipole of methyl acrylate. F22 also has a large dipole moment (1.4 D) and it can donate a proton to the basic methyl acrylate group. In these two cases the single-phase region extends to 50 °C and 100 bar compared to 2000 bar needed with ethylene.

Similar large shifts in cloud-point curves are observed for poly(ethylene-*co*-acrylic acid) (EAA_x, where x is the mole percent acid in the backbone)−SCF solvent mixtures. However, in this case, a very small percent of acid groups in the backbone of the copolymer has a large impact on the phase behavior since the strength of hydrogen bonding interactions far outweigh other types of interactions. Figure 16 shows the phase behavior for $EAA_{3.9}$ in butane, butene, and DME.[28] The shift in the butene cloud-point curve relative to the butane curve is attributed to both polar interactions and π-acid complexing that is supported by spectroscopic studies.[92,93] Notice that the butane and butene curves exhibit very steep slopes as the temperature is lowered which is more pronounced than that observed with the EMA_{31}−SCF phase behavior shown in Figure 15. As the temperature is lowered the amount of interchain and intrachain acid dimerization increases, which makes it exceedingly difficult to dissolve $EAA_{3.9}$ in a nonpolar or slightly polar solvent. The $EAA_{3.9}$−DME curve remains essentially flat near 400 bar regardless of temperature due to acid−ether hydrogen bonding. All three cloud-point curves appear to coincide at temperatures above 200 °C. Evidently, the amount of acid dimer formation is reduced to a very low level at these high temperatures where $EAA_{3.9}$ behaves more like nonpolar PE.

2. Molecular Weight, Branching, and Backbone Architecture

Although polymer molecular weight can play a role in determining the location of the cloud-point curve, its impact is attenuated if there is a large energetic mismatch between the copolymer and the solvent. Radosz and co-workers investigated the impact of copolymer molecular weight on the phase behavior of mixtures containing alternating poly(ethylene-*co*-propylene) (PEP) and 1-butene[84] and ethylene.[87] With butene at 160 °C there is a 60 bar difference in the cloud-point pressures for PEP fractions of M_w of 790 and 5900. The pressure differential decreases to only 15 bar for PEP fractions with M_w of 26 000 and 96 000. Ethylene has a smaller polarizability and a larger effective polarity than propylene, which makes ethylene a weaker SCF solvent for a nonpolar copolymer. Hence, with ethylene the phase behavior is even more sensitive to PEP molecular weight in the same 5900 to 96 000 weight range. For example, there is a 450 bar difference in the cloud-point pressures for PEP fractions with M_w of 5900 and 96 000 at 160 °C. Even though the investigators do not present cloud-point data for higher molecular weight polymers, the trend of diminishing effect of copolymer molecular weight is apparent, in agreement with the trend found with homopolymer−SCF solvent systems. In addition, the effect of molecular weight is more pronounced the weaker the SCF solvent.

Rätzsch and co-workers[94] investigated the effect of molecular weight on the poly(ethylene-*co*-14 mol % vinyl acetate) (EVA_{14})−ethylene system. This mixture exhibits type IV phase behavior with fairly flat cloud-point curves. Cloud-point pressures are 990, 1170, and 1215 bar at 120 °C for three EVA_{14} fractions with weight-average molecular weights of 8200, 40 800, 60 300, respectively. There is a ∼180 bar differential in the cloud-point pressures between the 8200 and 40 800 fractions, which reduces to a ∼40 bar difference between the 40 800 and 60 300 fractions. Although these EVA_{14} molecular weights are modest, the trend of diminishing molecular weight effect is still apparent. Meilchen et al. showed similar molecular weight trends for the EMA_{31}−chlorodifluoromethane (F22) system that exhibits type III LCST behavior.[91] The single-phase region decreases as the copolymer molecular weight increases and the effect diminishes once the molecular weight becomes larger than ∼40 000. For this system F22, a proton donor, is expected to hydrogen bond to the acrylate groups in EMA_{31}, but F22 does not self-associate.

Figure 17 shows a comparison of the impact of molecular weight and acrylate content for EMA_x (where x is the mol % of acrylate groups in the chain backbone) in butane. Several different EMA_x copoly-

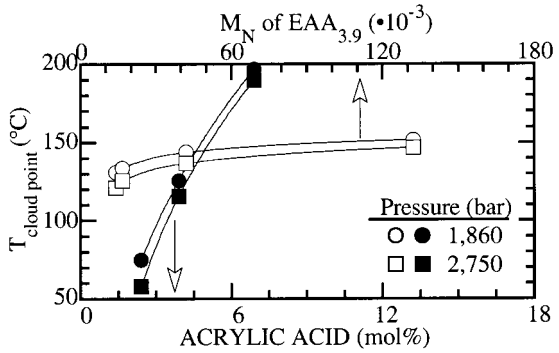

Figure 18. Impact of acrylic acid units in the copolymer backbone (open symbols) relative to copolymer molecular weight for mixtures (closed symbols) of 5 wt % poly(ethylene-*co*-acrylic acid) in butene.[28]

mers were fractionated with an SCF solvent to obtain samples with narrow molecular weight and chemical composition distributions.[90] The isobaric cloud-point temperatures in this figure are obtained from the UCST-portion of the EMA_{31} curves that have differing copolymer molecular weights or the curves with differing acrylate content at a constant M_w of ~120 000. The cloud-point temperature only changes by ~20 °C as the weight average molecular weight varies from 70 000 to 280 000 with molecular weight polydispersities near 1.3. In contrast, the cloud-point temperature at 2000 bar varies by more that 150 °C as the acrylate content is increased from 18 to 41 mol %. This is a dramatic example of the significant impact of backbone architecture relative to molecular weight, especially since the molecular weight data are obtained in the range where it should have the largest impact. Byun et al.[95] also show that the molecular weight dependence of poly(ethylene-*co*-butyl acrylate) (EBA_x) in ethylene is very modest for molecular weights in the range of 57 000−400 000. There is only a 100 bar differential between the EBA_{17} cloud-point curves with molecular weights of 57 000 and 283 000. The pressure differential decreases to only 50 bar for EBA_{25} cloud-point curves with molecular weights of 268 000 and 404 000.

Figure 18 shows a comparison of the impact of molecular weight and acid content for EAA_x copolymers in butene.[28] The EAA_x copolymers were also fractionated supercritically,[96] producing fractions with narrow molecular weight distributions of 1.6 and with narrow chemical composition distributions. The isobaric cloud-point temperatures in Figure 18 are from the UCST portion of the appropriate cloud-point curves similar to the data in Figure 17. In this instance, the cloud-point temperature only changes by 35 °C as the number average molecular weight varies from 13 000 to 130 000 which is equivalent to an increase from 20 000 to 200 000 in the weight average molecular weight. However, the cloud-point temperature of the EAA_x copolymers in butene varies by more than 130 °C as the acid content increases from 2.4 to 6.9 mol %. It is interesting to note that the cloud-point curves for the $EAA_{3.9}$−butene mixtures order with respect to M_n not M_w as is normally observed. The ordering of the acid copolymer curves with M_n is a result of intrapolymer hydrogen bonding that depends on the number of acid groups rather

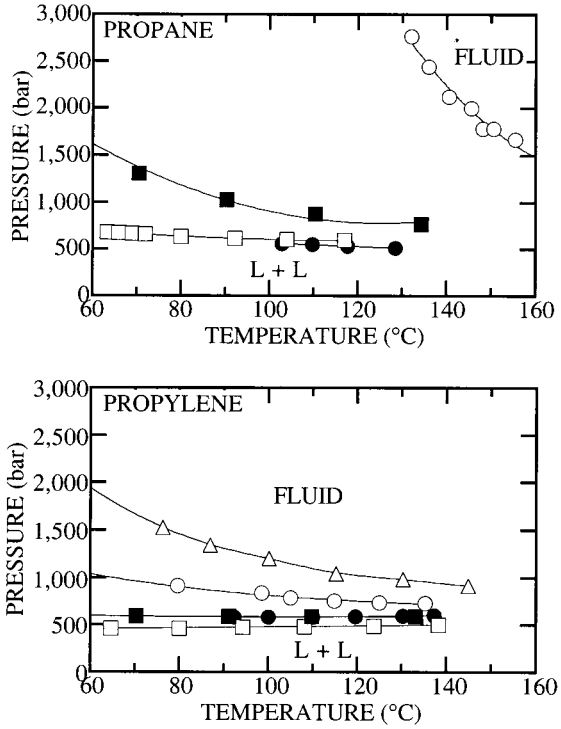

Figure 19. Impact of the amount of methyl acrylate units in the backbone of EMA_x copolymers (where x is the mol % methyl acrylate) on the phase in propane and in propylene:[39,99,100] closed circles, $x = 0$; open squares, $x = 10$; closed squares, $x = 18$; open circles, $x = 31$; and open triangles, $x = 41$. The copolymer concentration is approximately 5 wt % in all cases.

than on their weight. In a related study Chang and Morawetz use spectroscopy and osmometry to show that the methacrylic acid repeat units in poly(styrene-*co*-methacrylic acid) (SMAA) preferentially form intrapolymer hydrogen-bonded acid dimers at 30 °C in tetrachloroethane if the copolymer acid content is below ~5 mol %.[97,98] They argue that hydrogen bonding between acid groups depends more on the molar copolymer acid content rather than on the overall copolymer concentration in solution. Care must be exercised when determining the extent of intra- and intercopolymer hydrogen bonding since the properties of the solvent can play a large role in determining this ratio. Nevertheless, these studies are in agreement with the results shown in Figure 18. It is also interesting to note that the cloud-point curves for the EMA_x−F22 system order with respect to M_w even though copolymer−solvent hydrogen bonding occurs.

It is difficult to separate the impact of branching from backbone architecture since the comonomer introduces a branch point as well as a different functional group into the backbone of the polymer. However, the impact of backbone architecture is expected to be significantly greater with polar branches. A preview of the effect of backbone architecture has already been described for EMA_x copolymers in butane (Figure 17) and EAA_x copolymers in butene (Figure 18). Figure 19 shows another example of the impact of acrylate content on the location of EMA_x copolymers in propane and propylene.[39,99,100] It is evident that it takes increased temperatures and

pressures to dissolve EMA_x copolymers in propane as the acrylate content increases. For example with propane at 130 °C it takes approximately 2000 bar to obtain a single phase with EMA_{31}, but with propylene it only takes 700 bar. Propane and propylene have very similar polarizabilities so the increased solvent quality of propylene is attributed to the double bond that makes propylene slightly polar. Notice once again that the pressure of the cloud-point curves with the highest acrylate content decrease significantly with increasing temperature, which is expected behavior as polar interactions decrease with increasing temperature. The phase behavior of poly(ethylene-*co*-vinyl acetate)−ethylene mixtures,[94,101,102] exhibit trends analogous to those observed for EMA_x−ethylene mixtures.

Similar phase behavior is observed when comparing the phase behavior of EAA_x copolymers in a variety of different SCF solvents.[28] A small amount of acid groups has a large impact on the location of the cloud-point curve since the acid groups preferentially hydrogen bond to one another rather than to interact with the solvent unless the solvent can also hydrogen bond to the acid group. Luft and coworkers have also demonstrated that the addition of acrylic acid to the backbone of a nonpolar copolymer causes far more dramatic shifts in the location of the cloud-point curves than the addition of a nonself-associating comonomer such as vinyl acetate.[102,103]

Polar comonomers from the same chemical family can have very different effects on the copolymer−SCF solvent phase behavior. Byun et al.[95] compare the phase behavior of ethylene−methyl acrylate and ethylene−butyl acrylate copolymers in ethylene. Although from the same chemical family, butyl and methyl acrylate have different physicochemical properties. Both acrylate monomers have approximately the same dipole moments, however, since the strength of dipolar interactions scales inversely with the square root of the molar volume,[5] the increase in polarity per polar repeat unit is greater for methyl acrylate. Polar interactions scale roughly with inverse temperature, so the system temperature is expected to have a large affect on the cloud-point pressures. Another characteristic difference between EMA and EBA copolymers is that the free volume of the EBA copolymers should be greater than that of the EMA copolymers with equivalent numbers of acrylate groups. Therefore, as long as the temperature is high enough that polar interactions do not control solubility behavior, it should be easier to dissolve EBA copolymers. Figure 20 shows that the cloud-point pressure of EMA_x in ethylene initially decreases with increasing copolymer MA content, but it then increases quite rapidly at 75 and 125 °C. The impact of MA content on the cloud-point pressure disappears when the temperature is raised to 200 °C where polar interactions are diminished. In contrast, Figure 21 shows that the cloud-point pressure decreases rapidly as butyl acrylate is incorporated in the EBA_x backbone even at temperatures as high as 250 °C. In fact, EBA_x cloud-point pressures are significantly lower than those of EMA_x with equivalent amounts of acrylate content. These data demonstrate that in certain instances a strong synergy can occur between energetic and free volume effects to improve solubility behavior.

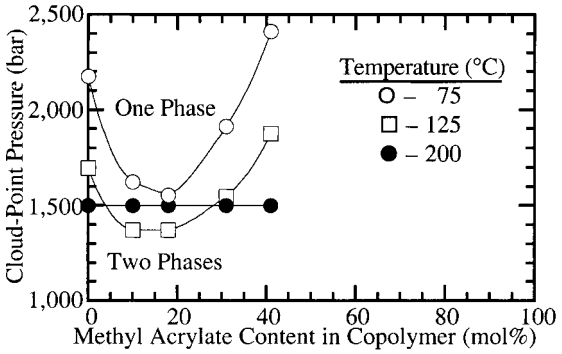

Figure 20. Impact of methyl acrylate content in the copolymer on the cloud-point pressure of EMA copolymers in ethylene. The cloud-point pressures for polyethylene at 75 and 125 °C are extrapolations of the cloud-point curve to lower temperatures disregarding that PE may crystallize. (Reprinted from ref 95. Copyright 1996 American Chemical Society.)

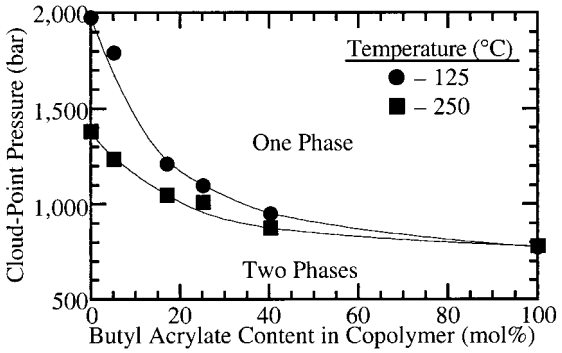

Figure 21. Impact of butyl acrylate content in the copolymer on the cloud-point pressure of EBA copolymers in ethylene. The cloud-point pressure for polyethylene at 125 °C is obtained by extrapolating the cloud-point curve disregarding that PE may solidify. The copolymer concentration is approximately 5 wt % in all cases. (Reprinted from ref 95. Copyright 1996 American Chemical Society.)

3. Cosolvent/Antisolvent Effects

A liquid cosolvent can expand the region of miscibility if it increases the solvent density, which reduces the free volume difference between the solvent and copolymer. The region of miscibility is further expanded with polar copolymers if the cosolvent is also polar and if it can hydrogen bond or π-complex with the polar repeat units in the copolymer. In contrast, the region of miscibility can be reduced substantially if an expanded SCF antisolvent is added to a copolymer−solvent mixture. Consider, for example the effect of adding ethylene as an antisolvent to PEP−hexene and PEP−butene mixtures.[85,86] The experimental results show that the addition of ethylene to either mixture causes the phase behavior to change from type III to type IV. The LCST curve is shifted to lower temperatures until it eventually merges with the UCST curve and shifts to high pressures. This change from type III to type IV phase behavior occurs at ~7 wt % ethylene in 1-butene, and at ~30 wt % ethylene in 1-hexene. The addition of ethylene decreases the density of the

overall solution and thus decreases the region of miscibility. In addition to reducing the solution density, ethylene also shifts the interchange energy to promote ethylene−ethylene quadrupolar interactions relative to ethylene−nonpolar PEP interactions. The effect of the quadrupole moment of ethylene is exacerbated because the molar volume of ethylene is quite small relative to quadrupole or dipole effects expected with butene and hexene. It has already been shown in this review that ethylene is a worse solvent than ethane for nonpolar PE, even though ethane and ethylene have virtually the same densities.

As previously mentioned, a cosolvent can have a large effect on the location of the cloud-point curve when the physicochemical properties of the two comonomers differ considerably from one another. It has already been shown that the location of the cloud-point curve for a nonpolar/polar copolymer is very sensitive to polar comonomer content and solvent quality so it is expected that a polar cosolvent will have a large effect on the phase behavior of these type mixtures. The EVA_x−ethylene−vinyl acetate system is perhaps the first copolymer−SCF solvent−cosolvent system reported in any detail as a result of the commercial importance of EVA_x copolymers. As noted in the Introduction, EVA_x copolymers can be synthesized with the same high-pressure, free-radical process used to make PE except in this case both ethylene and vinyl acetate are fed to the reactor simultaneously. The vinyl acetate that does not copolymerize with ethylene serves as a cosolvent that helps dissolve EVA_x. Rätzsch and co-workers were the first to show the effect of unreacted vinyl acetate, here called free VA, on the phase behavior of the EVA_x−ethylene system.[104,105] The cloud-point in the temperature range of 160−240 °C is lowered by as much as 400 bar when the amount of free VA in solution matches the amount of VA units in the copolymer. The effect of free VA in solution is more pronounced the lower the temperature, consistent with the notion that polar interactions between free VA and VA units in the copolymer increase with decreasing temperature. Recently, Wohlfarth published more details on the phase behavior of this ternary system along with modeling results.[106] In a related study, Luft and Subramanian[107] have shown that free methyl acrylate in solution increases the region of miscibility of the poly(ethylene-*co*-methyl acrylate)−ethylene system. Although it is industrially relevant to determine the phase behavior of copolymer−comonomer−comonomer mixtures, in the previously described studies it can be difficult distinguishing the effect of ethylene, a quadrupolar solvent, from that of vinyl acetate or methyl acrylate, also a polar molecule.

McHugh and co-workers show that the effect of a polar cosolvent on copolymer−SCF behavior is magnified for a family of EMA_x copolymers in nonpolar propane.[44,108] In these instances acetone and ethanol are the cosolvents. Ethanol has a greater effect than an equal quantity of acetone since ethanol can hydrogen bond to the acrylate groups in the backbone of the EMA_x copolymers. At low ethanol concentrations the acrylate groups available for cross

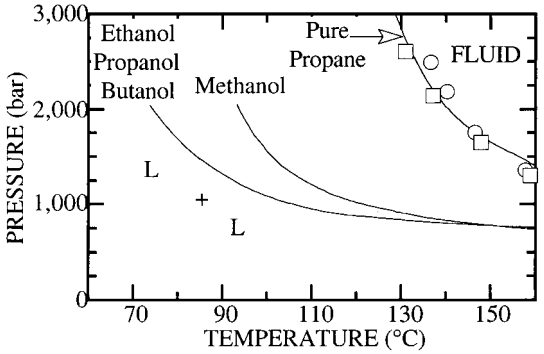

Figure 22. Impact of different cosolvents, all at ~9.6 wt %, on the phase behavior of the 5 wt % EMA_{31} in propane.[64] The data points for the EMA_{31}−propane−alcohol mixtures are not shown on this figure to avoid clutter. The open squares are hexane and the open circles are hexene cosolvent.

association outnumber the ethanol molecules available to self-associate. As the acrylate groups are saturated with ethanol molecules, the further addition of ethanol results in ethanol−ethanol hydrogen bonding which makes the mixed solvent highly polar and induces the copolymer to precipitate from solution. However, because acetone does not self-associate, much more acetone can be added to the solution, which results in a larger single-phase region compared to that obtained with ethanol. The effect of these polar cosolvents is impressive considering that the EMA_x copolymers used in these studies contain greater than 60 mol % nonpolar ethylene groups and that these two cosolvents can be used to precipitate PE from solution. It is readily apparent that the incorporation of polar acrylate groups into the backbone of PE changes polymer properties in a highly nonlinear manner.

The question still remains whether the cosolvent effect is due to enhanced interactions or to increased solvent density. LoStracco et al.[64] addressed this issue by investigating the phase behavior of EMA_{31} in propane with hexane, 1-hexene, and several alcohols. It should be possible to determine whether increasing the density of compressed propane shifts the location of the cloud-point curve by comparing the C_6 curves to the binary EMA_{31}−propane system and to assess the impact of hydrogen bonding by comparing the C_6 curves to those of the alcohols. Figure 22 shows that hexane and hexene have virtually no impact on the location of the EMA_{31}−propane cloud-point curve, whereas the alcohol cosolvents shift the curve by ~50−70 °C. Perhaps it is not surprising that cosolvent density has little impact on the cloud-point curve since the density of propane is greater than approximately 0.5 g cm^{-3} at the elevated pressures shown in Figure 22.[109] Note that the alcohol cloud-point curves increase rapidly in pressure with decreasing temperature due to an increase in alcohol self-association. The methanol curve is ~20 °C higher temperature than the other alcohols since methanol exhibits a stronger energy of self-association while having roughly the same energy of cross association with methyl acrylate.[64] It is also shown that the beneficial effect of an alcohol cosolvent decreases as its concentration increases

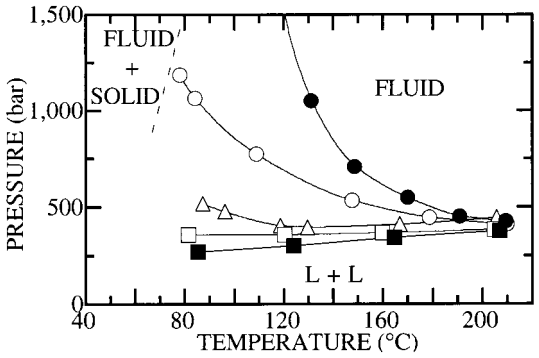

Figure 23. Influence of dimethyl ether (DME) on the phase behavior of 5 wt % poly(ethylene-*co*-methacrylic acid) in butane.[40] Weight percent DME: closed circles, 0; open circles, 5.5; open triangles, 94.9 (pure DME); open squares, 21.1; and closed squares, 36.1.

since the amount of alcohol self-association will dominate that of alcohol−acrylate complex formation for these solutions that have only 5 wt % EMA_{31}.

The effect of a cosolvent can also be very dramatic if the copolymer has polar groups that can self-associate. Consider, for example, the effect of DME on the cloud-point behavior of the poly(ethylene-*co*-3.1 mol % methacrylic acid) ($EMAA_{3.1}$)−butane system shown in Figure 23.[40] The pressures needed to dissolve $EMAA_{3.1}$ in butane decrease significantly when DME is added to the solution since DME hydrogen bonds with the methacrylic acid repeat units. At high temperatures, where acid dimerization is reduced,[110,111] the impact of DME is much less. It is interesting that pure DME is poorer solvent than a mixture of 38 wt % DME and 62 wt % butane. $EMAA_{3.1}$ only has 3.1 mol % acid groups so that once all the methacrylic acid sites are titrated with DME, further addition of DME diminishes the strength of the solvent since it has a smaller polarizability than butane and it is polar.

Figure 24 shows the effect of small amounts of ethanol on the phase behavior of $EMAA_{3.1}$−butane mixtures.[40] Ethanol is a much better cosolvent than DME. The addition of only 1.1 wt % ethanol to the $EMAA_{3.1}$−butane system decreases the cloud-point pressure by 800 bar at 120 °C. At ethanol concentrations greater than 10 wt %, the cloud-point curves are at very low pressures and they exhibit positive slopes. However, the cosolvent effect of ethanol diminishes more rapidly than that of DME. The moles of ethanol sites capable of hydrogen bonding is twice the number of moles of ethanol in solution since both the hydroxyl hydrogen and oxygen in ethanol can participate in hydrogen bonding with a single acrylic acid molecule. It is for this reason that ethanol, at low concentrations, is a better cosolvent than DME. Notice that the cloud-point pressures with ethanol are lower than those with DME probably due to the higher density of ethanol at these temperatures relative to DME, which itself is supercritical.

Figure 24 also shows that the phase behavior changes quite drastically with high concentrations of ethanol.[40] At an ethanol concentration of 15 wt % there are 62 times as many ethanol molecules as compared to methacrylic acid repeat units. Therefore,

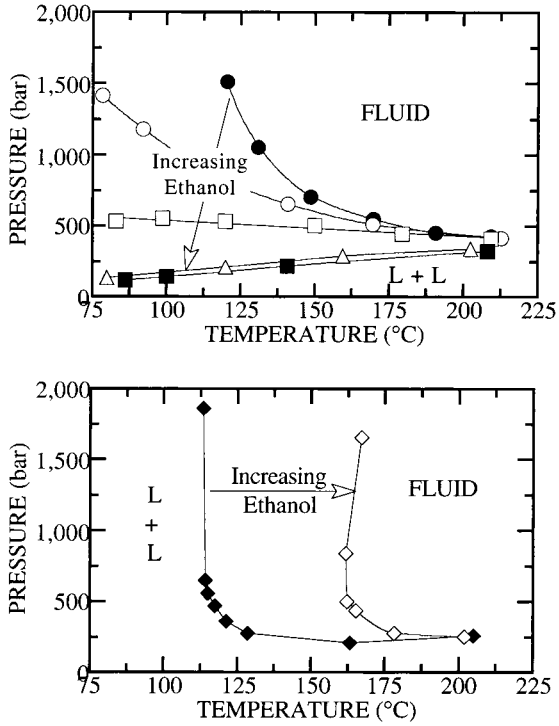

Figure 24. Influence of ethanol on the phase behavior of the poly(ethylene-*co*-methacrylic acid)−butane system.[40] The concentration of copolymer is 5 wt %. Weight percent ethanol: closed circles, 0; open circles, 1.1; open squares, 2.5; open triangles, 10.0; closed squares, 15.1; closed diamonds, 42.2; and open diamonds, 53.5.

the ethanol molecules in excess of the number needed to "saturate" the acrylic acid sites of $EMAA_{3.1}$ are expected to self-associate. At 42.4 wt % ethanol, there are 176 times as many ethanol molecules as compared to methacrylic acid repeat units. The cloud-point curve at this concentration exhibits a sudden increase in pressure at 115 °C, which suggests that the interchange energy is now dominated by the self-association of ethanol that does not favor the formation of a single phase. If the concentration of ethanol is further increased to 53.5 wt %, the cloud-point curve again exhibits a sudden increase in pressure, but now this pressure increase occurs at 160 °C. At 53.5 wt % ethanol, there is a larger concentration of ethanol in excess of that needed to titrate the acid sites as compared to the 42.4 wt % solution. Since the interchange energy depends on the number as well as the strength of ethanol−ethanol associations, temperature has a large impact on the cloud-point behavior. It is not possible to dissolve $EMAA_{3.1}$ in pure ethanol even at 250 °C and 2000 bar.

Although it might be envisioned that a copolymer with a slightly different backbone composition would be a cosolvent for the same type of copolymer in an SCF solvent, in fact, just the opposite cosolvent behavior occurs.[112] The addition of a second copolymer to the solution results in a cloud-point curve that is at higher temperatures than the curves for either of the two binary mixtures. For example, Figure 25 shows the cloud-point curves of PE, EMA_{19}, EMA_{41}, and a 1:1 EMA_{19}−EMA_{41} mixture in nonpolar butane. The cloud-point curve of the EMA_{19}−EMA_{41}−butane mixture does not fall between the curves of the EMA_{19}−butane and the EMA_{41}−butane systems, but

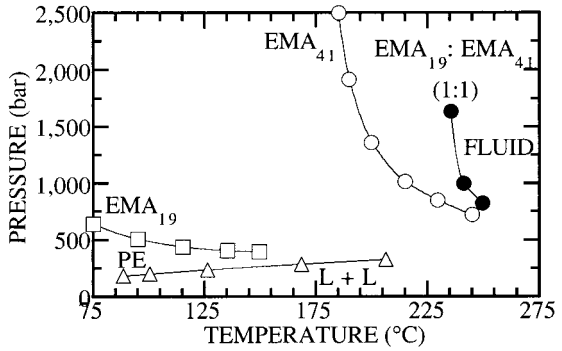

Figure 25. Cloud-point curves of PE, EMA_{19}, EMA_{41},[90] and a 1:1 EMA_{19}−EMA_{41} mixture in butane. A 1:1 mixture of PE and EMA_{41} in butane does not form a single phase to temperatures as high as 238 °C and pressures of 2200 bar. The weight ratio EMA_{19} to EMA_{41} is on a butane-free basis, and the overall copolymer concentration is ∼10 wt % for the copolymer−copolymer−SCF mixtures and ∼5 wt % for the copolymer−SCF solvent mixtures. (Reprinted with permission from ref 112. Copyright 1998 Elsevier.)

rather it is located at 40 °C higher temperatures at a fixed pressure of 1500 bar. In addition, it is not possible to obtain a single phase for a 1:1 mixture of PE with EMA_{41} even to 238 °C and 2200 bar. Similar, but less extreme behavior is observed with butene as the SCF solvent. This study shows that the phase behavior of copolymer−copolymer−solvent mixtures is very sensitive to the difference in chemical architecture of the two copolymers. These data are also consistent with the results from low-pressure studies that suggest that a very small difference in the intermolecular potential energies of the two polymers leads to phase separation.[113−122]

Although it is known that alcohols are good cosolvents for EMA_x copolymers, Lee and McHugh[112] also show that the cloud-point curve for a 1:2.4 EMA_{41}−poly(ethylene-*co*-10 mol % vinyl alcohol) ($EVOH_{10}$) mixture in butane is at higher temperatures than either of the two binary mixture curves. The attenuation of the impact of the hydroxyl groups in $EVOH_{10}$, relative to ethanol, is likely due to the steric hindrance of packing hydroxyl groups tethered to a long-chain, nonpolar polymer in close proximity to the acrylate groups. Also, there are a larger number of methyl acrylate groups in EMA_{41} so that not all of the MA groups are hydrogen bonded to a hydroxyl group.

VI. Fluoropolymer–SCF Phase Behavior

Fluoropolymers are treated as a self-standing section due to their specialty-end applications in the medical and electronics industry and as separation membranes. Very few systematic phase behavior studies have been done on fluorocopolymer−SCF mixtures since fluorinated polymers and copolymers, and particularly poly(tetrafluoroethylene) (PTFE), have generally been considered resistant to dissolution in most common solvents.[123] However, recent studies show that it is possible to dissolve PTFE and its copolymers in many halogenated solvents including tertiary perfluoroamines, perfluorinated olefins, perfluorokerosenes, perfluorinated oils, and polyhexafluoropropylene oxide oligomers.[123−125] Most of

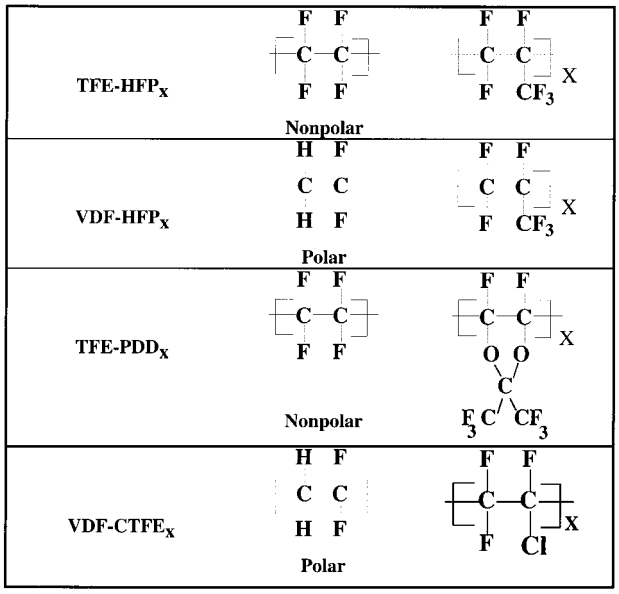

Figure 26. Chemical structure of the repeat units in several fluorocopolymers along with their acronym.

these studies are performed at temperatures near the melting point of PTFE, $T_{melt} \approx 330$ °C, and at atmospheric pressure since solid PTFE remains essentially insoluble in these solvents until it melts. Tuminello et al.[126] demonstrate that low boiling halocarbons, nonsolvents for PTFE at atmospheric pressure, dissolve PTFE at elevated pressures, and they suggest that for these particular halocarbons, solvent density controls solubility once the PTFE melts. A linear relationship exists between the critical temperature of these low boiling halocarbons and the cloud-point pressures for their respective PTFE−solvent mixtures which is not surprising since polarizability scales with critical temperature for nonpolar solvents from the same chemical family. In addition, lower pressure is needed to dissolve PTFE with a solvent that has a higher critical temperature since less pressure is required to densify this less-volatile halocarbon.

In this section data are presented on the solubility of a variety of fluoro(co)polymers in several SCF solvents whose properties are given in Table 1. Figure 26 shows the structures of the fluorocopolymers reported in the literature and the acronyms used with these copolymers. A variety of comonomers are polymerized with tetrafluoroethylene to synthesize copolymers that retain the chemical inertness of PTFE and yet exhibit improved or more facile processing characteristics.

1. Solvent Quality

Figure 27 shows the phase behavior of nonpolar poly(tetrafluoroethylene-*co*-19 mol % hexafluoropropylene) (FEP_{19}) in the fluorinated alkanes that should have closely matched intermolecular potential energies with that of a repeat unit.[30] With 19 mol % hexafluoropropylene added randomly to the backbone of PTFE, the peak melting point is lowered from 327 °C for PTFE to 147 °C for FEP_{19}. Dispersion-type interactions are expected to be the dominant type of intermolecular force of attraction between segments

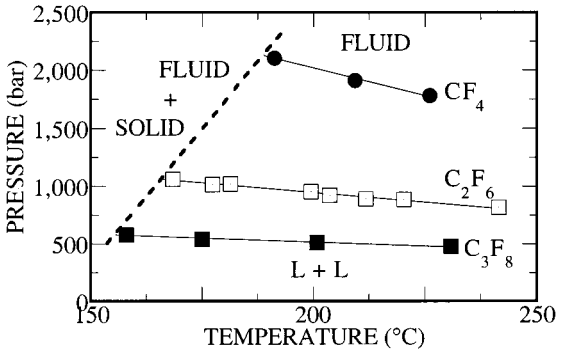

Figure 27. Comparison of the cloud-point curves of ~5 wt % FEP_{19} in CF_4, C_2F_6, and C_3F_8. The dashed line denotes the crystallization boundary. (Reprinted from ref 30. Copyright 1996 American Chemical Society.)

of FEP_{19} given that the hexafluoropropylene incorporated into the copolymer backbone exhibits characteristics of nonpolar hexafluoropropane. The FEP_{19} has a weight-average molecular weight of ~210 000[127] and contains 1000 mass ppm carboxylic acid end groups which should not have a significant effect on the behavior of this polymer. Although CF_4 is a nonpolar fluoroalkane that has properties similar to a repeat unit of FEP_{19}, CF_4 has a small polarizability, which makes it a very feeble SCF solvent. Figure 27 shows that very high pressures are needed to obtain sufficient CF_4 solvent density to solubilize FEP_{19} since CF_4 is highly expanded at 180−260 °C. Note that the crystallization boundary of FEP_{19} in CF_4 occurs at approximately 189 °C at pressures of ~2000 bar compared to a peak melting temperature of 147 °C at atmospheric pressure for pure FEP_{19}. In the presence of solvent at high pressures there are two competing effects that fix the location of the crystallization boundary. One is hydrostatic pressure that increases the melting temperature at a rate of ~1.0 °C/10 bar, which is the rate observed for PTFE.[128,129] The other effect is the melting point depression of FEP_{19} that results from the solubility of CF_4 in the FEP_{19}-rich liquid phase. Thus, while 2000 bar of hydrostatic pressure raises the melting point of pure FEP_{19} from 147 °C to ~347 °C, the presence of CF_4 in the FEP_{19}-rich liquid-phase reduces the temperature of crystallization to ~189 °C at the same pressure.[30]

FEP_{19} cloud-point pressures with C_2F_6 are 700−1000 bar lower than those with CF_4. While CF_4 has a higher molar density than C_2F_6 at the same temperature at their respective cloud-point pressures, the large decrease in cloud-point pressure is attributed to the higher polarizability of C_2F_6 compared to CF_4. Thus, favorable dispersion forces must dominate density effects in this case, making C_2F_6 the better solvent of the two. Also note that the crystallization boundary in C_2F_6 is ~20 °C lower than in CF_4 due to the lower cloud-point pressures in C_2F_6 and to the likely higher solubility of C_2F_6 in the FEP_{19}-rich liquid phase. C_3F_8 has a greater solvent power for FEP_{19} than the other two perfluoroalkanes due to its larger polarizability, despite C_3F_8 having a lower molar density at the same temperatures at their respective cloud-point pressures.[30] Once again, the favorable dispersion forces dominate density effects, making C_3F_8 an even better solvent for FEP_{19}. The difference between the cloud-point pressures in C_3F_8 compared to C_2F_6 is only 300 bar, whereas the difference in C_2F_6 relative to CF_4 is ~1000 bar. The trend of decreasing cloud-point pressure differences with increasing solvent carbon number is similar to that exhibited by PE−normal alkane mixtures.[39,42] The crystallization boundary for the C_3F_8 system occurs at ~158 °C, which is ~10 °C lower than that of the C_2F_6 system and ~33 °C lower than that of the CF_4 system. In fact, the high solubility of C_3F_8 in the FEP_{19}-rich liquid phase, which is implied by the low cloud-point pressures relative to that of the other two fluoroalkanes, virtually offsets the expected 50 °C increase in freezing point of FEP_{19} due to hydrostatic pressure alone.

Mertdogan et al.[30] distinguish the effects of polarity, polarizability, and density from one another by comparing the phase behavior of FEP_{19} in several different fluorocarbon solvents. They show that the cloud-point pressures of FEP_{19} in slightly polar C_3F_6 and $CClF_3$ are similar to those observed in nonpolar C_3F_8 at comparable temperatures. Evidently solvent polar interactions are not significant in this instance since the magnitude of the dipole moments of the two polar solvents are much less than 1 Debye and the effectiveness of these polar moments scale inversely with the square root of the molar volume.[5] The cloud-point pressures in $CClF_3$ are ~1300 bar less than those in CF_4 as a direct consequence of the larger polarizability of $CClF_3$ since it has a smaller molar density than CF_4 at the same temperatures and at their respective cloud-point pressures. On the other hand, Mertdogan finds that the cloud-point pressures for the $CClF_3$ system are lower than those for the C_2F_6 system even though both solvents have essentially the same polarizability. In this case, $CClF_3$ has a slightly higher critical temperature compared to C_2F_6, 28.8 °C vs 19.7 °C, which implies that $CClF_3$ is easier to densify. Also, the crystallization temperature of FEP_{19} in $CClF_3$, ~138 °C, is 30 °C lower than that of FEP_{19} in C_2F_6 which suggests that $CClF_3$ is more soluble in the FEP_{19}-rich liquid phase than is C_2F_6. The difference in the solubility behavior of the $CClF_3$ and C_2F_6 systems is probably due to both the differences in density and in interaction energies.

Sulfur hexafluoride is an interesting solvent for FEP_{19} since it has a modest critical temperature and it is nonpolar with a polarizability that is greater than that of C_2F_6. Figure 28 compares the cloud-point behavior of FEP_{19} in C_3F_8, $CClF_3$, and SF_6. The pressures needed to obtain a single phase are lower in SF_6 except at temperatures greater than 200 °C where cloud-point pressures are lowest for the C_3F_8−FEP_{19} system. The cloud-point curve of the SF_6 system is closest to, but, generally at lower pressures than, the C_3F_8 system. Also, the crystallization boundary in SF_6 is ~30 °C lower than that in C_3F_8. Although SF_6 has a smaller polarizability than C_3F_8, it is a better solvent for FEP_{19} since the molar density of SF_6 is approximately 25% greater than that of C_3F_8 at the same temperature and at their respective cloud-point pressures. Compared to $CClF_3$, SF_6 has a higher polarizability and critical temperature but

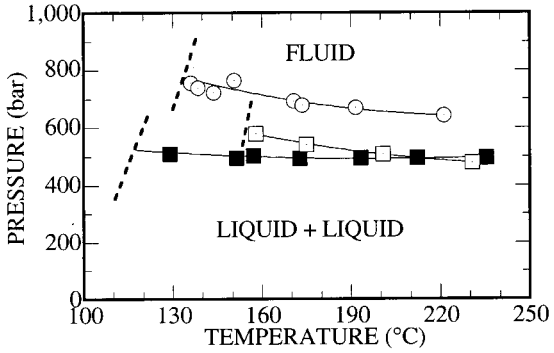

Figure 28. Comparison of the cloud-point curves of ~5 wt % FEP_{19} in $CClF_3$ (open circles), C_3F_8 (open squares), and SF_6 (closed squares). The dashed lines denote the crystallization boundaries. (Reprinted from ref 30. Copyright 1996 American Chemical Society.)

a lower molar density at cloud-point conditions. Nevertheless, SF_6 is a better solvent for FEP_{19} due to the favorable dispersion forces between nonpolar SF_6 and FEP_{19}, which overpowers the effect of density.

2. Branching

To the best of our knowledge, the study that compares the phase behavior of FEP_{19} to FEP_{48} is the only one reporting the effect of branching on phase behavior for a fluorocopolymer−SCF mixture.[130] Figure 29 shows that the cloud-point curves for FEP_{19} and FEP_{48} in CF_4. At temperatures greater than 190 °C, the FEP_{48} curve is shifted 400−500 bar lower in pressure compared to the FEP_{19} curve. The location of the cloud-point curve is determined both by the energy of interaction and the entropy of mixing. The entropic term includes the combinatorial entropy of mixing and the conformational entropy of mixing, the so-called equation of state contribution that is related to the free volume difference between the solvent and the polymer. Adding HFP groups to the backbone of FEP_x copolymers has only a modest effect on the energetics of interaction, but it does increase the free volume of the copolymer that favors dissolution of the copolymer. Also, branching reduces the intermolecular interactions between polymer segments that arise due to short-range molecular orientation of polymers with a high content of linear segments with few pendant groups.[54] Hence, the decrease in cloud-point pressure is a consequence of both the increased free volume of FEP_{48} relative to that of FEP_{19} and the reduced amount of segment−segment interactions expected with FEP_{48}. Similar trends are observed with the phase behavior of supercritical ethane and propane with LLDPE with differing amounts of chain branching as described earlier.[56] The FEP_{48}−CF_4 curve extends to temperatures lower than 190 °C since it does not crystallize. Both cloud-point curves exhibit only a small negative slopes since nonpolar, dispersion interactions are the dominant type of interaction in these systems.

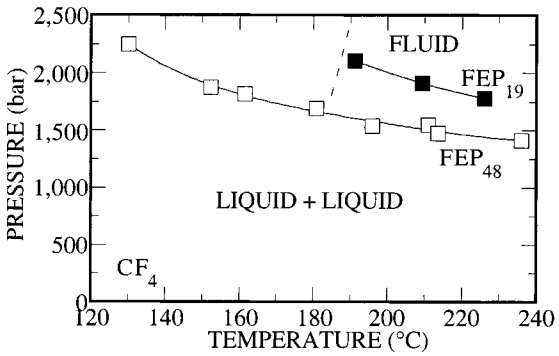

Figure 29. Impact of hexafluoropropylene content in the copolymer backbone on the solubility of poly(tetrafluoroethylene-*co*-hexafluoropropylene) copolymer with 19 mol % HFP (FEP_{19}) and 48 mol % HFP (FEP_{48}) in CF_4. The crystallization boundary of FEP_{19} is denoted by a dashed line and the copolymer concentrations are approximately 5 wt %. (Reprinted from ref 130. Copyright 1998 American Chemical Society.)

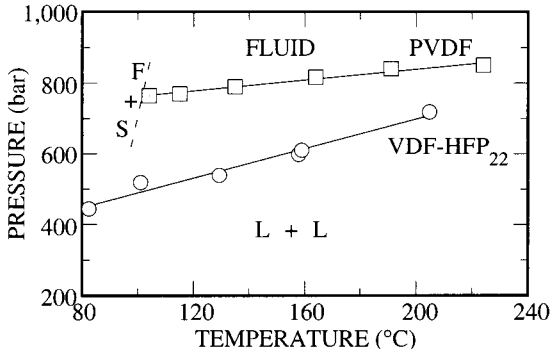

Figure 30. Comparison of the behavior of poly(vinylidene fluoride) (PVDF) and poly(vinylidene fluoride-*co*-22 mol % hexafluoropropylene) (VDF−HFP22) in CH_2F_2.[33] The polymer and copolymer concentrations are ~5 wt %.

McHugh and co-workers[130] also demonstrate that the impact of chain branching on the cloud-point location diminishes as the quality of the solvent increases, as was observed with LLDPE−SCF alkane mixtures.[56] For example, with SF_6 the cloud-point pressures are well below 1000 bar since SF_6 has a much larger polarizability than CF_4. The FEP_{48} curve superposes with the FEP_{19} curve at temperatures greater than 120 °C, but it exhibits a slight positive slope as the temperature is lowered which is at lower pressures than the extrapolated FEP_{19} curve.

DiNoia et al. show the effect of backbone branching on the phase behavior with a comparison of the behavior of poly(vinylidene fluoride) (PVDF) and VDF−HFP_{22} in CH_2F_2.[33] PVDF has a melting point of 170 °C while VDF−HFP_{22} is amorphous. Figure 30 shows that the melting point of PVDF is reduced from 170 °C to 100 °C due to the solubility of CH_2F_2 in the polymer-rich liquid phase. Also note that the VDF−HFP_{22} curve is ~250 bar lower in pressure at temperatures near 100 °C but is only ~125 bar lower at temperatures near 200 °C. The lower pressures and temperatures of the VDF−HFP_{22} curve are a consequence of both energetic and entropic considerations. The increased free volume of VDF−HFP_{22} enhances the mixing process with CH_2F_2 and the hexafluoropropylene in the backbone of VDF−HFP_{22} reduces the number of copolymer segment−segment polar interactions, which makes the interchange energy more favorable for dissolving in CH_2F_2.

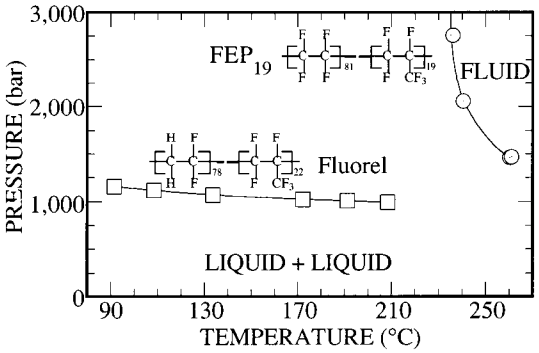

Figure 31. Comparison of the cloud-point curves of poly(vinylidene fluoride-*co*-22.0 mol % hexafluoropropylene) (Fluorel, VDF−HFP_{22})[131] to that of poly(tetrafluoroethylene-*co*-19.3 mol % hexafluoropropylene) (FEP_{19}) in CHF_3.[222] The copolymer concentrations are ∼5 wt %. (Reprinted from ref 131. Copyright 1997 American Chemical Society.)

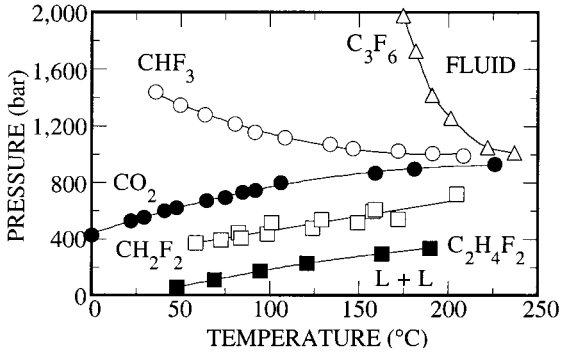

Figure 32. Comparison of the cloud-point curves of 5 wt % poly(vinylidene fluoride-*co*-22.0 mol % hexafluoropropylene) in several SCF solvents.[33]

3. Backbone Architecture

Fluorinated polymers have unique wetting and lubrication properties but generally these polymers are difficult to process because they do not dissolve until melted, and the melting temperatures are very high. For example, poly(vinyl fluoride) melts at 189 °C, poly(vinylidene fluoride) melts at 170 °C, and poly(tetrafluoroethylene) (Teflon) melts at greater than 325 °C. It is possible to copolymerize many fluorovinyl groups with hexafluoropropylene which provides CF_3 branches that disrupt the ability of the copolymer to align in solution and hence to crystallize. As noted with the hydrocarbon copolymers, the type and structure of the comonomer has a strong influence on the temperatures and pressures needed for a single phase. Likewise, as is shown in the following paragraphs, solvent quality also has a significant affect on the location of the cloud-point.

Let us consider the phase behavior of VDF−HFP_{22} in several different SCF solvents.[131] Figure 31 contrasts the behavior of VDF−HFP_{22} with that of FEP_{19} in CHF3, a polar SCF solvent. Notice that the FEP_{19}−CHF_3 cloud-point curve exhibits a very steep slope at ∼230 °C, which suggests that there is an extreme energy mismatch between the nonpolar repeat units in FEP_{19} and polar CHF_3 even at elevated temperatures where configurational polar interactions should be diminished. On the other hand the VDF−HFP_{22}−CHF_3 cloud-point curve is relatively flat near 1000 bar and extends to 30 °C. In this instance there are favorable polar interactions between the VDF groups in the copolymer with polar CHF_3 even at very low temperatures. Pressures of ∼1000 bar are needed to increase the density of CHF_3 sufficiently to modulate the strength of its intermolecular potential so that it is capable of dissolving VDF−HFP_{22}.

Figure 32 shows a comparison of VDF−HFP_{22} cloud-point curves in a series of SCF solvents to reveal the interplay between polarizability and dipole moment. Table 1 shows that both CH_2F_2 and CHF_3 have similar values for polarizability, but CH_2F_2 has a slightly greater dipole which is more than likely the reason the CH_2F_2 cloud-point curve is at lower pressures than the CHF_3 curve. It is readily apparent that CH_2F_2 is the better solvent if the reduced or effective dipole moment, μ_i/(molar volume)$^{0.5}$, is compared. Not surprisingly, the $C_2H_4F_2$ curve is at the lowest pressures since it has the larger polarizability, dipole moment, and solvent densities compared to CH_2F_2 and CHF_3. Although the magnitude of the polarizability is important, the solvent must have a sufficiently large dipole moment to dissolve VDF−HFP_{22}. Notice that the C_3F_6 curve exhibits a very steep slope at ∼150 °C even though this solvent has a larger polarizability compared to the other solvents just described. However, C_3F_6 has a very modest dipole moment so that the interchange favors VDF−VDF interactions as the temperature is reduced below 150 °C and the copolymer falls out of solution. For comparison the cloud-point curve for VDF−HFP_{22} in CO_2 is also shown in this figure. The cloud-point curve falls between those of CHF_3 and CH_2F_2. All three of these SCF solvents have very similar polarizabilities. CHF_3 and CH_2F_2 both have dipole moments and CO_2 has a quadrupole moment. Although it is difficult to predict á priori the behavior of these three copolymer−SCF solvent mixtures, the data in Figure 32 suggest that CO_2 has many of the characteristics of CHF_3 and CH_2F_2, which makes it a candidate replacement solvent for these two fluorocarbon solvents. More information is provide on CO_2 in the next section of this review.

VII. Polymer–CO_2 Behavior

Carbon dioxide has been touted as the solvent of choice for many industrial applications because it is nonhazardous and inexpensive. CO_2, whose properties are listed in Table 1, has a critical temperature near room temperature, a modest critical pressure, and a density higher than most supercritical fluids. It remains a challenge to predict the solvent properties of CO_2 quantitatively since the solution theories that describe intermolecular interactions between solvents and solutes in a dense fluid state are still in a nascent state of development. Several authors have argued that the solvent properties of CO_2 should be compared to those of toluene,[132] acetone,[133] and hexane.[132] These seemingly widely varying opinions on the solvent characteristics of CO_2 reinforce the complexity of definitively categorizing solvent power. Nevertheless, considerable insight into the solvent characteristics of CO_2 is reported here based on well-

characterized and systematic solubility studies that are available in the literature with a wide range of polymers and copolymers.

Before proceeding to a presentation of experimental homopolymer− and copolymer−CO_2 studies, it is worthwhile to revisit briefly the molecular thermodynamic framework developed in an earlier section to characterize the expected solvent properties of CO_2. The pressures and temperatures needed to dissolve a polymer in CO_2 depend on the intermolecular forces between solvent−solvent, solvent−polymer segment, and polymer segment−segment pairs in solution as given by the interchange energy, and on the free volume difference between the polymer and CO_2. Table 1 shows that the polarizability of CO_2 is similar in value to that of perfluoromethane, fluoroform, and dihydrodifluoromethane and it is also close to that of methane. It is intuitively obvious that methane will not be a good SCF solvent unless the system pressure is exceptionally high, or stated differently, unless the density of methane is increased considerably. Hence, by analogy, CO_2 is not expected to be a good solvent at high operating temperatures where dispersion interactions are dominant. Due to structural symmetry, CO_2 does not have a dipole moment, but it does have a substantial quadrupole moment that operates over a much shorter distance than dipolar interactions. CO_2 is a dense solvent at modest temperatures and pressures which magnifies quadrupolar interactions that scale with inverse molar volume to the $^5/_6$ power. As will be shown, CO_2 is a weak solvent for nonpolar polymers since CO_2 quadrupolar interactions dominate the interchange energy as the temperature is lowered. Conversely, CO_2 is a feeble solvent for very polar polymers since dipole interactions outweigh quadrupole interactions, especially at low temperatures where polar interactions are magnified.

Kazarian and co-workers have used spectroscopic techniques to characterize the interactions between CO_2 and polymers.[134] They demonstrate that polymers possessing electron-donating groups, such as carbonyls, exhibit specific interactions with CO_2. The carbon atom of CO_2 acts as an electron acceptor and the carbonyl oxygen in the polymer acts as an electron donator. Kazarian and co-workers show that the strength of the complex between CO_2 and a polymer segment is generally less than 1 kcal/mol which makes it only slightly stronger than dispersion interactions. In certain instances, CO_2−polymer complex formation can be an important consideration when interpreting data at low to moderate temperatures where complexing is expected to be significant. O'Shea and co-workers report similar observations on polar and hydrogen bonding interactions for small molecule−CO_2 mixtures from spectroscopy studies.[135]

Before proceeding to a discussion of polymer−CO_2 phase behavior, a very brief synopsis is given for the many polymerization reaction studies with CO_2 since they contain some information on polymer solubility. It is beyond the scope of this review to detail all of the SCF reaction studies that have been performed and, therefore, only a select few of them are mentioned here to reveal trends concerning polymer solubility in CO_2. A large body of work has been generated demonstrating that CO_2 dissolves hydrocarbon polymers containing fluorinated octyl acrylates.[136−144] Hydrocarbon−fluorocarbon block and graft copolymers also exhibit a high degree of solubility in CO_2.[145−148] It is argued that copolymer solubility depends on the number of fluorinated side groups and on the molecular weight of the side groups relative to the molecular weight of the hydrocarbon main chain. The recurring theme in all of these studies is that fluorinated groups play a significant role in polymer solubility and that some polarity in the polymer also plays a role in fixing solubility levels. It has been suggested that CO_2 may either form a weak complex or that it preferentially clusters near the fluorine of the C−F bonds that are more polar than C−H bonds.[6,134,149] Hence, the fluorinated side groups shield the hydrocarbon main chain from interacting with CO_2. Although creative synthetic chemistry can be used to improve polymer solubility in CO_2, the results from these studies only provide limited insight into why most polymers do not dissolve in CO_2 regardless of temperature and pressure. For example, although fluorinating a polymer enhances its solubility severalfold in CO_2, Mertdogan and co-workers show that fluorination alone does not ensure that the polymer will be soluble in CO_2 at temperatures below 100 °C.[30]

1. Homopolymer–CO_2 Phase Behavior

Krukonis has shown that CO_2 at or near room temperature and at pressures typically below 600 bar dissolves many poly(dimethyl)- and poly(phenylmethyl)silicones, perfluoroalkylpolyethers, and chloro- and bromotrifluoroethylene polymers.[8,150,151] Beckman and co-workers have described the solubility of poly(perfluoropropylene oxide) and also poly(dimethyl siloxane) in CO_2.[152,153] Barton[154,155] and Kiran[156] have also reported on the high solubility of poly(dimethyl siloxane) in CO_2 at approximately 450 bar. The polymers reported to have solubility in CO_2 all possesses some degree of polarity due to oxygen or other electronegative groups such as chlorine or bromine incorporated into the backbone of the polymer. The exceptions are the silicone and siloxane-type polymers. The solubility of the poly(dimethyl) and poly(phenylmethyl) silicones in CO_2 is likely due to the very flexible nature of these polymers that endows them with much larger free volumes as compared to other polymers.

CO_2 does not dissolve polyolefins to any great extent unless the molecular weight is very low. Gregg and co-workers show that a three-arm-star polyisobutylene with a molecular weight of 4000 does not dissolve in CO_2 to temperatures of 200 °C and pressures of 2000 bar.[196] Hagiwara et al. also showed that polyethylene does not dissolve in CO_2 although they provide no information on molecular weight.[157,158] For example, Rindfleisch has shown that nonpolar PE, with an M_w of 108 900, does not dissolve in CO_2 even to temperatures of 270 °C and pressures of 2750 bar.[159] CO_2 can dissolve octane, hexadecane, and squalane, but these nonpolar solutes have molecular weights in the range of 100−500. Figure 33 shows

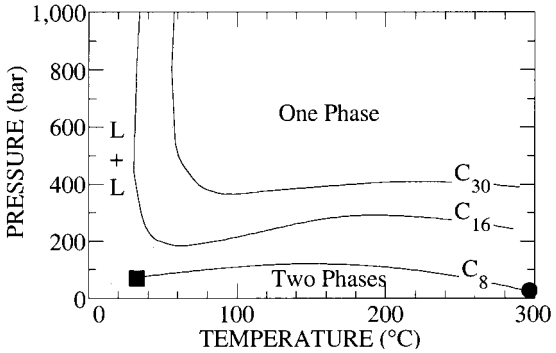

Figure 33. Critical-mixture curves for CO_2 with octane (C_8), hexadecane (C_{16}), and squalane (C_{30}).[221] The closed square and circle are the critical points of CO_2 and octane, respectively. Below each curve two phases exist and at pressure above the curves a single phase exists. Smoothed data curves are presented rather than individual data points.

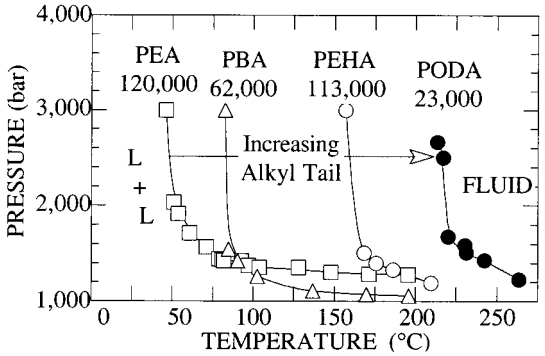

Figure 34. Impact of the nonpolar alkyl tail of the acrylate group on the cloud-point curves of poly(ethyl acrylate) (PEA), poly(butyl acrylate) (PBA), poly(ethylhexyl acrylate) (PEHA), and poly(octadecyl acrylate) (PODA) in CO_2.[159] Listed on each curve is the respective weight average molecular weight, M_w. The polymer concentration is ~5 wt % in each case.

that the characteristics of the hexadecane−CO_2 phase behavior are similar to those exhibited by mixtures of a nonpolar component with a polar one depicted schematically in Figure 4.[160] The cloud-point curve (i.e., the critical-mixture curve in this instance) has a maximum near 300 bar and it shows a sharp upturn in pressure near 30 °C. At these modest temperatures the phase behavior is usually attributed to enthalpic interactions since the curve exhibits UCST-like characteristics. Rindfleisch et al.[159] argue that the sharp increase in the critical-mixture pressure results from a large energy mismatch between CO_2 and hexadecane that is dominated by CO_2−CO_2 quadrupolar interactions rather than CO_2−hexadecane dispersion or induction interactions. For this binary mixture, CO_2 becomes too polar for hexadecane once the temperature is reduced below 30 °C since quadrupolar interactions scale with inverse temperature. If the molecular size of the nonpolar hydrocarbon is approximately doubled to a C_{30}, the critical-mixture curve is shifted to higher pressures and the sharp increase in the critical pressure occurs at 60 °C. The results shown in Figure 33 suggest strongly that CO_2 is too polar to dissolve nonpolar PE even at temperatures in excess of 270 °C. A polymer or copolymer must have some polarity before it will exhibit any solubility in CO_2.

CO_2 can dissolve very low molecular weight, slightly polar polymers, such as polystyrene or telechelic polyisobutylene if the molecular weights are below 1000[8,150,151,161,162] so as to minimize excluded volume interactions that make many high molecular weight polymers difficult to dissolve. Rindfleisch et al.[159] also show that polystyrene with an M_w of 106 000 does not dissolve in CO_2 even to temperatures of 225 °C and pressures of 2100 bar. At first glance this result is somewhat surprising since the aromatic ring in PS has a quadrupole moment that interacts favorably with the quadrupole of CO_2. However, PS has a high glass transition temperature, ~103 °C, that indicates a high hindrance potential for chain segment rotations resulting in enhanced segment−segment interactions that do not favor dissolution.

How much polarity is needed to make a polymer soluble in CO_2? Rindfleisch et al.[159] addressed this issue by determining the cloud-point behavior of a family of poly(acrylates) in CO_2. Figure 34 shows the cloud-point curves for poly(ethyl acrylate) (PEA), poly(butyl acrylate) (PBA), poly(ethylhexyl acrylate) (PEHA), and poly(octadecyl acrylate) (PODA) in CO_2 and the M_w of the polymers. As the alkyl tail on the acrylate increases, the effective polarity decreases since reduced dipole interactions scale inversely with the square root of the molar volume.[5] Likewise, the sharp upturn in cloud-point pressure shifts to higher temperatures with increasing alkyl tail length. PODA has the lowest M_w but the PODA−CO_2 curve turns up sharply in pressure at 215 °C, which is surprising since it suggests that even at this very high temperature, CO_2 is too polar to dissolve PODA. Conversely, as the alkyl tail on the acrylate is decreased, the polymer remains in solution to lower temperatures suggesting that dipole−quadrupole interactions between the acrylate group and CO_2 promote solubility. Note that the free volume difference between the poly(acrylate) and CO_2 decreases with increasing alkyl tail length, but, the gain in conformational entropy of mixing does not outweigh the increased mismatch in energetics accompanying this structural change. The weak solvent character of CO_2 for these poly(acrylates) is manifest in the very high pressures needed to obtain a single phase even at high temperatures where polar interactions are diminished. It is the very low polarizability of CO_2 that results in the need for extremely high pressures to dissolve these polymers.

Interpreting the phase behavior of polymers in CO_2 or any supercritical fluid solvent can be perplexing since the connectivity of the monomer units and the conformation of the polymer in solution affects both the energy and entropy of mixing. For example, even though PMA dissolves in CO_2 at high pressures, poly(methyl methacrylate) with an M_w of 93 300 is not soluble in CO_2 to temperatures of 255 °C and pressures of 2550 bar. This observation is a bit surprising since the strength of PMA−CO_2 intermolecular interactions are expected to be similar to those of PMMA−CO_2. Likewise, poly(ethyl methacrylate) with an M_w of 340 000 also does not dissolve in CO_2 to

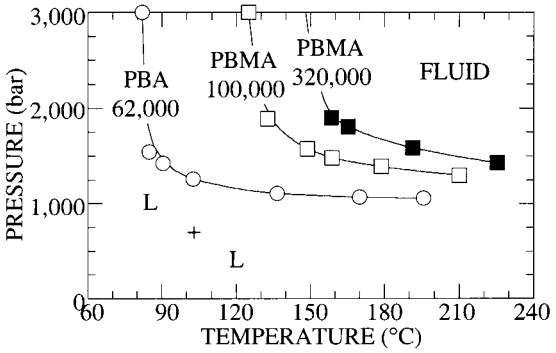

Figure 35. Comparison of the CO_2−poly(butyl acrylate) (PBA) cloud-point curve to two CO_2−poly(butyl methacrylate) (PBMA) curves. The weight average molecular weight, M_w, is given in the figure, and the polymer concentrations are ~5 wt % in each case. (Reprinted from ref 159. Copyright 1996 American Chemical Society.)

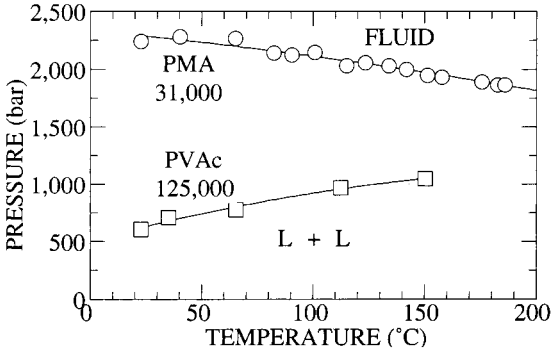

Figure 36. Comparison of the CO_2−poly(methyl acrylate) (PMA) and CO_2−poly(vinyl acetate) (PVAc) cloud-point curves. The weight average molecular weight, M_w, is given in the figure, and the polymer concentrations are ~5 wt % in each case. (Reprinted from ref 159. Copyright 1996 American Chemical Society.)

temperatures of 285 °C and pressures of 2550 bar even though PEA does dissolve. One major difference between these two poly(acrylates) and poly(methacrylates) are that the T_g's are 80−100 °C higher for the methacrylates compared to the acrylates. Enhanced segment−segment interactions are expected for the poly(methacrylates) since the rotation of a methacrylate chain segment is more hindered than a rotation of an acrylate chain segment. CO_2 does dissolve poly(butyl methacrylate) (PBMA) as shown in Figure 35 although in this case the T_g for PBMA is only 70 °C higher than that of PBA. Both PBMA cloud-point curves are shifted to higher temperatures compared to the curve for PBA. The effect of M_w can be quantified by plotting the inverse of the cloud-point temperatures of the two PBMA curves at a fixed pressure with respect to $1/M_w^{0.5}$.[163] At 2500 bar an estimated cloud-point temperature of 116 °C is obtained for PBMA with an M_w of 62 000 which is 33 °C higher than that found for PBA.

On the basis of the phase behavior results presented in the previous figures it is apparent that CO_2 is a very weak supercritical solvent that is sensitive to polymer architecture and to the chemical type and intermolecular potential energy of the repeat units. Figure 36 shows an interesting comparison of the cloud-point curves of PMA and poly(vinyl acetate) (PVAc) in CO_2. The difference between the location of these two curves is quite dramatic. At 30 °C the PMA cloud-point curve is more than 1500 bar higher than the PVAc curve even though the molecular weight of PVAc is four times greater than that of PMA. Both PMA and PVAc are polar, but the T_g for PVAc is approximately 21 °C higher than the T_g of PMA. The slightly higher T_g of PVAc is a reflection of stronger polar interactions between vinyl acetate groups as compared to methyl acrylate groups when these groups are tethered to a polymer chain. CO_2 can more easily access the carbonyl group in PVAc than in PMA, which makes PVAc more soluble in CO_2 with decreasing temperature. Easier access to the carbonyl group in PVAc also makes it easier for CO_2 to form a weak complex with PVAc especially at moderate temperatures.[134]

The preceding examples of polymer solubility in CO_2 demonstrate that hydrocarbon polymers and copolymers must have some polarity to dissolve in CO_2. However, very polar polymers or polymers that are water-soluble are not expected to dissolve in CO_2 even at high temperatures. For example, poly(acrylic acid) does not dissolve in CO_2 to temperatures of 272 °C and pressures of 2220 bar.

2. Copolymer–CO_2 Behavior

The question of how much polarity is needed for CO_2 solubility is probably better addressed by examining the cloud-point curves for poly(ethylene-*co*-methyl acrylate) (EMA_x, where x represents the mole fraction of methyl acrylate groups in the backbone)−CO_2 mixtures shown in Figure 37. As the methyl acrylate content increases in this statistically random copolymer, the cloud-point curve shifts to lower temperatures, suggesting that the energy mismatch is relaxed by dipole−quadrupole interactions between methyl acrylate repeat units and CO_2. In this instance, the acrylate groups in the backbone of the copolymer act as an internal cosolvent. It is also interesting that the cloud-point curves appear to level off in pressure at approximately 1400 bar, which indicates that CO_2 must be highly compressed before it can dissolve these copolymers. As already noted, the high temperature, high-pressure behavior with CO_2 appears with many other polymers and copoly-

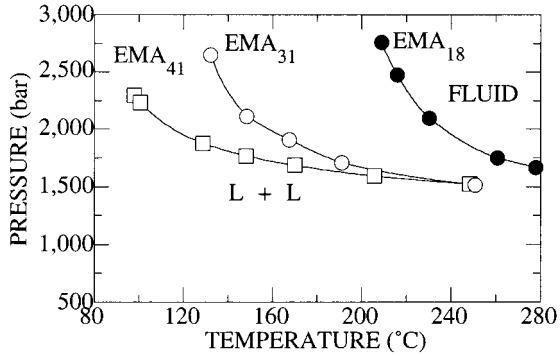

Figure 37. Impact of polar methyl acrylate groups on the location of the cloud-point curves of CO_2−EMA_x mixtures, where x represents the mole fraction of methyl acrylate groups in the copolymer. The copolymer concentrations are ~5 wt % in each case. (Reprinted from ref 159. Copyright 1996 American Chemical Society.)

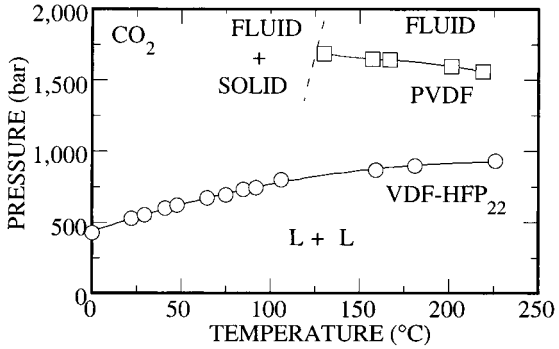

Figure 38. Comparison of the cloud-point behavior of poly(vinylidene fluoride) (PVDF) to that of poly(vinylidene fluoride-*co*-22 mol % hexafluoropropylene) (VDF−HFP_{22}) in CO_2.[33] The polymer and copolymer concentrations are ∼5 wt % in each case.

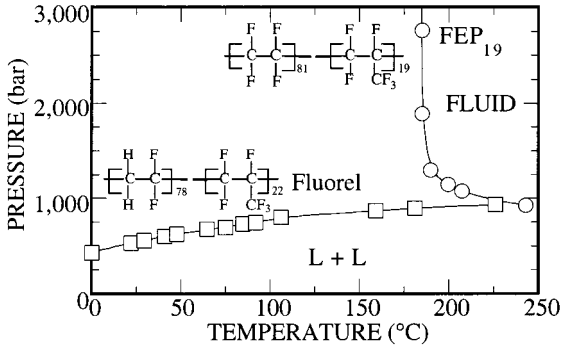

Figure 39. Comparison of the poly(tetrafluoroethylene-*co*-hexafluoropropylene) (TFE-HFP_{19})−CO_2 cloud-point curve[30] and the poly(vinylidene fluoride-*co*-hexafluoropropylene) (Fluorel, VDF−HFP_{22})−CO_2 cloud-point curve.[131] The subscripts on the chemical formulas represent the mole fraction of each comonomer in the backbone of the copolymer. The copolymer concentration is ∼5 wt % in each case. (Reprinted from ref 131. Copyright 1997 American Chemical Society.)

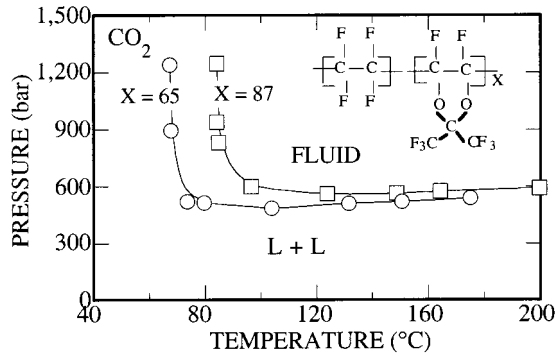

Figure 40. Comparison of the cloud-point behavior of TFE−TDD_{65} (TeflonAF 1600) with 65 mol % dioxole and TFE−TDD_{87} (TeflonAF 2400) with 87 mol % dioxole in CO_2.[33] The copolymer concentration is ∼5 wt % in each case.

mers and it is more than likely a consequence of the very low polarizability of CO_2.

A large body of work has recently been developed on the solubility of fluorinated polymers and copolymers in CO_2. DeSimone and co-workers have measured the solubility of poly(1,1-dihydroperfluorooctylacrylate) (PFOA) in CO_2.[217,218] PFOA is one of the very few fluorocopolymers that dissolves in CO_2 at near room temperatures and pressures of less than 300 bar. PFOA is a good example of utilizing creative chemistry to design a CO_2-soluble polymer. DiNoia et al.[33] report that poly(vinylidene fluoride) (PVDF) dissolves in CO_2 but that poly(vinyl fluoride) (PVF) does not dissolve even at temperatures of 300 °C and pressures of 2750 bar. DiNoia et al. point out that in an earlier study PVDF did not dissolve in CO_2, however, the PVDF used in the earlier study contained a large amount of cross-linked, gel material that is a result of the synthesis technique. Both of these fluoropolymers have very high melting temperatures which is a consequence of strong segment−segment polar interactions. Evidently the dipole moment of PVF is too strong compared to the dipole moment of PVDF. Figure 38 shows that cloud-point pressures in CO_2 decrease if the polarity of PVDF is reduced by randomly mixing 22 mol % hexafluoropropylene (VDF−HFP_{22}) in the backbone of the polymer. The PVDF−CO_2 curve is at pressures of 1500−1700 bar, and it terminates at a crystallization boundary at 130 °C. In contrast, the VDF−HFP_{22}−CO_2 curve is at pressures less than 1000 bar and it extends to 0 °C and 400 bar. Figure 39 shows that if all of the polarity is removed from the copolymer, now an 81 mol % tetrafluoroethylene−19 mol % hexafluoropropylene (TFE-HFP_{19}) copolymer, then very high temperatures are needed to dissolve it in CO_2. The shape of the TFE−HFP_{19} curve is similar to that described earlier for this same copolymer in CHF_3, an SCF solvent with a large dipole moment, 1.7 D, and a polarizability similar in value to that of CO_2. The CHF_3 cloud-point curve exhibits a very steep slope at ∼230 °C due to an energy mismatch between nonpolar TFE−HFP_{19} and polar CHF_3 even at elevated temperatures where configurational polar interactions should be diminished. Pressures of ∼1200 bar are needed to dissolve TFE−HFP_{19} in CHF_3 similar to those found with CO_2. This side by side comparison suggests that CO_2 is not as polar as CHF_3 and that the small polarizabilities of both SCF solvents translates to a need for very high pressures to dissolve TFE−HFP_{19} in the high-temperature region of the phase diagram.

Rindfleisch et al.[159] and DiNoia et al.[33] report that Teflon AF, a random copolymer of tetrafluoroethylene and dioxole, dissolves in CO_2. Figure 40 shows that the cloud-point curve for the copolymer with 87 mol % dioxole groups exhibits a sharp increase in pressure near 85 °C while the curve for the copolymer with 65 mol % has a very similar shape but it is shifted 20 °C lower in temperature. Both copolymers dissolve at pressures of 500−600 bar. The sharp increase in pressure of the cloud-point curve reflects the change in the interchange energy that becomes dominated either by CO_2 quadrupole−quadrupole interactions or by Teflon AF dipole−dipole interactions as the temperature is lowered. It is interesting that these copolymers dissolve in CO_2 even though they both have very high T_g's, 160 °C for the 65 mol % copolymer and 240 °C for the 87 mol % copolymer. The very high T_g is a consequence of the bulky size of the dioxole group that reduces the rotational flexibility of the chain segments. However, as the temperature is lowered, the polar dioxole groups in

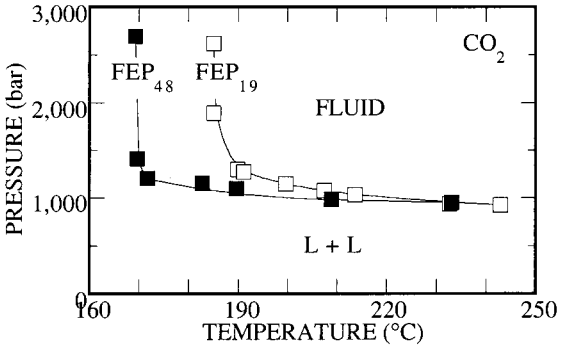

Figure 41. Impact of copolymer hexafluoropropylene content on the solubility of poly(tetrafluoroethylene-*co*-hexafluoropropylene) copolymer with 19 mol % HFP (FEP_{19}) and 48 mol % HFP (FEP_{48}) in CO_2. The copolymer concentration is ~5 wt % in each case. (Reprinted from ref 130. Copyright 1998 American Chemical Society.)

Teflon AF interact favorably with polar CO_2 so that the copolymer remains in solution to moderately low temperatures.

The impact of free volume is shown in Figure 41 that compares cloud-point data for nonpolar TFE−HFP_{19} and TFE−HFP_{48} in CO_2.[130] Both cloud-point curves exhibit the same characteristic shapes even though TFE−HFP_{19} has a peak melting point at 147 °C and TFE−HFP_{48} is amorphous. At high temperatures it takes approximately 1000 bar to dissolve either copolymer in CO_2 which is a consequence of the small polarizability of CO_2. Increasing the hexafluoropropylene (HFP) comonomer content from 19 to 48 mol % shifts the low-temperature portion of the cloud-point curve from 190 to 170 °C. The sharp upturn in cloud-point pressure in both cases is a consequence of quadrupolar interactions between CO_2 molecules that makes the interchange energy unfavorable for dissolving nonpolar TFE−HFP_x.

Certainly fluorinating a polymer or a copolymer makes it CO_2-soluble, but, the pressures needed to solubilize fluorinated copolymers can be very high and they can be extremely temperature sensitive, depending on the polarity of the polymer. It should now be evident why relatively mild pressures and temperatures are needed to dissolve the fluorinated acrylates mentioned previously. The fluorinated acrylate polymers are partially fluorinated, they have bulky fluorinated alkyl tails, and they have carboxyl groups that give them some polarity. All of these features enhance solubility in CO_2.

VIII. Modeling

As mentioned in the Introduction, the incorporation of SCF solvent-based technology for polymer processing would be greatly facilitated if it were possible to simulate different process scenarios with an accurate equation of state. A major objective with modeling is to predict the changes in phase behavior observed as a function of solvent quality or as a function of polymer architecture with a minimum number of fitted parameters. There are several different equations of state that can be used to calculate polymer−SCF solvent phase behavior,[21,37,106,164−169] but only two equations of state are described here, the Sanchez−Lacombe (SL)[170−174] and the Statistical Associating Fluid Theory (SAFT) equation.[88,175−177] These two equations are widely used in the polymer solution thermodynamics community and they are representative examples of the lattice−gas and perturbation models used to describe polymer solution behavior. The Sanchez−Lacombe equation of state is a lattice−gas model in which each component is divided into parts or "mers" that are placed into a lattice and are allowed to interact with a mean-field intermolecular potential. An appropriate number of holes are placed in the lattice to obtain the correct solution density. SAFT is a perturbation-based equation that represents molecules as covalently bonded chains of segments that may contain sites capable of forming associative complexes. A mean-field attractive term is used as a perturbation of the reference equation that consists of terms accounting for the connectivity of the hard segments in the main chain, the hard-sphere repulsion of the segments, and the energy of site−site specific interactions of segments. The merits of each of these polymer solution models are briefly described. The effect of molecular weight or backbone composition polydispersity is not accounted for in the following discussion. Once the formalism is established for calculating polymer−SCF solvent phase behavior, in principle it is not difficult to account for the effects of polydispersity. The goal of this section is to demonstrate how these two equations of state are used to calculate the phase diagram for a polymer−SCF solvent mixture with the minimum of fitted mixture parameters.

1. Sanchez–Lacombe Equation of State

The SL equation of state is derived from a lattice−fluid model that accounts for the compressibility of a solution, or the "free-volume," by introducing holes into the lattice.[172] The SL lattice−gas equation is comprised of a van der Waals-type attractive term with a lattice−gas repulsive term. In reduced form, the equation of state is

$$\tilde{\rho}^2 + \tilde{P} + \tilde{T}\left[\ln(1-\tilde{\rho}) + \left(1 - \frac{1}{r}\right)\tilde{\rho}\right] = 0 \qquad (5)$$

where $\tilde{P}$, $\tilde{T}$, and $\tilde{\rho}$ are the reduced pressure, temperature, and density, respectively. The number of lattice sites occupied by a molecule, r, is

$$r = \frac{MP^*}{RT^*\rho^*} \qquad (6)$$

The reduced parameters for a pure component are

$$\tilde{T} = T/T^* \quad \text{where} \quad T^* = \epsilon^*/R \qquad (7)$$

$$\tilde{P} = P/P^* \quad \text{where} \quad P^* = \epsilon^*/v^* \qquad (8)$$

$$\tilde{v} = 1/\tilde{\rho} = V/V^* \quad \text{where} \quad V^* = N((rv^*) \qquad (9)$$

$$\tilde{\rho} = \rho/\rho^* \quad \text{where} \quad \rho^* = M/rv^* \qquad (10)$$

where T is absolute temperature, ϵ^* is the interaction energy per mer, R is the gas constant, P is the system pressure, v^* is the close-packed molar volume of a mer, V^* is the close-packed volume of the mixture, ρ

is the solution density, and M is the molecular weight. The three characteristic parameters, T^*, P^*, and ρ^* or, equivalently, ϵ^*, v^*, and r, are obtained from fitting the Sanchez−Lacombe equation to pure-component PVT data such as saturated liquid densities and vapor pressures.

For binary and multicomponent mixtures, it is necessary to define a characteristic mixture temperature, pressure, and close-packed molar volume. The characteristic mixture temperature is

$$T^*_{\mathrm{mix}} = \frac{\epsilon^*_{\mathrm{mix}}}{R} \tag{11}$$

where the mixing rule for $\epsilon^*_{\mathrm{mix}}$ is

$$\epsilon^*_{\mathrm{mix}} = \frac{1}{v^*_{\mathrm{mix}}} \Sigma\Sigma \varphi_i \varphi_j \epsilon^*_{ij} v^*_{ij} \tag{12}$$

and the cross term, ϵ^*_{ij}, is

$$\epsilon^*_{ij} = (\epsilon^*_{ii}\, \epsilon^*_{jj})^{0.5}(1 - k_{ij}) \tag{13}$$

where k_{ij} is a fitted, binary mixture parameter that corrects the energy of the mixture for specific binary interactions between components i and j not accounted for by a simple geometric-mean average. The volume fraction a component, φ_i, is

$$\varphi_i = \frac{\dfrac{m_i}{(\rho_i v_i)}}{\displaystyle\sum_c \frac{m_c}{(\rho_c v_c)}} \tag{14}$$

where m_i is the mass fraction of component i.

The mixing rule for v^*_{mix} is

$$v^*_{\mathrm{mix}} = \Sigma\Sigma \varphi_i \varphi_j v^*_{ij} \tag{15}$$

where the cross term, v^*_{ij}, is the arithmetic mean of the two pure-component characteristic volumes,

$$v^*_{ij} = {}^1/_2(v^*_{ii} + v^*_{jj})\,(1 - \eta_{ij}) \tag{16}$$

where η_{ij} is a fitted mixture parameter that accounts for the packing of a polymer segment with a solvent segment. The adjustable binary mixture parameters, k_{ij} and η_{ij}, are determined by fitting experimental binary pressure−composition (P−x) isotherms. In general, reasonable values of k_{ij} and η_{ij} are between ±0.2. These two parameters are expected to be close to zero for a mixture of components that come from the same chemical family and therefore have similar intermolecular potential energy functions.

The mixing rule for the number of sites that a mixture occupies is

$$\frac{1}{r_{\mathrm{mix}}} = \Sigma \varphi_i / r_i \tag{17}$$

The characteristic pressure of the mixture is

$$P^*_{\mathrm{mix}} = \frac{R T^*_{\mathrm{mix}}}{V^*_{\mathrm{mix}}} \tag{18}$$

At equilibrium, the fugacity of each of the components present in each of the phases must be equal. For a two-phase, L_1−L_2 system, the fugacity relationships are

$$F_i^{L_1} = F_i^{L_2} \quad \text{or} \quad y_i \phi_i^{L_1} = x_i \phi_i^{L_2}$$
$$i = 1, 2 \tag{19}$$

where F_i is the fugacity of component i, x, and y are mole fractions in each of the phases, ϕ is the fugacity coefficient, and L_1 and L_2 represent the two liquid phases, respectively. Oftentimes, it is convenient to recast the fugacity relationships in terms of chemical potential, μ_i

$$\exp\left[\frac{\mu_i^{L_1} - \mu_i^{L_2}}{RT}\right] = 1 \tag{20}$$

For details on the mechanics of polymer−SCF solvent phase equilibrium calculations, the reader is directed to the work of Koak and Heidemann[178] which describes the peculiarities associated with these type of calculations. At most pressures the calculated concentrations of polymer in the SCF-rich solvent phase can be less than the underflow limit of the computer. Hence, the polymer mass fraction should be fixed at a very low value such as 10^{-75} and the equality of the polymer chemical potential in each of the phases is removed from the calculation. In addition, successive substitution can become oscillatory and divergent, which can be remedied if the substitution is damped. However, damping does increase the time needed to calculate a tie line.

The chemical potential is obtained from the thermodynamic relationship

$$\mu_i = \left(\frac{\partial G}{\partial N_i}\right)_{T,P,N_{i\neq j}} \tag{21}$$

where the Gibbs free energy of the mixture is derived using the SL equation of state.[171] Note that N_i is the number of moles of component i. With the SL equation the chemical potential of component i in a mixture is

$$\mu_i = RT\left[\ln \varphi_i + \left(1 - \frac{r_i}{r_{\mathrm{mix}}}\right)\right] + r_i\left\{-\tilde{\rho}[2/v^*_{\mathrm{mix}}(\sum_{j=1}^{c} \varphi_j v^*_{ij}(\epsilon^*_{ij} - \epsilon^*_{\mathrm{mix}})) + \epsilon^*_{\mathrm{mix}}] + RT\tilde{v}\left[(1 - \tilde{\rho})\ln(1 - \tilde{\rho}) + \frac{\tilde{\rho}}{r_i}\ln\tilde{\rho}\right] + P\tilde{v}[2\sum_{j=1}^{c} \varphi_j v^*_{ij} - v^*_{\mathrm{mix}}]\right\} \tag{22}$$

Pure-component parameters, T^*, P^*, and ρ^*, are fit to saturated liquid density and vapor pressure data to within 50 °C of the critical temperature for the solvent and to PVT data for the polymers. The SL equation of state is not expected to predict accurately the critical point of a pure component since it is a mean-field equation.[171] The determination of SCF pure-component parameters is sensitive to the number of liquid density data points used in the fitting routine. If it is important to fit the critical point of the solvent accurately it is necessary to reduce the number of liquid density data points used in the fitting routine. However, a good fit of the solvent critical point usually results in calculated saturated liquid densities that are ~20% lower than experimental values.

Compilations of characteristic parameters for polymers and low molecular weight substances can be found in the literature.[170,171] Rogers[179] presents PVT data for a large number of polymers and some copolymers that can be used to regress pure-component polymer parameters. The parameters for statistically random copolymers can also be estimated with the mixing rules given in equations 12−17. In this instance, the parameters of the two homopolymers that comprise the copolymer are used in the mixing rules along with the volume percent of each comonomer present in the backbone of the copolymer.[180] The mixture parameters, k_{ij} and η_{ij}, that are now homopolymer−homopolymer parameters rather than polymer−solvent parameters, typically have little effect on the calculated cloud-point curves and should be set equal to zero.

The SL equation of state has been used to model polymer−SCF solvent and polymer−SCF solvent−cosolvent phase behavior with varying degrees of success. Usually it is necessary to allow both binary mixture parameters, k_{ij} and η_{ij}, to be functions of temperature to obtain a good representation of the phase behavior even if the polymer and SCF solvent are both nonpolar.[30,39,44,91,181,182] In an alternative approach, Kiran and co-workers advocate allowing k_{ij} to vary with the molecular weight of the polymer.[52,181−183] Of course, if k_{ij} is allowed to vary, more fitted parameters are introduced. However, it is not apparent how to extrapolate the values of these parameters from one system to another since there is no fundamental basis for choosing a particular functional form for the temperature or molecular weight dependence. Another difficulty with predicting phase behavior as opposed to fitting it, is that the calculated cloud-point curves are very sensitive to the value used for k_{ij} which is usually determined after fitting at least a small amount of binary data.

The SL equation has also been used to calculate poly(ethylene-*co*-methyl acrylate) (EMA_x)−SCF solvent phase behavior with modest success.[31,39,44,56,91] As noted earlier, a good representation of the phase behavior is obtained only if the binary mixture parameters are allowed to vary with temperature. The dilemma of this approach is that mixture data are needed to obtain a reasonable estimate of the mixture parameters, that is, you need to know the answer to get the answer! As more methyl acrylate is added to the copolymer backbone, k_{ij} values increase and become strong functions of temperature to account for polar interactions. The values of η_{ij} are large and negative for most crystalline copolymers and it is necessary to make η_{ij} a function of temperature. It is not too surprising that the SL model does a poor job modeling polar copolymer−SCF solvent phase behavior since this is a mean-field equation of state with mixing rules that assume that the mixture is random. Hence, polar configurational interactions are not taken into consideration except through a temperature-dependent k_{ij}. The need for a temperature-dependent packing parameter, η_{ij}, even for nonpolar PE−ethane mixtures,[56] probably is a consequence of the conformational properties of the polymer chain that affects the packing of solvent molecules around segments of the polymer. Chain dimensions in solution are expected to be sensitive to temperature. The major benefit of the SL equation is that it is very tractable and it can be used to interpolate data. It is also possible to use the SL to calculate the phase behavior of ternary polymer−SCF solvent-cosolvent mixtures,[44,52,181,183] but once again, the performance of this equation is only fair.

If any of the components in the solution can hydrogen bond or form a complex, a different version of the SL equation is needed.[184] Panayiotou and Sanchez[185] used a "quasi-chemical" approach to decompose the partition function into contributions from associative and nonassociative interactions where the nonassociative partition function is that of the original Sanchez−Lacombe equation of state. The partition function for association is determined by calculating the number of ways that hydrogen bonds can be distributed in the system with the constraint that the total hydrogen bonding energy remains constant. Given the limitations of the SL equation for calculating polymer−SCF solvent phase behavior, it is recommended that the SAFT equation be used for mixtures that have components that can cross-associate or self-associate.

2. SAFT Equation of State

SAFT is a perturbation-based equation that represents molecules as covalently bonded chains of segments that may contain sites capable of forming associative complexes. A mean-field attractive term is used as a perturbation of the reference equation that consists of terms accounting for the connectivity of the hard segments in the main chain, the hard-sphere repulsion of the segments, and the energy of site−site specific interactions of the segments with themselves or other segments. With this approach, the residual Helmholtz free energy relative to an ideal gas reference state is

$$a^{\mathrm{res}} = (a^{\mathrm{hs}} + a^{\mathrm{chain}} + a^{\mathrm{assoc}}) + a^{\mathrm{disp}} \qquad (23)$$

where a^{hs} accounts for segment−segment, hard-sphere repulsion,[186] a^{chain} accounts for connectivity of the segments,[176,177] a^{assoc} accounts for site−site specific interactions[176,177] such as hydrogen bonding based on Wertheim's associating fluid theory,[187−190] and a^{disp} accounts for the mean-field, dispersion

attraction between segments.[191] The Helmholtz free energy expressions, both for pure components and mixtures, are given in detail in the literature[88,175] and are not reproduced here.

The equation for the fugacity coefficient, ϕ_i, is obtained from

$$\ln \phi_i = \left(\frac{\partial(\mathrm{Na}^{\mathrm{res}}/RT)}{\partial N_i}\right)_{T,V,N_{j\neq i}} - \ln Z \qquad (24)$$

where Z is the compressibility of the mixture, R is the gas constant, T is the temperature, N is the total number of moles in the system, V is the total system volume, and N_i is the number of moles of component i in the system. Equation 24 can be rewritten in terms of the residual Helmholtz energy as

$$\ln \phi_i = \left\{\frac{\partial\left[\frac{a^{\mathrm{res}}}{RT}\right]}{\partial x_i}\right\}_{T,V,N_{j\neq i}} - \sum x_j \left\{\frac{\partial\left[\frac{a^{\mathrm{res}}}{RT}\right]}{\partial x_j}\right\}_{T,V,N_{j\neq i}} + a^{\mathrm{res}}/RT + (Z-1) - \ln Z \qquad (25)$$

where x_i is the mole fraction of component i. Huang and Radosz provide the derivatives in eq 25 in a parametrized form.[88]

There are five pure-component parameters in the SAFT equation: v^{oo}, the temperature-independent volume of a segment, u^o/k, the temperature-independent, nonspecific energy of attraction between two segments, m, the number of segments in a molecule, ϵ/k, the energy of association between sites on a molecule, and v, the volume of association. A square-well model is used for association interactions where the energy of association, ϵ/k, is the depth of the well and the volume of association, v, is the width of the well.[176,177,192] Estimates for the energy of hydrogen bonding can be made from spectroscopic measurements with liquids that have the same functional groups as found in the SCF solvent or in the polymer. Estimates for v can be made by analogy to the tabulated values regressed from pure-component data.[88]

The mixing rules for the volume of a segment, v^o, the energy of attraction, u, and the number of segments in the mixture, m, are

$$v^0 = \sum_i \sum_j x_i x_j m_i m_j v_{ij}^0 \quad \text{where} \quad v_{ij}^0 = \frac{1}{8}[v_i^{0\,1/3} + v_j^{0\,1/3}]^3 \qquad (26)$$

$$\frac{u}{kT} = \frac{1}{v^0}\sum_i \sum_j x_i x_j m_i m_j \left[\frac{u_{ij}}{kT}\right] v_{ij}^0 \quad \text{where} \quad u_{ij} = (u_{ii}\, u_{jj})^{1/2}(1 - k_{ij}) \qquad (27)$$

and

$$m = \sum_i \sum_j x_i x_j m_{ij} \quad \text{where} \quad m_{ij} = \frac{1}{2}(m_i + m_j)(1 - \eta_{ij}) \qquad (28)$$

Equations 27 and 28 contain binary mixture parameters, k_{ij} and η_{ij}, that are fitted to experimental data. Typically η_{ij} is set equal to zero since it has essentially the same affect on the location of the cloud-point curve as does k_{ij}.

Pure-component parameters for small molecule systems are reported in the literature.[175] Although PVT data are available for many polymers[179] a regression of polymer parameters from PVT data leads to completely wrong phase equilibrium calculations.[61,193,194] From the regression of PVT data the values for v^{oo} and u^o/k are usually overestimated, while the value for m tends to be underestimated. The dilemma with SAFT is that calculated polymer densities are not very sensitive to variations in pure-component parameters while phase equilibria calculations are very sensitive to these parameters. Consider, for example, calculations for the phase behavior of the PEA−ethylene system presented earlier. The pure-component parameters for PEA, obtained from a fit of density data[179] to within 2%, are 17.17 cm^3/mol for v^{oo}, 778.5 for m, and 367.4 K for u^o/k. With these values, and with k_{ij} set equal to zero, the calculated cloud-point curve is more than 7000 bar too high relative to the experimental curve! If k_{ij} is set equal to −0.150, a large negative value, a portion of the cloud-point curve is in reasonable agreement with the experimental data, but, the calculated curve has a positive slope indicative of LCST-type behavior, while the experimental curve has a negative slope. The primary reason that cloud-point calculations are so far off in this instance is that the value of u^o/k is much too large.[193]

A number of different schemes have been suggested for determining m, v^{oo}, and u^o/k for a polymer. Radosz and co-workers propose that m be determined from the correlation found for n-alkanes,[84,85−87,161,162,195,196] which should work reasonably well for polyolefins with modest side-chain branching or with ethylene-acrylate,[85,95,193,197] ethylene-vinyl acetate,[102] or ethylene-acid,[195,197−199] copolymers with modest amounts of comonomer in the backbone. Radosz and co-workers also propose that v^{oo} for a polymer be set equal to 12.0 cm^3/mol that follows from a fit of alkane data.[84−87,161,162,195,196] Fixing the value of v^{oo} is not unreasonable since changing it by ∼10% has only a modest affect on the calculated phase behavior.[200] The difficulty once again is how to determine a reasonable estimate for u^o/k. In many cases Radosz and co-workers set u^o/k equal to 210 K, the value for an infinite molecular weight alkane, which is reasonable for their calculations since they are mainly concerned with polyolefin−SCF solvent phase behavior. The issue still remains how to determine u^o/k for other classes of polymers since fitting polymer PVT data does not provide a reasonable estimate for u^o/k.[61,193,201]

Fortunately the values for m and v^{oo} follow regular trends depending on the structural features of the species under consideration, which suggests that a group-contribution method can be used for their determination. Lora and McHugh[61,201] extend the group-contribution approach of Huang and Radosz[88,175] for calculating m and v^{oo} for polymers as a

function of the values for a repeat unit and with m corrected for the size of the polymer utilizing the number average molecular weight. However, the group contribution approach cannot be used to calculate the energy parameter of a segment, u^o/k, since for a given chemical family this parameter varies in a nonlinear manner with respect to molecule size. Lora and McHugh[61,201] suggest that it is possible to determine a value for u^o/k by two different methods. In one case u^o/k is calculated for the monomer from a fit of vapor pressure and liquid density data, and then this value is used for the corresponding polymer. A value of k_{ij} is obtained from a fit of monomer-solvent phase behavior data. In the second approach a single polymer−SCF solvent cloud-point curve is used to determine u^o/k for the polymer and k_{ij} for the polymer−solvent pair. The value of u^o/k then remains fixed for all other polymer−SCF solvent pairs.

Several examples are provided where reasonable values of the monomer parameters are obtained from the group contribution approach coupled with the fit of liquid density and vapor pressure data.[61,201] However, in many cases the calculated cloud-point curve does not agree even qualitatively with the experimental curve if the value of u^o/k for the polymer is set equal to that of the monomer and if k_{ij} is set equal to zero. A good fit of the polymer−SCF solvent cloud-point curve is obtained if both u^o/k for the polymer and if k_{ij} are allowed to vary. In most cases the value of k_{ij} found from a fit of monomer-SCF solvent phase behavior is very different from the value found from a fit of polymer−SCF solvent behavior. Another general finding[61,201] is that the difference between $(u^o/k)_{\text{polymer}}$ obtained from a fit of a cloud-point curve and $(u^o/k)_{\text{monomer}}$ increases with increasing polarity of the repeat groups.

The predictive power of the SAFT equation for polymer−supercritical solvent systems is limited since a nonzero value of k_{ij} is needed to obtain a reasonable representation of the phase behavior. As more systematic modeling studies are performed with polymer−supercritical solvent mixtures it may be possible to provide general guidelines for estimating k_{ij} much in the same manner as is done with the Peng−Robinson equation for small molecule mixtures. Further work is needed to extend the group contribution approach to other chemical families, and to find a more accurate method to calculate the energy parameter of strongly polar polymers since it is not possible to use the value regressed for the monomer. Nevertheless, the SAFT model has been used to calculate the phase behavior of many different polymer−SCF solvent mixtures,[61,84−87,95,102,161,162,182,193−202] which has sparked a great deal of research to address its current limitations.

IX. Conclusions

Several trends can be gleaned from the large body of polymer−SCF phase behavior studies reported in this review. Supercritical fluids are weak solvents for polymers especially those SCF solvents that are the lowest molecular weight members of a chemical family. The relative improvement in solvent quality diminishes as the molecular weight of the SCF solvent increases as long as the solvents come from the same chemical family. The phase behavior of polymer−SCF mixtures falls essentially into only two different classes. In one class the cloud-point curve exhibits a positive slope in P−T space, so-called LCST behavior. In the other class, the cloud-point curve exhibits a steep increase in pressure as the temperature is lowered which occurs if either the SCF solvent or the polymer is polar and the other component is nonpolar. The larger the difference in polarity between these two components, the higher the temperature where the slope in the cloud-point curve suddenly increases. Polymer−SCF solvent hydrogen bonding or complexing dramatically improves solvent quality that, in turn, lowers the pressures and temperatures needed to obtain a single phase. However, if the polymer self-associates, it is virtually impossible to dissolve it in a nonpolar solvent. Polymer architecture plays a very important role in determining solubility in an SCF solvent. In fact, SCF solvents are such weak solvents that even the interactions of end groups can dictate solubility for polymers with molecular weights in excess of 100 000.

CO_2, perhaps the most widely promoted SCF solvent, exhibits both polar and nonpolar character although the nonpolar character of CO_2 is very modest and is similar to that of methane and perfluoromethane, which are weak SCF solvents. CO_2 does not dissolve polyolefins as long as the molecular is greater than a few thousand. Several studies have demonstrated that fluorinating a hydrocarbon polymer can improve its solubility in supercritical CO_2, but, some polarity must be added to the polymer to significantly reduce cloud-point pressures and temperatures. At present it remains a challenge to quantify the amount of polarity in the polymer that is needed to ensure solubility. Although not reviewed here, high-pressure NMR has also been used successfully to elucidate specific CO_2−fluorocarbon interactions in low molecular weight fluorocarbon solvents[203] and fluorocarbon repeat units in different fluorinated polymers and copolymers.[204] These data provide valuable insight for interpreting the unique solvent characteristics of supercritical CO_2.

Equations of state still need further refinement before they can be used to predict polymer−SCF solvent phase behavior rather than to model and characterize the phase behavior after the fact. Many of the difficulties inherent in predicting and interpreting polymer−SCF behavior reside in the entropy of mixing. ΔS_{mix} depends on both the combinatorial entropy of mixing and the noncombinatorial contribution associated with the volume change on mixing. As shown in this review, high molecular weight polymers typically dissolve in SCF solvents at temperatures and pressures very far removed from the critical point of the solvent. At high pressures SCF densities are the same order of magnitude as that of a typical organic liquid and are relatively insensitive to changes in pressure or temperature. Hence, the combinatorial entropy of mixing a polymer with an SCF solvent should not vary significantly with tem-

perature and pressure near the conditions where the polymer dissolves in solution and, it should be noted that the combinatorial entropy always promotes the mixing of a polymer with a solvent. The central issues, then, for interpreting polymer−SCF solution behavior are the determination of the energetics of mixing and the conformational entropy of the polymer which contributes to the noncombinatorial entropy of mixing. In this review we demonstrated that it is possible to obtain a coarse-grain indication of the energetics of mixing as described by the balance of SCF−polymer interactions relative to SCF−SCF and polymer segment−segment interactions from the characteristics exhibited by the cloud-point curve. The location in P−T space and the shape of the cloud-point curve for a given polymer can shift significantly when substituting one SCF solvent for another since most low molecular weight supercritical fluids are extremely weak solvents in the absence of hydrogen bonding. However, it is not possible to assert that the characteristics of the binodal curve are a consequence of strictly energetic considerations since the conformation of the polymer chain responds to its local environment and it affects the entropy of mixing. In addition, polymer chain conformation has a major impact on the accessibility of the solvent to the repeat units of the coil. Information on the role of chain conformation on solubility is slowly emerging as light, X-ray, and neutron scattering studies are reported quantifying the impact of polymer chain dimensions and polymer−SCF solvent interactions on the breadth of the single-phase region.[205,206,207] These scattering techniques are themselves challenging since a radiation source and detector must be coupled to a high-pressure cell with well defined geometrical characteristics so that artifacts of the apparatus are kept to a minimum. However, the benefits of these techniques can be significant since SCF properties are tunable which means that it is possible to traverse the entire good-to-θ-to-poor solvent quality spectrum by adjusting solvent density with changes in pressure at a single temperature and in a single solvent. These supramolecular to macromolecular to submacromolecular length scale studies will provide deeper insight into role of microscopic level interactions on macroscopically observed phase behavior.

X. Acknowledgments

The authors acknowledge the National Science Foundation for partial support of this project under Grant CTS-9729720, and they acknowledge the donors of the Petroleum Research Society administered by the ACS.

XI. References

(1) Ehrlich, P.; Mortimer, G. A. *Adv. Polym. Sci.* **1970**, *7*, 386.
(2) Whelan, T. *Polymer Technology Dictionary*; Chapman and Hall: London, 1994.
(3) Hsu, T. T.-P.; Langer, R. *J. Biomed. Mater. Res.* **1985**, *19*, 445.
(4) Saltzman, W. M.; Sheppard, N.; McHugh, M. A.; Dause, R. B.; Pratt, J. A.; Dodrill, A. M. *J. Appl. Polym. Sci.* **1993**, *48*, 1493.
(5) Prausnitz, J. M.; Lichtenthaler, R. N.; Azevedo, E. G. *Molecular Thermodynamics of Fluid Phase Equilibria*, 2nd ed.; Prentice Hall: Englewood Cliffs, NJ, 1986.
(6) Patterson, D. *Polym. Eng. Sci.* **1982**, *22*, 64.
(7) Lee, L. L. *Molecular Thermodynamics of Nonideal Fluids*; Butterworth Publishers: Stoneham, MA, 1988.
(8) McHugh, M. A.; Krukonis, V. J. *Supercritical Fluid Extraction: Principles and Practice*, 2nd ed.; Butterworth Publishers: Stoneham, MA, 1994.
(9) Scott, R. L. *Ber. Bunsen-Ges. Phys. Chem.* **1972**, *76*, 296.
(10) Scott, R. L.; van Konynenburg, P. B. *Discuss. Faraday Soc.* **1970**, *49*, 87.
(11) Bardin, J. M.; Patterson, D. *Polymer* **1969**, *10*, 247.
(12) Rowlinson, J. S.; Swinton, F. L. *Liquids and Liquid Mixtures*, 3rd ed.; Butterworth Publishers: Boston, 1982.
(13) Freeman, P. I.; Rowlinson, J. S. *Polymer* **1960**, *1*, 20.
(14) Allen, B.; Baker, C. H. *Polymer* **1965**, *6*, 181.
(15) Baker, C. H.; Clemson, C. S.; Allen, G. *Polymer* **1966**, *1*, 525.
(16) Zeman, L.; Biros, J.; Delmas, G.; Patterson, D. *J. Phys. Chem.* **1972**, *76*, 1206.
(17) Zeman, L.; Patterson, D. J. *J. Phys. Chem.* **1972**, *76*, 1214.
(18) Saeki, S.; Konno, S.; Kuwahara, N.; Nakata, M.; Kaneko, M. *Macromolecules* **1974**, *7*, 521.
(19) Cowie, J. M. G.; McEwen, I. J. *Macromolecules* **1974**, *7*, 291.
(20) Koningsveld, R.; Staverman, A. J. *J. Polym. Sci.: Part C* **1967**, *16*, 1775.
(21) de Loos, T. W.; Lichtenthaler, R. N.; Diepen, G. A. *Macromolecules* **1983**, *16*, 117.
(22) de Loos, T. W.; Poot, W.; Diepen, G. A. *Macromolecules* **1983**, *16*, 111.
(23) Koningsveld, R.; Staverman, A. J. *J. Polym. Sci: Part A-2* **1968**, *6*, 305.
(24) Koningsveld, R.; Staverman, A. J. *J. Polym. Sci: Part A-2* **1968**, *6*, 325.
(25) Koningsveld, R.; Staverman, A. J. *J. Polym. Sci: Part A-2* **1968**, *6*, 349.
(26) Solc, K. *Macromolecules* **1970**, *3*, 665.
(27) Irani, C. A.; Cozewith, C. *J. Appl. Polym. Sci.* **1986**, *31*, 1879.
(28) Lee, S.-H.; LoStracco, M. A.; Hasch, B. M.; McHugh, M. A. *J. Phys. Chem.* **1994**, *98*, 4055.
(29) de Loos, Th. W.; Poot, W.; Lichtenthaler, R. N. *J. Supercrit. Fluids* **1995**, *8*, 282.
(30) Mertdogan, C. A.; Byun, H.-S.; McHugh, M. A.; Tuminello, W. H. *Macromolecules* **1996**, *29*, 6548.
(31) Meilchen, M. A.; Hasch, B. M.; McHugh, M. A. *Macromolecules* **1991**, *24*, 4878.
(32) Saeki, S.; Kuwahara, N.; Konno, S.; Kaneko, M. *Macromolecules* **1973**, *6*, 246.
(33) DiNoia, T. P.; Conway, S. E.; Lim, J. S.; McHugh, M. A. *Macromolecules*, submitted for publication.
(34) Liu, T.; Nace, V. M.; Chu, B. *J. Phys. Chem.* **1997**, *101*, 8074.
(35) Ehrlich, P. *Polym. Sci. A* **1965**, *3*, 131.
(36) Swelheim, T.; de Swaan Arons, J.; Diepen, G. A. M. *Recueil* **1965**, *84*, 261.
(37) Walsh, D. J.; Dee, G. T. *Polymer* **1988**, *29*, 656.
(38) Condo, P. D.; Coleman, E. J.; Ehrlich, P. *Macromolecules* **1992**, *25*, 750.
(39) Hasch, B. M.; Meilchen, M. A.; Lee, S.-H.; McHugh, M. A. *J. Polym. Sci.: Part B, Polym. Phys. Ed.* **1992**, *30*, 1365.
(40) Lee, S.-H.; McHugh, M. A. *Polymer* **1997**, *38*, 1317.
(41) Lee, S.-H. Unpublished data.
(42) Ehrlich, P.; Kurpen, J. J. *J. Polym. Sci.; Part A* **1963**, *1*, 3217.
(43) Whaley, P. D.; Winter, H. H.; Ehrlich, P. *Macromolecules* **1997**, *30*, 4882.
(44) Hasch, B. M.; Meilchen, M. A.; Lee, S.-H.; McHugh, M. A. *J. Polym. Sci.: Part B, Polym. Phys. Ed.* **1993**, *31*, 429.
(45) Spahl, R.; Luft, G. *Ber. Bunsen-Ges. Phys. Chem.* **1982**, *86*, 621.
(46) Linder, A.; Luft, G. *High Temp. − High Press.* **1977**, *9*, 563.
(47) Luft, G.; Linder, A. *Angewandte Makromol. Chemie* **1976**, *56*, 99.
(48) Hamada, F.; Fujisawa, K.; Nakajima, A. *Polymer J.* **1973**, *4*, 316.
(49) Kiran, E.; Zhuang, W. In *Supercritical fluids, extraction and pollution prevention*; American Chemical Society: Washington, DC, 1997; Chapter 1, p 2−36.
(50) Kiran, E.; Zhuang, W. *Polymer* **1992**, *33*, 5259.
(51) Kiran, E.; Zhuang, W.; Sen, Y. L. *J. Appl. Sci.* **1993**, *47*, 895
(52) Xiong, Y.; Kiran, E. *J. Appl. Polym. Sci.* **1994**, *53*, 1179.
(53) Conway, S. E.; McHugh, M. A.; Wang, J. D.; Mandel, F. S. *J. Appl. Polym. Sci.*, submitted for publication.
(54) Charlet, G.; Ducasse, R.; Delmas, G. *Polymer* **1981**, *22*, 1190.
(55) Kleintjens, L. A.; Koningsveld, R.; Gordon, M. *Macromolecules* **1980**, *13*, 303.
(56) Hasch, B. M.; Lee, S.-H.; McHugh, M. A.; Watkins, J. J.; Krukonis, V. J. *Polymer* **1993**, *34*, 2554.
(57) Watkins, J. J.; Krukonis, V. J.; Condo, P. J.; Pradhan, D.; Ehrlich, P. *J. Supercrit. Fluids* **1991**, *4*, 24.
(58) Chen, S.-J.; Banaszak, M.; Radosz, M. *Macromolecules* **1995**, *28*, 1812.
(59) Han, S. J.; Lohse, D. J.; Radosz, M.; Sperling, L. H. *PMSE* **1996**, *75*, 279; also, *Macromolecules* **1998**, *31*, 2533.
(60) Whaley, P. D.; Winter, H. H.; Ehrlich, P. *Macromolecules* **1997**, *30*, 4887.

(61) Lora, M.; Rindfleisch, F.; McHugh, M. A. *J. Appl. Polym. Sci.*, in press.
(62) Cowie, J. M. G.; McEwen, I. J. *J. Chem. Soc., Faraday Trans.* **1974**, *70*, 171.
(63) Wolf, B. A.; Blaum, G. *Polym. Sci.: Part B: Polym. Phys.* **1975**, *13*, 1115.
(64) LoStracco, M. A.; Lee, S.-H.; McHugh, M. A. *Polymer* **1994**, *35*, 3272.
(65) Cowie, J. M. G.; McCrindle, J. T. *Eur. Polym. J.*, **1972**, *8*, 1185.
(66) Cowie, J. M. G.; McCrindle, J. T. *Eur. Polym. J.* **1972**, *8*, 1325.
(67) Cowie, J. M. G.; McEwen, I. J. *Polymer* **1983**, *24*, 1449.
(68) Katime, I. A.; Sasia, P. M.; Eguia, B. *Eur. Polym. J.* **1988**, *24*, 1159.
(69) Blanco, M. D.; Teijon, J. M.; Katime, I. A. *Eur. Polym. J.* **1990**, *26*, 249.
(70) Palaiologou, M.; Viras, F.; Viras, K. *Eur. Polym. J.* **1988**, *24*, 1191.
(71) Viras, F.; Viras, K. *J. Polym. Sci.: Part B: Polym. Phys.* **1988**, *26*, 2525.
(72) Wolf, B. A.; Blaum, G. *Makromol. Chem.* **1976**, *177*, 1073.
(73) McHugh, M. A.; Rindfleisch, R.; Kuntz, P. T.; Schmaltz, C.; Buback, M. *Polymer* **1998**, *39*, 6049.
(74) Irani, C. A.; Cozewith, C.; Kasegrande, S. S. U.S. Patent 4,319, 021, 1982.
(75) McHugh, M. A.; Guckes, T. L. *Macromolecules* **1985**, *18*, 674.
(76) McClellan, A. K.; Bauman, E. G.; McHugh, M. A. Polymer solution-supercritical fluid phase behavior, Paper presented at the AIChE Annual Meeting, San Francisco, CA. 1984.
(77) McClellan, A. K.; McHugh, M. A. *J. Polym. Sci. Eng.* **1985**, *25*, 1088.
(78) Seckner, A. J.; McClellan, A. K.; McHugh, M. A. *AIChE J.* **1988**, *34*, 9.
(79) Guckes, T. L.; McHugh, M. A.; Cozewith, C.; Hazelton, R. L. U.S. Patent 4,946, 940, 1990.
(80) Kiran, E.; Xiong, Y. *J. Supercrit. Fluids* **1998**, *11*, 173.
(81) Xiong, Y.; Kiran, E. *Polymer* **1997**, *38*, 5185.
(82) Kiamos, A. A.; Donohue, M. D. *Macromolecules* **1994**, *27*, 357.
(83) Kennis, H. A. J.; de Loos, Th. W.; de Swann Arons, J.; van der Haegan, R.; Kleintjens, L. A. *Chem. Eng. Sci.* **1990**, *45*, 1875.
(84) Chen, S.-J.; Radosz, M. *Macromolecules* **1992**, *25*, 3089.
(85) Chen, S.-J.; Economou, I. G.; Radosz, M. *Macromolecules* **1992**, *25*, 4987.
(86) Chen, S.-J.; Economou, I. G.; Radosz, M. *Fluid Phase Equilib.* **1993**, *83*, 391.
(87) Gregg, C. J.; Chen, S.-J.; Stein, F. P.; Radosz, M. *Fluid Phase Equilib.* **1993**, *83*, 375.
(88) Huang, S. H.; Radosz, M. *Ind. Eng. Chem. Res.* **1991**, *30*, 1994. [See Huang, S. H.; Radosz, M. *Ind. Eng. Chem. Res.* **1993**, *32*, 762 for correct form of equation A24.]
(89) Lee, S.-H. Unpublished EMA_{31}−DME data.
(90) Pratt, J. A.; Lee, S.-H.; McHugh, M. A. *J. Appl. Polym. Sci.* **1993**, *49*, 953.
(91) Meilchen, M. A.; Hasch, B. M.; McHugh, M. A. *Macromolecules* **1991**, *24*, 4874.
(92) Van Ness, H. C.; Van Winkle, J.; Richtol, H. H.; Hollinger, H. B. *J. Phys. Chem.* **1967**, *71*, 1483.
(93) Yoshida, Z.; Osawa, E. *J. Am. Chem. Soc.* **1966**, *88*, 4019.
(94) Rätzsch, M. T.; Wagner, P.; Wohlfarth, C.; Gleditzsch, S. *Acta Polym.* **1983**, ***34***, 340.
(95) Byun, H.-S.; Hasch, B. M.; McHugh, M. A.; Mähling, F.−O.; Busch, M.; Buback, M. *Macromolecules* **1996**, *29*, 1625.
(96) Pratt, J. A.; McHugh, M. A. *J. Supercrit. Fluids* **1996**, *9*, 61.
(97) Chang, S. Y.; Morawetz, H. *J. Phys. Chem.* **1956**, *60*, 782.
(98) Morawetz, H.; Gobran, R. H. *J. Poly Sci.* **1954**, *12*, 133.
(99) McHugh, M. A. *NATO ASI Series E* **1994**, *273*, 599.
(100) Hasch, B. M.; Lee, S.-H.; McHugh, M. A. *Fluid Phase Equilib.* **1993**, *83*, 341.
(101) Rätzsch, M. T.; Wagner, P.; Wohlfarth, C.; Heise, D. *Acta Polym.* **1982**, *33*, 463.
(102) Folie, B.; Gregg, C.; Luft, G.; Radosz, M. *Fluid Phase Equilib.* **1996**, *120*, 11.
(103) Luft, G.; Wind, R. W. *Chem. Ing. Tech.* **1992**, *64*, 1114.
(104) Wohlfarth, C.; Wagner, P.; Glindemann, D.; Völkner, M.; Rätzsch, M. T. *Acta Polym.* **1984**, *35*, 498.
(105) Rätzsch, M. T.; Findeison, R.; Sernow, V. S. *Z. Phys. Chem.* **1980**, *261*, 995.
(106) Finck, U.; Wohlfarth, C.; Heuer, T. *Ber. Bunsen-Ges. Phys. Chem.* **1992**, *96*, 179.
(107) Luft, G.; Subramanian, N. S. *Ind. Eng. Chem. Res.* **1987**, *26*, 750.
(108) Meilchen, M. A.; Hasch, B. M.; Lee, S.-H.; McHugh, M. A. *Polymer* **1992**, *33*, 1922.
(109) Vargaftik, N. B. *Handbook of Physical Properties of Liquids and Gases*, 2nd ed.; Hemisphere: Washington, 1983.
(110) Buback, M.; Mähling, F. *J. Supercrit. Fluids* **1995**, *8*, 119.
(111) MacKnight, W. J.; Taggart, W. P.; McKenna, L. *J. Polym. Sci.* **1974**, *46*, 83.
(112) Lee, S.-H.; McHugh, M. A. *Polymer* **1998**, *39*, 5447.
(113) Dobry, A.; Boyer-Kawenoki, F. *J. Polym. Sci.* **1947**, *2*, 90.
(114) Tong, Z.; Einaga, Y.; Miyashita, H.; Fujita, H. *Macromolecules* **1987**, *20*, 1888.
(115) Berek, D.; Lath, D.; Durdovic, V. J. *Polym. Sci., Part C* **1967**, *16*, 659.
(116) Narasimhan, V.; Lloyd, D. R.; Burns, C. M. *J. Appl. Polym. Sci.* **1979**, *23*, 749.
(117) Narasimhan, V.; Huang, R. Y. M.; Burns, C. M. *J. Polym. Sci., Polym. Phys. Ed.* **1983**, *21*, 1993 (see also refs 4−27 herein).
(118) Lau, W. W. Y.; Burns, C. M.; Huang, R. Y. M. *J. Appl. Polym. Sci.* **1984**, *29*, 1531.
(119) Robled-Muniz, J. G.; Tseng, H. S.; Lloyd, D. R.; Ward, T. C. *Polym. Eng. Sci.* **1985**, *25*, 934.
(120) Narasimhan, V.; Huang, R. Y. M.; Burns, C. M. *J. Polym. Sci., Polym. Symp.* **1986**, *74*, 265.
(121) Tseng, H. S.; Lloyd, D. R.; Ward, T. C. *J. Polym. Sci., Polym. Phys. Ed.* **1987**, *25*, 325.
(122) Walsh, D. J.; Higgins, J. S.; Rostami, S. *Macromolecules* **1983**, *16*, 388.
(123) Smith, P.; Gardner, K. H. *Macromolecules* **1987**, *18*, 1222.
(124) McCain, G. H.; Covitch, M. J. *J. Electrochem. Soc.* **1984**, *31*, 1350.
(125) Tuminello, W. H.; Dee, G. T. *Macromolecules* **1994**, *27*, 669.
(126) Tuminello, W. H.; Brill, D. J.; Walsh, D. J.; Paulaitis, M. E. *J. Appl. Polym. Sci.* **1995**, *56*, 495.
(127) Tuminello, W. H. *Int. J. Polym. Anal. Character.* **1996**, *2*, 141.
(128) Tuminello, W. H.; Dee, G. T.; McHugh, M. A. *Macromolecules* **1995**, *28*, 1506.
(129) Zoller, P. *J. Appl. Polym. Sci.* **1978**, *22*, 633.
(130) McHugh, M. A.; Mertdogan, C. A.; DiNoia, T. P.; Anolick, C.; Tuminello, W. H.; Wheland, R. *Macromolecules* **1998**, 31, 2252.
(131) Mertdogan, C. A.; DiNoia, T. P.; McHugh, M. A. *Macromolecules* **1997**, *30*, 7511.
(132) Hyatt, J. A. *J. Org. Chem.* **1984**, *49*, 5097.
(133) Walsh, J. M.; Ikonomou, G. D.; Donohue, M. D. *Fluid Phase Equilib.* **1987**, *33*, 295.
(134) Kazarian, S. G.; Vincent, M. F.; Bright, F. V.; Liotta, C. L.; Eckert, C. A. *J. Am. Chem. Soc.* **1996**, *118*, 1729.
(135) O'Shea, K. E.; Kirmse, K. M.; Fox, M. A.; Johnston, K. P. *J. Phys. Chem.* **1991**, *95*, 7863.
(136) DeSimone, J. M.; Zhibin, G.; Elsbernd, C. S. *Science* **1992**, *257*, 945.
(137) DeSimone, J. M.; Maury, E. E.; Menceloglu, Y. Z.; McClain, J. B.; Romack, T. J.; Combles, J. R. *Science* **1994**, *265*, 356.
(138) Maury, E. E.; DeSimone, J. M. *Polym. Prepr.* **1994**, *35*, 8.
(139) Guan, Z.; Combes, J. R.; Menceloglu, Y. Z.; DeSimone, J. M. *Macromolecules* **1993**, *26*, 2663.
(140) Guan, Z.; DeSimone, J. M. *Macromolecules* **1994**, *27*, 5527.
(141) Romack, T. J.; Maury, E. E.; DeSimone, J. M. *Macromolecules* **1995**, *28*, 912.
(142) DeSimone, J. M.; Maury, E. E.; Lemert, R. M.; Combes, J. R. *Makromol. Chem. Makromol. Symp.* **1993**, *67*, 251.
(143) Shaffer, K. A.; DeSimone, J. M. *Trends Polym. Sci.* **1995**, *3*, 146.
(144) Hsiao, Y. L.; Maury, E. E.; DeSimone, J. M.; Mawson, S.; Johnston, K. P. *Macromolecules* **1995**, *28*, 8159.
(145) Canelas, D. A.; Betts, D. E.; DeSimone, J. M. *Macromolecules* **1996**, *29*, 2818.
(146) Adamsky, F. A.; Beckman, E. J. *Macromolecules* **1994**, *27*, 312.
(147) Hoefling, T. A.; Newman, D. A.; Enick, R. M.; Beckman, E. J. *J. Supercrit. Fluids* **1993**, *6*, 165.
(148) Newman, D. A.; Hoefling, T. A.; Beitle, R. R.; Beckman, E. J.; Enick, R. M. *J. Supercrit. Fluids* **1993**, *5*, 205.
(149) Shah, V. M.; Hardy, B. J.; Stern, S. A. *J. Polym. Sci., Polym. Phys. Ed.* **1993**, *31*, 313.
(150) Yilgor, I.; McGrath, J. E.; Krukonis, V. J. *J. Polym. Bul.* **1984**, *12*, 499.
(151) Krukonis, V. J. *J. Polym. News* **1985**, *11*, 7.
(152) Hoefling, T. A.; Enick, R. M.; Beckman, E. J. *J. Phys. Chem.* **1991**, *95*, 7127.
(153) Hoefling, T. A.; Stofesky, D.; Reid, M.; Beckman, E. J.; Enick, R. M. *J. Supercrit. Fluids* **1992**, *5*, 237.
(154) Dris, G.; Barton, S. W. *Polym. Mater. Sci. Eng.* **1996**, *74*, 226.
(155) Zhao, X.; Watkins, R.; Barton, S. W. *J. Appl. Polym. Sci.* **1995**, *55*, 773.
(156) Xiang, Y.; Kiran, E. *Polymer* **1995**, *36*, 4817.
(157) Hagiwara, M.; Mistui, H.; Machi, S.; Kagiya, T. *J. Polym. Sci.: Part A-1* **1968**, 6, 603.
(158) Hagiwara, M.; Mistui, H.; Machi, S.; Kagiya, T. *J. Polym. Sci.: Part A-1* **1968**, 6, 609.
(159) Rindfleisch, F.; DiNoia, T. P.; McHugh, M. A. *J. Phys. Chem.* **1996**, *100*, 15581.
(160) Liphard, K. G.; Schneider, G. M. *J. Chem. Thermodyn.* **1975**, *7*, 805.
(161) Gregg, C. J.; Stein, F. P.; Radosz, M. *Macromolecules* **1994**, *27*, 4972.
(162) Gregg, C. J.; Stein, F. P.; Radosz, M. *Macromolecules* **1994**, *27*, 4981.
(163) Sun, S. F. *Physical Chemistry of Macromolecules*; John Wiley and Sons: New York, 1994.
(164) Song, Y.; Lambert, S. M.; Prausnitz, J. M. *Macromolecules* **1994**, *27*, 441.

(165) Sako. T.; Wu, A. H.; Prausnitz, J. M. *J. Appl. Polym. Sci.* **1989**, *38*, 1839.
(166) Chen, S.-J.; Radosz, M. *Macromolecules* **1992**, *25*, 3089.
(167) Rudolf, B.; Kressler, J.; Shimomai, K.; Ougizawa, T.; Inoue, T. *Acta Polym.* **1995**, *46*, 312.
(168) Wohlfarth, C.; Finck, U.; Schultz, R.; Heuer, T. *Angew. Makromol. Chem.* **1992**, *198*, 91.
(169) Kiran, E.; Saraf, V. P.; Sen, Y. L. *Int. J. Thermophys.* **1989**, *10*, 437.
(170) Sanchez, I. C.; Lacombe, R. H. *J. Phys. Chem.* **1976**, *80*, 2568.
(171) Sanchez, I. C.; Lacombe, R. H. *Macromolecules* **1978**, *11*, 1145.
(172) Sanchez, I. C. *J. Macromol. Sci.-Phys.* **1980**, *3*, 565.
(173) Sanchez, I. C.; Balazs, A. C. *Macromolecules* **1989**, *22*, 2325.
(174) Shim, J.-J.; Johnston, K. P. *AIChE J.* **1991**, *37*, 607.
(175) Huang, S. H.; Radosz, M. *Ind. Eng. Chem. Res.* **1990**, *29*, 2284.
(176) Chapman, W. G.; Gubbins, K. E.; Jackson, G.; Radosz, M. *Fluid Phase Equilib.* **1989**, *52*, 31.
(177) Chapman, W. G.; Gubbins, K. E.; Jackson, G.; Radosz, M. *Ind. Eng. Chem. Res.* **1990**, *29*, 1709.
(178) Koak, N.; Heidemann, R. A. *Ind. Eng. Chem. Res.* **1996**, *35*, 4301.
(179) Rodgers, P. A. *J. Appl. Polym. Sci.* **1993**, *48*, 1061
(180) Panayiotou, C. G. *Makromol. Chem.* **1987**, *188*, 2733.
(181) Kiran, E.; Xiong, Y.; Zhuang, W. *J. Supercrit. Fluids* **1993**, *6*, 193.
(182) Xiong, Y.; Kiran, E. *J. Appl. Polym. Sci.* **1995**, *55*, 1805.
(183) Xiong, Y.; Kiran, E. *Polymer* **1994**, *35*, 4408.
(184) Haschets, C. W.; Shine, A. D. *Macromolecules* **1993**, *26*, 5052.
(185) Panayiotou, C.; Sanchez, I. C. *Macromolecules* **1991**, *24*, 6231.
(186) Carnahan, N. F.; Starling, K. E. *J. Chem. Phys.* **1969**, *51*, 635.
(187) Wertheim, M. S. *J. Stat. Phys.* **1984**, *35*, 19.
(188) Wertheim, M. S. *J. Stat. Phys.* **1984**, *35*, 35.
(189) Wertheim, M. S. *J. Stat. Phys.* **1986**, *42*, 459.
(190) Wertheim, M. S. *J. Stat. Phys.* **1986**, *42*, 477.
(191) Alder, B. J.; Young, D. A.; Mark, M. A. *J. Chem. Phys.* **1972**, *56*, 3013.
(192) Chapman, W. G.; Gubbins, K. E.; Joslin, C. G.; Gray, C. G. *Pure Appl. Chem.* **1987**, *59*, 53.
(193) Hasch, B. M.; Lee, S.-H.; McHugh, M. A. *J. Appl. Polym. Sci.* **1996**, *59*, 1107.
(194) Hasch, B. M.; McHugh, M. A. *J. Polym. Sci.: Polym. Phys. Ed.* **1995**, *33*, 715.
(195) Banaszak, M.; Chen, C. K.; Radosz, M. *Macromolecules* **1996**, *29*, 6481.
(196) Gregg, C. J.; Stein, F. P.; Radosz, M.*J. Phys. Chem.* **1994**, *98*, 10634.
(197) McHugh, M. A. In *Supercritical Fluids*; Levelt Sengers, J. M. H., Kiran, E., Eds.; Kluwer Academic Publishers: Boston, 1994; p 599.
(198) Lee, S. H.; LoStracco, M. A.; McHugh, M. A. *Macromolecules* **1996**, *29*, 1349.
(199) Lee, S. H.; Hasch, B. M.; McHugh, M. A. *Fluid Phase Equilib.* **1996**, *117*, 61.
(200) Lee, S.-H.; LoStracco, M. A.; McHugh, M. A. *Macromolecules* **1994**, *27*, 4652.
(201) Lora, M.; McHugh, M. A. *Fluid Phase Equilib.*, in press.
(202) Suresh, J.; Enick, R.; Beckman, E. *Macromolecules* **1994**, *27*, 348.
(203) Dardin, A.; DeSimone, J. M.; Samulski, E. T. *J. Phys. Chem. B* **1998**, *102*, 1775.
(204) Dardin, A.; Cain, J. B.; DeSimone, J. M.; Johnson, Jr., C. S.; Samulski, E. T. *Macromolecules* **1997**, *30*, 3593.
(205) McClain, J. B.; Londono, D.; Combes, J. R.; Romack, T. J.; Canelas, D. A.; Betts, D. E.; Wignall, G. D.; Samulski, E. T.; DeSimone, J. M. *J. Am. Chem. Soc.* **1996**, *118*, 917.
(206) Fulton, J. L.; Pfund, D. M.; McClain, J. B.; Romack, T. J.; Maury, E. E.; Combes, J. R.; Samulski, E. T.; DeSimone, J. M.; Capel, M. *Langmuir* **1995**, *11*, 4241.
(207) Chillura-Martino, D.; Triolo, R.; McClain, J. B.; Combes, J. R.; Betts, D. E.; Canelas, D. A.; DeSimone, J. M.; Samulski, E. T.; Cochran, H. D.; Londono, D.; Wignall, G. D. **1996**, *383*, 3.
(208) Reid, R. C.; Prausnitz, J. M.; Poling B. E. *The Properties of Gases and Liquids*, 4th ed.; McGraw-Hill: New York, 1987.
(209) Braker, W.; Mossman, A. L. *Matheson Gas Data Book*, 6th ed.; Matheson: Lyndhurst, NJ, 1980.
(210) Miller, K. J.; Savchik, J. A. *J. Am. Chem. Soc.* **1979**, *101*, 7206.
(211) Ali, S. *Z. Phys. Chem.* **1983**, *137*, 13.
(212) Bungert, B.; Sadowski, G.; Arlt, W. *Fluid Phase Equilib.* **1997**, *139*, 349.
(213) Haschets, C. W.; Blackwood, T. A.; Shine, A. D. *Polym. Prepr.* **1993**, *34*, 602.
(214) Lele, A. K.; Shine, A. D. *Ind. Eng. Chem. Res.* **1994**, *33*, 1476.
(215) Maderek, E.; Schulz, G. V.; Wolf, B. A. *Eur. Polym. J.* **1983**, *19*, 963.
(216) Lora, M.; Lim, J. S.; McHugh, M. A. *J. Phys. Chem.* **1998**, submitted for publication.
(217) Luna-Barcenas, G.; Mawson, S.; Takishima, S.; DeSimone, J. M.; Sanchez, I. C.; Johnston, K. P. *Fluid Phase Equilib.* **1998**, *146*, 325.
(218) Hsiao, Y.-L.; Maury, E. E.; DeSimone, J. M.; Mawson, S.; Johnston, K. P. *Macromolecules* **1995**, *28*, 8159.
(219) DiNoia, T. P.; McHugh, M. A.; Cocchiaro, J. E.; Morris, J. B. *Waste Manage.* **1997**, *17*, 151.
(220) Mawson, S.; Johnston, K. P.; Combes, J. R.; DeSimone, J. M. *Macromolecules* **1995**, *28*, 3182.
(221) Liphard, K. G.; Schneider, G. M. *J. Chem. Thermodyn.* **1975**, *7*, 805.
(222) Mertdogan, C. A.; McHugh, M. A.; Tuminello, W. H. *J. Appl. Polym. Sci.* **1999**, submitted for publication.

CR970046J